

Aus der  
Medizinischen Klinik und Poliklinik I  
Klinik der Ludwig-Maximilians-Universität München



***Plasmacytoid Dendritic Cells Play a Role in Megakaryopoiesis in the  
Bone Marrow***

Dissertation  
zum Erwerb des Doktorgrades der Medizin  
an der Medizinischen Fakultät der  
Ludwig-Maximilians-Universität München

vorgelegt von

Chenglong Guo  
aus

Henan, China

Jahr

2022

---

Mit Genehmigung der Medizinischen Fakultät der  
Ludwig-Maximilians-Universität zu München

Erster Gutachter: Prof. Dr. Med. Steffen Massberg  
Zweiter Gutachter: Prof. Dr. rer. nat. Annete Müller-Taubenberger  
Dritter Gutachter: Prof. Dr. Med. Michael Spannagl  
  
Mitbetreuung durch den  
promovierten Mitarbeiter: Dr. Hellen Ishikawa-Ankerhold  
Dekan: Prof. Dr. med. Thomas Gudermann  
  
Tag der mündlichen Prüfung: 11.05.2022

## Table of content

Abstract .....	1
Zusammenfassung.....	2
1 Introduction .....	3
1.1 Background .....	3
1.1.1 Bone marrow megakaryocytes.....	3
1.1.1.1 MK maturation stages in the bone marrow .....	3
1.1.1.2 The process of megakaryocytes developing into platelets in the bone marrow .....	4
1.1.1.3 Megakaryocyte apoptosis in the bone marrow.....	6
1.1.2 Bone marrow plasmacytoid dendritic cells (pDCs) .....	8
1.1.2.1 pDCs development .....	8
1.1.2.2 Identification of pDCs.....	9
1.1.2.3 Function of pDCs .....	10
1.1.3 Megakaryopoiesis in the bone marrow .....	11
1.1.3.1 The process of megakaryopoiesis .....	11
1.1.3.2 The potential regulators of megakaryopoiesis .....	13
1.1.3.2.1 Sinusoidal vascular niche as a microenvironment for megakaryopoiesis .....	13
1.1.3.2.2 Thrombopoietin as a dominant cytokine for megakaryopoiesis .....	13
1.1.3.2.3 The potential role of pDCs in megakaryopoiesis .....	15
1.2 Objective .....	16
2 Materials & Methods.....	18
2.1 Mouse strains .....	18
2.2 Reagents and antibodies .....	18
2.3 Measurement of platelets .....	19
2.3.1 Platelets measurement.....	19
2.3.2 Consecutive platelets measurement .....	20
2.4 Whole-mount immunofluorescence staining and imaging .....	20
2.5 Calvarium bone marrow intravital imaging by Two-Photon microscopy .....	22
2.6 Image processing.....	23
2.7 Isolation of bone marrow cells.....	23
2.8 Megakaryocyte colony forming unit (CFU-MK) assay .....	23

2.9 Megakaryocyte colony staining and imaging .....	24
2.10 Statistics .....	25
3 Results .....	26
3.1 The regulation of pDCs on megakaryopoiesis in the steady state .....	26
3.1.1 Interaction between pDCs and MKs in the steady state.....	26
3.1.1.1 Observation of the interaction between pDCs and MKs by bone marrow whole-mount immunostaining .....	26
3.1.1.2 Observation of the dynamic interaction between pDCs and MKs <i>in vivo</i>	29
3.1.2 The impact of pDCs depletion on megakaryopoiesis in the steady state....	32
3.2 The regulation of pDCs in megakaryopoiesis under thrombocytopenia.....	35
3.2.1 The interaction of pDCs with MKs under thrombocytopenia.....	35
3.2.2 Apoptotic MK numbers under thrombocytopenia .....	38
3.2.3 The impact of pDCs absence on megakaryopoiesis under thrombocytopenia .....	40
3.3 The impact of IFN- $\alpha$ on megakaryopoiesis.....	43
3.3.1 The impact of IFN- $\alpha$ on megakaryopoiesis <i>in vivo</i> .....	43
3.3.2 The impact of IFN- $\alpha$ on megakaryopoiesis <i>in vitro</i> .....	45
3.3.3 Effects of IFN $\alpha$ R deficiency on megakaryopoiesis <i>in vivo</i> .....	49
3.3.4 IFN- $\alpha$ impacting megakaryopoiesis mainly released by pDCs .....	51
4. Discussion .....	54
4.1 Methodology discussion.....	54
4.1.1 Identification of MKs, MKPs and pDCs.....	54
4.2 Results discussion .....	55
4.2.1 pDCs serve as the BM scanners sensing apoptotic MKs .....	56
4.2.2 Absence of pDCs impairs megakaryopoiesis both in the steady state and under emergency thrombocytopenia .....	56
4.2.3 IFN- $\alpha$ promotes megakaryopoiesis in the bone marrow.....	57
4.2.3.1 IFN- $\alpha$ plays a role in promoting the development of MKs.....	57
4.2.3.2 The source of IFN- $\alpha$ for promoting megakaryopoiesis in the bone marrow .....	58
4.3 Clinical implications .....	58
5. References .....	60
6 Appendix .....	79
Abbreviations .....	79
Acknowledgement.....	82

Affidavit .....83

## List of figures

Figure 1 Different phases of MK maturation.....	4
Figure 2 Overview of megakaryocyte producing platelets .....	6
Figure 3 Intrinsic and extrinsic apoptosis pathways .....	7
Figure 4 Plasmacytoid dendritic cell differentiation.....	9
Figure 5 The main functions of pDCs.....	11
Figure 6 Megakaryocyte differentiation pathways in the bone marrow .....	12
Figure 7 TPO measurements after platelet depletion.. .....	14
Figure 8 Quantification of MKs and MKPS in the bone marrow after TPO treatment..	15
Figure 9 Model of the whole-mount staining of the tibial bone marrow in mice .	21
Figure 10 Representative whole-mount staining images of pDC-MK interactions in control (left) and MK apoptotic (right) groups .....	27
Figure 11 Quantification of pDC and MK numbers under MK apoptotic conditions .....	27
Figure 12 MK apoptotic quantification.....	28
Figure 13 Quantification of pDC interacting with MK in the bone marrow .....	28
Figure 14 Representative intravital calvarial bone marrow imaging in control group (left) and MK apoptotic group (right) by two-photon microscopy .....	29
Figure 15 Single pDC dynamical interaction with MK surface.....	30
Figure 16 Single pDC dynamical diving into MK body .....	31
Figure 17 3D reconstructed images of single pDC dynamical interaction with MK in control group (upper) and MK apoptotic group (lower) .....	31
Figure 18 Speed of each pDC processing the interaction with MKs in control group compared with MK apoptotic group .....	31
Figure 19 pDC depletion in the bone marrow.....	32
Figure 20 Platelet quantification under pDC depletion conditions. ....	33
Figure 21 Representative whole-mount immunostaining in control group (left) and pDC depletion group (right).....	34
Figure 22 MK and MKP quantifications under pDC depletion conditions .....	34
Figure 23 Representative bone marrow whole-mount immunostaining (upper) and 3D reconstructed images (lower) in control group (left) and platelet depletion group (right) .....	35
Figure 24 MK-pDC interaction under thrombocytopenia.....	36
Figure 25 Representative intravital calvarial bone marrow imaging in platelet depleted mice by two-photon microscopy .....	37

Figure 26 3D reconstructed images of single pDC dynamic interaction with MK in control group (upper) and platelet depletion group (lower).....	37
Figure 27 Speed of each pDC interacting with MKs in control group compared with platelet depletion group.....	38
Figure 28 Representative whole-mount staining images in control group .....	39
Figure 29 Representative whole-mount staining images in thrombocytopenia group .....	39
Figure 30 MK apoptotic quantification under thrombocytopenia.....	40
Figure 31 Platelets recovery under emergency thrombocytopenia .....	41
Figure 32 Representative whole-mount staining images in platelet depletion mice (left) and platelet depletion + pDC depletion mice (right).....	42
Figure 33 pDC, MK and MKP quantifications under thrombocytopenia.....	42
Figure 34 Platelet numbers under interferon treatment.....	43
Figure 35 Representative whole-mount immunostaining in control (upper-left), IFN- $\alpha$ treated 2h (upper-right), IFN- $\alpha$ treated 4h (lower-left) and IFN- $\alpha$ treated 24h (lower-right) mice.....	44
Figure 36 MK and MKP quantifications under interferon treatment.....	45
Figure 37 Representative MK-CFU staining images in control group. ....	46
Figure 38 Representative MK-CFU staining images in experimental group.....	47
Figure 39 CFU-MK fold in vWF $\times$ IFNaRflox cre <sup>-</sup> mice (control group) (n=6mice). .....	47
Figure 40. CFU-MK fold in vWF $\times$ IFNaRflox cre <sup>+</sup> mice (experimental group) (n=6mice).....	48
Figure 41 CFU-MK fold in vWF $\times$ IFNaRflox cre <sup>-</sup> mice (control group) and vWF $\times$ IFNaRflox cre <sup>+</sup> mice (experimental group) .....	48
Figure 42 Platelets fold relative to control group.....	49
Figure 43 Representative whole-mount immunostaining in control group (left) and IFNaR-KO group (right) .....	50
Figure 44 pDC, MK and MKP quantifications under IFNaR deficiency condition .....	50
Figure 45 Representative whole-mount immunostaining in pDC depletion group (left) and pDC-DTR x IFNaR-KO group (right).....	51
Figure 46 Representative whole-mount immunostaining in platelet depletion + pDC depletion mice (left) and platelet depletion + pDC-DTR x IFNaR-KO mice (right).....	52
Figure 47 MK and MKP quantifications under absence of pDC and IFNaR knock out condition.....	52

Figure 48 MK and MKP quantifications in the absence of pDC and IFNaR knock  
out under thrombocytopenia .....53

## **Abstract**

The hematopoietic system gives rise to a heterogeneous cell population in the bone marrow (BM), which will fulfill their roles in immunity, blood clotting and tissue oxygenation. Hematopoietic stem cells (HSCs) are at the apex of a hierarchically organized maturation cascade constantly replenishing the pool of differentiated cells to maintain blood cell homeostasis. Megakaryocytes (MKs) are niche cells of hematopoietic origin that support HSCs homeostasis and generate circulating platelets. The process of platelet generation by MK fragmentation or proplatelet release (thrombopoiesis) is well characterized. However, what is triggering MK progenitor cells (MKPs) to differentiate into mature MKs (megakaryopoiesis) after MK finishing platelets production, still remains unclear.

The results in this study revealed some input for the answer to this question. It is revealed that plasmacytoid dendritic cells (pDCs) are in closer contact with apoptotic MKs and they may release interferon  $\alpha$  (IFN- $\alpha$ ) into the MK niche. The released IFN- $\alpha$  can induce MKPs to develop into mature MKs, both in steady state and thrombocytopenia. Thus, we identify pDCs as crucial bone marrow niche cells to monitor the bone marrow for exhausted platelet-producing megakaryocytes and deliver IFN- $\alpha$  to the megakaryocytic niche to trigger local on-demand proliferation of megakaryocyte progenitors. This fine-tuned coordination between thrombopoiesis and megakaryopoiesis is crucial for megakaryocyte and platelet homeostasis in steady state and thrombocytopenia.

## **Zusammenfassung**

Das hämatopoetische System im Knochenmark (BM) bildet die Grundlage für die Generierung von terminal differenzierten Zellen, welche eine wesentliche Rolle bei der Blutgerinnung, Gewebeoxygenierung und Immunität spielen. Stamm- und Vorläuferzellen stehen an der Spitze einer hierarchisch organisierten Reifungskaskade, um den Pool differenzierter Zellen ständig aufzufüllen und die Homöostase der Blutzellen aufrecht zu erhalten. Megakaryozyten (MKs) sind Nischenzellen, die die Homöostase von hämatopoetischen Stammzellen (HSCs) unterstützen und die zirkulierenden Blutplättchen (Thrombozyten) erzeugen. Obwohl der Prozess der Blutplättchenbildung durch Fragmentierung von MKs (Thrombopoese) umfassend untersucht wurde, bleibt der Prozess der Neubildung von Megakaryozyten aus Vorläuferzellen (Megakaryopoese) und die dafür erforderlichen zellulären und molekularen Mechanismen, unklar.

In der vorliegenden Arbeit wurde gezeigt, dass plasmazytoide dendritische Zellen (pDCs) im Knochenmark in Kontakt mit apoptotischen MKs stehen, welches zu einer potentiellen Freisetzung von Interferon alpha ( $\text{IFN-}\alpha$ ) führt.  $\text{IFN}\alpha$  indiziert dann die Entwicklung von Megakaryozyten-Vorläufer zu MKs im Steady-State, sowie bei Thrombozytopenie. Diese Ergebnisse legen nahe, dass pDCs die entscheidenden Nischenzellen des Knochenmarks darstellen, die das Knochenmark auf erschöpfte Thrombozyten-produzierende Megakaryozyten hin überwachen und  $\text{IFN-}\alpha$  an die megakaryocytische Nische liefern und eine lokale bedarfsgesteuerte Proliferation von MK-Vorläufern vermittelt. Diese fein abgestimmte Koordination zwischen Thrombopoese und Megakaryopoese ist entscheidend für die Megakaryozyten- und Thrombozytenhomöostase im Steady-State und bei Thrombozytopenie.

# **1 Introduction**

## **1.1 Background**

### **1.1.1 Bone marrow megakaryocytes**

#### 1.1.1.1 MK maturation stages in the bone marrow

Megakaryocytes (MKs) are polyploidy and rare cells mainly localized in the bone marrow (BM) sinusoids with a size of 50-100  $\mu\text{m}$  in diameter [1-3]. In maturation period, the cytoplasm of MK is filled up with proteins and organelles to be transferred to the newborn platelets [1-5]. MKs are differentiated from hematopoietic stem cells (HSCs) and undergo four different growth stages before they are mature to produce platelets. In the first stage, the MKs have a small size of 10-15  $\mu\text{m}$  in diameter, with round shape and single nucleus so called megakaryocyte progenitors (MKPs) [6]. MKPs have no demarcation membranous system (DMS) [7]. In the second stage, MKs present a larger nucleus where the chromosome numbers increase 4-8 folds [8] and with a diameter around 14-20  $\mu\text{m}$ . In this stage, some tube-like structures, called the pre-demarcation membrane system, start to appear [6]. In the third stage, MKs increase the size to 20-40  $\mu\text{m}$  and the cytoplasm is filled up with different types of organelles. In this stage, the MK ploidy increases with the predominant numbers of 8 N, 16 N, and 32 N [6]. In the last stage, MKs grow much bigger (40-100  $\mu\text{m}$ ) and become fully mature to initiate the production of cytoplasmic structure extension called proplatelet [9]. In this final stage, the DMS extends into so called proplatelets, which enter the blood stream to release platelets [10]. Figure 1 [6] illustrates the different phases of MKs maturation.

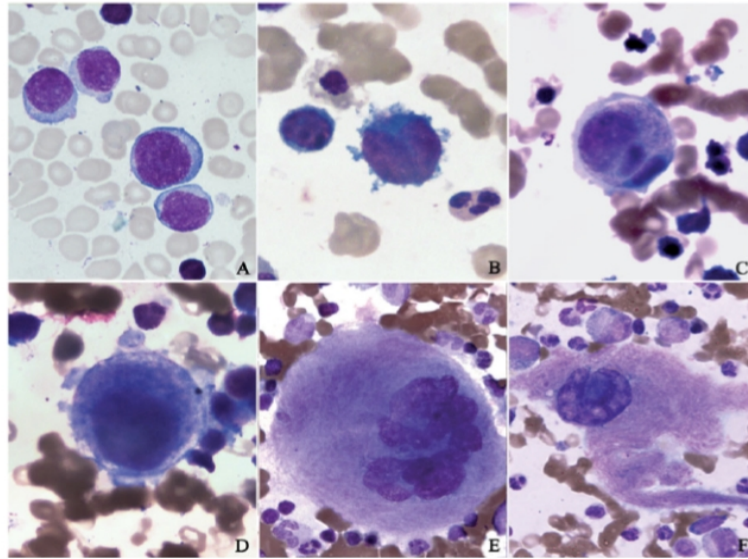


**Figure 1 Different phases of MK maturation.** (A) Phase I: It is composed by small cells denominate megakaryocytes progenitors (MKPs) with 10-15 $\mu$ m in diameter and a single nucleus. (B) Phase II: MKs increased in size to 15-20  $\mu$ m in diameter and have a bigger nucleus. (C, D) Phase III: MKs are with 20-40  $\mu$ m in diameter and high ploidy. (E) Phase IV: MKs are with 40  $\mu$ m in diameter and are preparing for extending proplatelet into the blood vessels. (F) Phase VII: The mature MK is releasing platelets (from Y.X.Ru, et al. [6])

The MK phases can be identified and separated by different cell surface markers. CD41 is used to label all stages of megakaryocyte development and is the most extensively accepted cell surface marker for MKs [11]. CD42 is usually used for labeling the mature MKs [12,13], thus MKPs could be defined as CD41<sup>+</sup> CD42<sup>-</sup> cells. Additionally, in mice the HSCs are defined as Lin<sup>-</sup> Sca-1<sup>+</sup> c-Kit<sup>+</sup> cells [14,15], and CD9 is used to label MK lineages [16]. Thus, MKPs can be differentiated as CD41<sup>+</sup>CD42<sup>-</sup>Lin<sup>-</sup> Sca-1<sup>+</sup> c-Kit<sup>+</sup> CD9<sup>+</sup> cells [17,18].

#### 1.1.1.2 The process of megakaryocytes development and platelet generation in the bone marrow

Mature MKs with a size of 100  $\mu$ m in diameter, can produce thousands of platelets daily [19-21]. MK bodies are full covered with abundant ribosomes responsible for the

production of specific proteins, that will be part of the platelets content, before MKs are capable to release platelets [22]. The expansion of MKs is conducted by several rounds of endomitosis, which is the process of chromosome numbers increase, by more than 64-fold, without nuclear division [1-3,23]. Thrombopoietin (TPO) promotes megakaryocyte endomitosis via binding to the c-Mpl receptor. Chromosome duplication and the nuclear envelope disruption occur during endomitosis. The failing separation of spindles and nuclear envelope reformation result in polyploid and multilobed nucleus in each MK [24]. Besides the high DNA content, mature MKs are characterized by the presence of granules, organelles as well as internal membrane systems. In particular, the DMS that is an extensive and interconnected membranous system, used for separating the MK cytoplasm into small areas for platelets release. Nowadays, it is recognized as a major reservoir surrounded by membranes responsible for proplatelets formatting and platelet release [24-26]. MKs usually initiate the process of platelet generation by forming one or more cytoplasmic extensions that elongate giving origin to proplatelets [24]. MK will continuously generate an expansive and complicated network of interconnected proplatelets, until its cytoplasm is completely used [27, 28]. In addition, the proplatelet tips are amplified by bending and branching [27], and become elongated by the microtubules cytoskeleton movement to the cell cortex. Parallely, organelles and granules travel to the proplatelet ends where the platelets are released. Eventually, the whole cytoplasm of MK is transformed into abundant mesh of proplatelets and the remaining nuclei are pressed out during the process of platelets released from their tips. See Figure 2 [24] for the process of MKs releasing platelets.

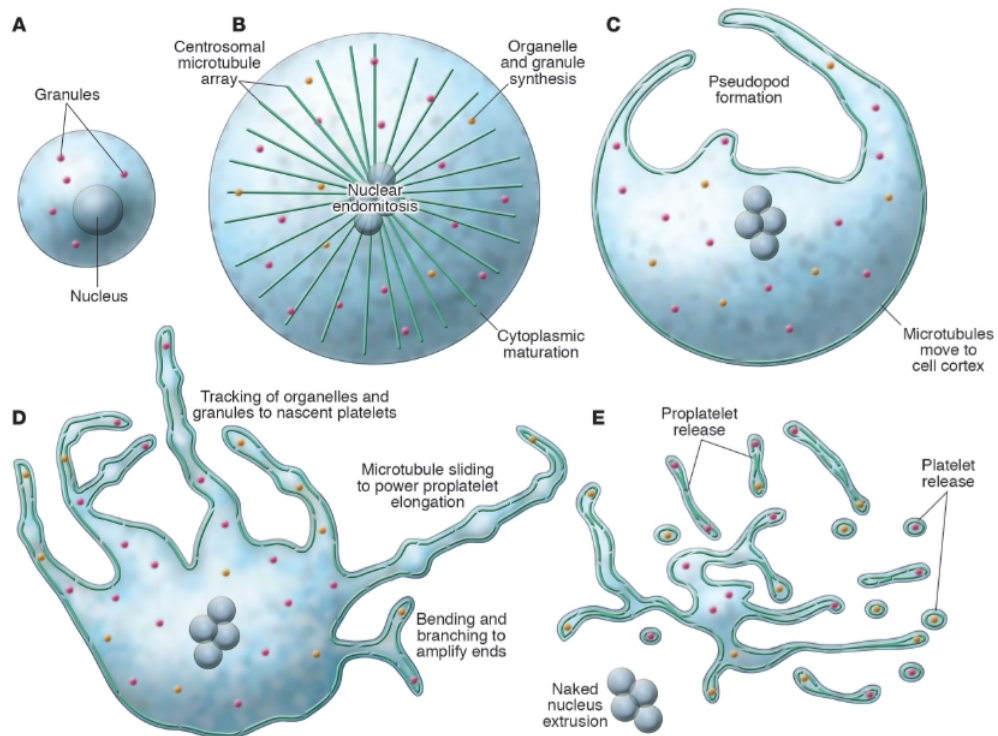


**Figure 2 Overview of megakaryocyte producing platelets.** (A) Immature MK. (B) MK chromosomes duplication with organelle assembly and cytoplasm maturation. (C) Microtubules are assembly in direction to cell cortex to promote proplatelet elongation. (D) Proplatelet elongation, organelles and granules travel to the proplatelet ends. (E) Proplatelets release the platelets and extrude the nuclei (from Patel SR, et al. [24])

### 1.1.1.3 Megakaryocyte apoptosis in the bone marrow

Apoptosis has been defined as a type of cell death with morphologically distinct mechanism [29], and now it is clear that apoptosis is a programmed cell death drive by the intrinsic or the extrinsic pathways [30]. The intrinsic pathway is regulated by BCL-2 family-proteins and it is taking place on the mitochondria. The main function of BCL-2 proteins is to inhibit the BAK and BAX proteins, to keep the cell surviving. Once some stress signals impair the BCL-2 protein members, BAK and BAX will be activated contributing to mitochondria membrane damage leading to release of mitochondrial constituents containing cytochrome c, that can trigger a series of responses of apoptotic caspase cascade. In the apoptotic cascade, caspase-9 is the first compound to be activated, and subsequently the caspase-3 and caspase-7, leading to DNA impairment, transcription and translation restrained [31]. The extrinsic pathway

is initiated by some death-ligands secreted from tumor necrosis factor (TNF). For example, by the FasL (a kind of death-ligands) binding to Fas receptor of cells, caspase-8 will be activated to trigger Caspase-3/7 executing the cell death program [32]. Additionally, the cleaved caspase-8 can activate the protein BID to release t-BID contributing to triggering the intrinsic pathway by activating BAK/BAX [33,34]. Figure 3 illustrates the two apoptosis pathways.

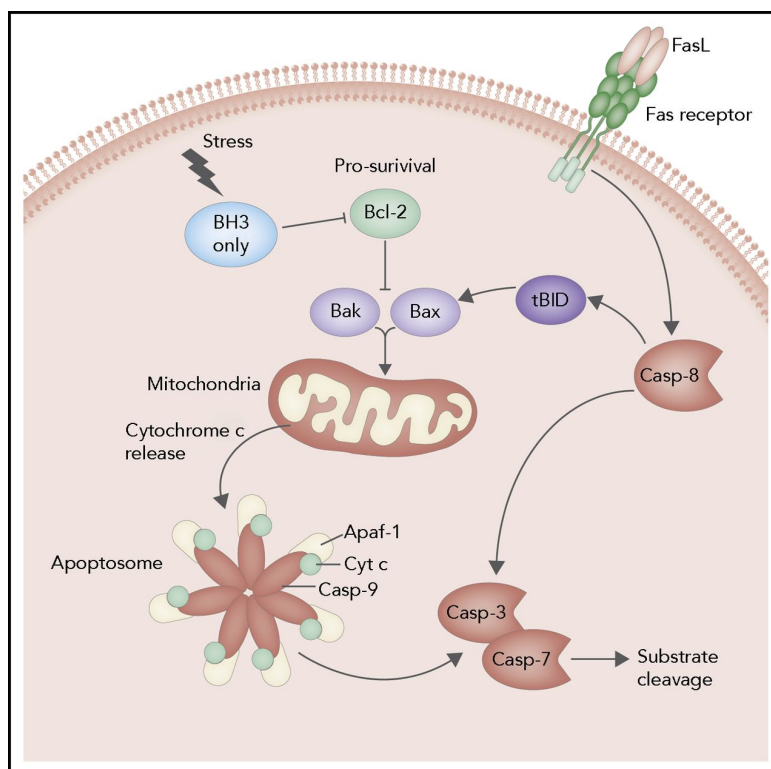


**Figure 3 Intrinsic and extrinsic apoptosis pathways.** Intrinsic pathway: Stress stimulus activates BH3-only, that inhibits the BCL-2 family-proteins. This inhibition leads to Bak/Bax activation and damage of the mitochondrial membrane. This results in cytochrome c release inducing caspase-9 activation. Afterwards, caspase-3/7 are subsequently activated by caspase-9. Extrinsic pathway: FasL binding to Fas receptor activates caspase-8 trigger caspase 3/7 activation (from McArthur K, et al. [35])

In MKs, MCL-1 and BCL-XL are the main proteins to restrain the intrinsic pathways, thus to maintain the growth and maturation of MKs [36,37]. There is a controversy if

MK apoptosis is indispensable for platelet production. Many studies found that mature MK apoptosis promotes the rearrangements of cytoskeleton which are required for platelet shedding [38-45]. Another study by Debili and his colleagues demonstrated that caspase inhibitors can impair the proplatelet formation in the culture of MKs. Therefore, they concluded that MK apoptosis is required for platelet production. Some studies shown oppose to this viewpoint found that there were no effects on platelets production by using mouse models of deficiency of BAK, BAX, caspase-8, or caspase-9 [36,46-50]. Although it has not reached a consensus about the necessity of MK apoptosis for producing platelets, it is clear that platelet release is followed by MK apoptosis. Other authors reported that the feature of “degenerative senescent” MK were distinguished by “naked” nuclei surrounded by a thin ring of cytoskeleton, that is consistent with MK death by apoptosis. Thus, they proposed that platelet shedding was happening parallel with MK apoptosis [51].

## **1.1.2 Bone marrow plasmacytoid dendritic cells (pDCs)**

### **1.1.2.1 pDCs development**

Plasmacytoid dendritic cell is one subtype of the dendritic cells (DCs) population, and it has been identified and characterized in the 1950s [52]. pDCs are developed from HSCs in the bone marrow. In the process of the pDC development, lymphoid primed multipotent progenitors (LMPPs) create myeloid and lymphoid pathways to differentiate into pDCs [53,54]. For the myeloid pathway, LMPPs can directly give rise to common DC progenitors (CDPs) or differentiate into myeloid macrophage DC progenitors (MDPs) first, then continue developing into CDPs [55]. CDPs which are defined as CD115<sup>+</sup> CD117<sup>+</sup> CD135<sup>+</sup> cells finally finish the differentiation into pDCs or classical DCs (cDCs) [56,57]. One subset of the CDPs without expressing CD115 but with high-level of E2-2 are committing more to contribute to pDCs differentiation, than CD115<sup>+</sup> CDPs [58,59]. CCR9<sup>low</sup> pDC-like cells differentiated from small parts of these CDPs expressing low level of E2-2 and high level of Id2 that can inhibit E2-2 activity,

suppress pDCs differentiation [60,61]. For the lymphoid pathway, LMPPs can give rise to common lymphoid progenitors (CLPs) then continue to develop into Ly-6D<sup>+</sup> LPs. Next, these LPs differentiate into Ly-6D<sup>+</sup> Siglec-H<sup>+</sup> pre-pDCs and finally develop into the pDCs [62]. Figure 4 [62] illustrates the development of pDCs.

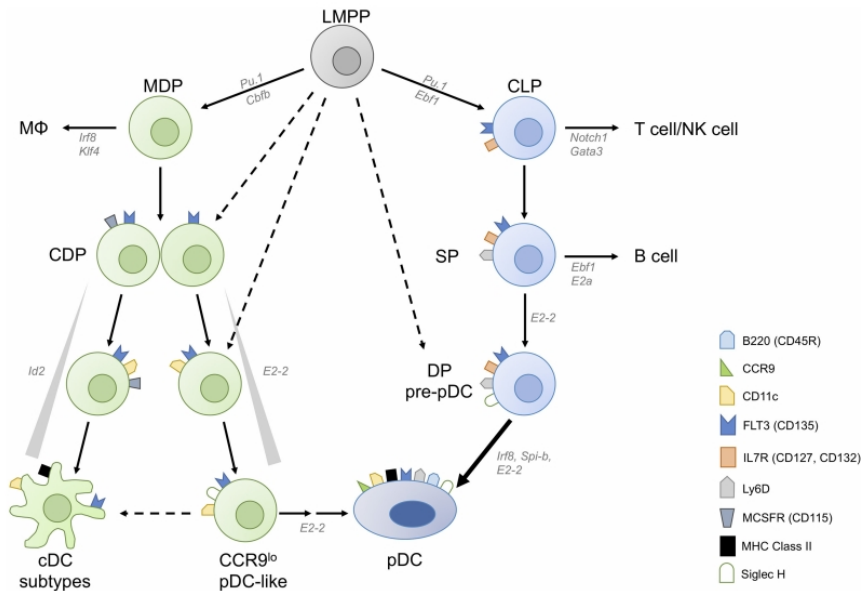


**Figure 4 Plasmacytoid dendritic cell differentiation.** Lymphoid primed multipotent progenitor (LMPP) can originate either macrophage-dendritic cell progenitor (MDP), that will develop into common dendritic cell progenitor (CDP) or directly differentiates into CDP. CDP can develop into classical dendritic cell (cDC) and plasmacytoid dendritic cell (pDC). pDC is also generated by the lymphoid pathway. LMPP gives rise to common lymphoid progenitor (CLP), then continues to develop into Ly-6D<sup>+</sup> LP and Ly-6D<sup>+</sup> Siglec-H<sup>+</sup> pre-pDCs, finally into the pDCs (from Andrea Musumeci, et al. [62])

#### 1.1.2.2 Identification of pDCs

Plasmacytoid dendritic cells can be differentiated from the cDC subtypes in mice and human by the expression of defined makers. In mice, the markers are B220, Ly-6D, Siglec-H and BST2. In human, pDCs can be identified by BDCA2/4, CD123 and CD45RA markers [62]. BST2 and Siglec-H are the most common markers to identify pDCs in mice. Especially, BST2 is very specific to pDCs in the bone marrow, while it

can label some other cells which are exposed to type I and II interferon [63]. Siglec-H expression is mostly defined as pDCs in cell suspensions from primary and secondary lymphoid organs [64,65]. However, it is also expressed on some subtypes of macrophages [66].

#### 1.1.2.3 Function of pDCs

The main function of pDCs is secreting IFN- $\alpha$  mostly mediated by toll like receptor 7/9 (TLR7/9) via MyD88-IRF7 pathway to promote the immunity responses [67,68]. TLR7/9 will be activated respectively by sensing RNA/DNA viruses, endogenous RNA/DNA as well as composite oligoribonucleotides/oligodeoxyribonucleotides to initiate the IFN- $\alpha$  production [69,70]. pDCs also can secrete the pro-inflammatory cytokines and chemokines mediated by TLR7 or TLR9 via the MyD88-NF- $\kappa$ B pathway, by recognizing the nucleic acids of pathogens [71]. IFN- $\alpha$  produced by pDCs can induce T<sub>H1</sub> cells polarization, enhance CD8<sup>+</sup> T cell augmentation, and stimulate the differentiation of plasma cells [72-74]. With the expression of CD80, CD86 and MHCII, pDCs commit the function of presenting antigens to CD4<sup>+</sup> T cells [75-77]. Furthermore, pDCs can drive CD4<sup>+</sup> T cells development into T<sub>H2</sub> and T<sub>reg</sub> cells to promote the immune tolerance with expressing indoleamine 2,3-dioxygenase (IDO), inducible co-stimulator ligand-L (ICOS-L) and OX40L [78,79]. In addition, pDCs can respond directly to apoptotic cells by producing IFN- $\alpha$  or/and some cytokines such as interleukin 6/10 (IL-6/10) [80]. Figure 5 [81] describes the main functions of pDCs concretely.

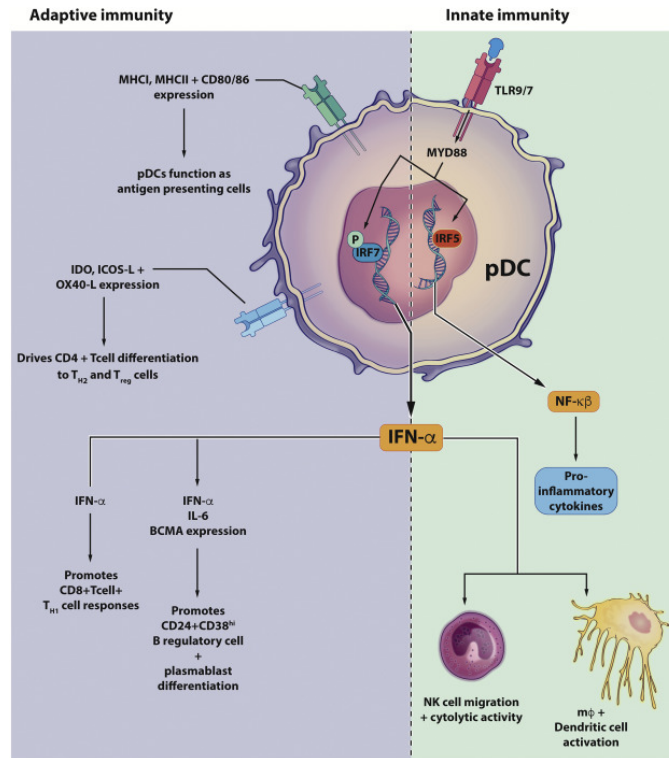


**Figure 5 The main functions of pDCs.** pDCs take part in both innate immunity and adaptive immunity. pDCs produce IFN- $\alpha$  via the TLR9/7. IFN- $\alpha$  promotes T<sub>H1</sub> cells and CD8<sup>+</sup> T cell survival and expansion. It also induces NK cell migration and activates the differentiation of plasma cells and macrophages. pDCs drive the CD4<sup>+</sup> T cells development to T<sub>H2</sub> and T<sub>reg</sub> cells when they express IDO, ICOS-L and OX40L. pDCs act as antigen presenting cells (APCs) presenting antigens to CD4<sup>+</sup> T cells (from Dana Mitchell, et al. [81])

### 1.1.3 Megakaryopoiesis in the bone marrow

#### 1.1.3.1 The process of megakaryopoiesis

What is megakaryopoiesis? In brief, it is a process of MK differentiation from the megakaryocyte precursors called megakaryocyte progenitors and some hematopoietic stem cells (HSCs) into mature megakaryocytes [82,83]. In detail, the long-term HSCs (LT-HSCs) break stationary phase and turn into the short-term HSCs (ST-HSCs), continuing to develop into the multipotent progenitors (MPPs) [84]. MPPs sequentially differentiate into the common myeloid progenitors (CMPs) which have the capacity to form granulocyte, monocyte-macrophage, erythrocyte as well as platelet-precursor [85].

CMPs continue division into megakaryocytic-erythrocytic progenitors (MEPs) and then finally differentiates into MKs [86-88]. Recent studies propose that there are three parallel lineage pathways in general for the megakaryopoiesis in the bone marrow (Figure 6) [18, 89-92]. ST-HSCs derived from LT-HSCs differentiate into MPPs1 as well as MPPs2 and continue to differentiate into MKs respectively with multiple steps in two different pathways (classic and alternative model). Notably, it is proposed that there are no proliferative potentials in both MPPs1 and MPPs2. While MPPs3, differentiated from LT-HSCs directly, are recognized as self-renewing cells committed to the development of MKs in myeloid bypass model [92,93]. In this model, MPPs3 can differentiate into myeloid repopulating progenitors including repopulating CMPs, MEPs and MKPs. It is proposed that the MK development in myeloid bypass model may be dynamic and sensitive to the change of environments such as inflammation, infection, and wound healing (92,94).

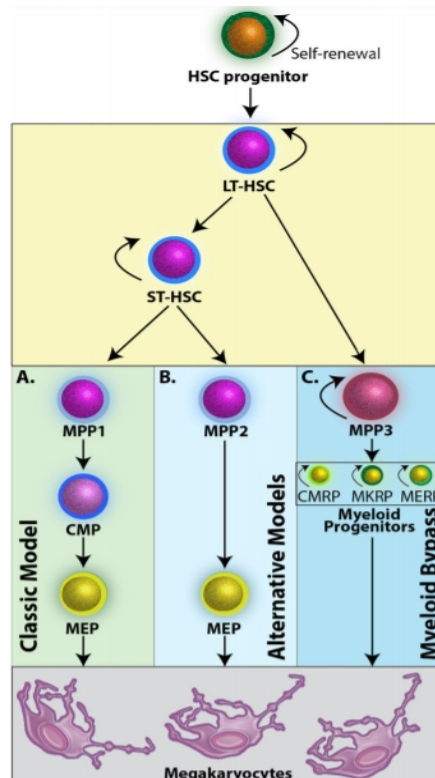


**Figure 6 Megakaryocyte differentiation pathways in the bone marrow.** LT-HSC gives rise to ST-HSC, and then continues to develop into MPP1, MPP2 and MPP3. (A) Classic model: MPP1 differentiates into CMP, then CMP gives to MEP and MEP develops into MK (B)

Alternative model: MPP2 differentiates into CMP, then CMP originate MEP and MEP develops into MK. (C) Myeloid bypass: MPP3 differentiates into CMRP, then CMRP gives to MERP and MERP develops into MK (from Bush LM, et al. [18])

### 1.1.3.2 The potential regulators of megakaryopoiesis

#### 1.1.3.2.1 Sinusoidal vascular niche as a microenvironment for megakaryopoiesis

Many studies found that most MKs, MKPs and even HSCs are the units of megakaryopoiesis located closer to the perivascular niche in the bone marrow [95,96]. Why megakaryopoiesis takes place at the perivascular niche? First, because the perivascular niche is a place with plenty oxygen and nutrients in which MKs release the platelets into the circulation more easily and effectively. Second, there are some cells secreting abundant factors to promote the progress of megakaryopoiesis such as endothelial cells and some reticular cells that are rich in CXCL12. Many studies found that these cells at the perivascular niche can produce a large amount of SDF-1 and SCF which are critical regulators contributing to regulating the HSCs [97-99]. c-kit is the cytokine receptor mainly expressed on HSCs, and SCF serves as the c-kit ligand inducing HSCs differentiation when they bind together [100-105]. Later, some studies discovered that c-kit was also expressed on MKs, and SCF/c-kit can promote MK maturation [106,107]. SDF-1 and FGF-4 were reported to increase platelet production by mediating the interaction between MKPs and bone marrow endothelial cells [96]. Above all, these studies make clear that sinusoidal vascular niche supplies an adaptive microenvironment for megakaryopoiesis.

#### 1.1.3.2.2 Thrombopoietin as a dominant cytokine for megakaryopoiesis

Thrombopoietin (TPO) is the critical protein for the development of MKs and it was first purified in 1994 [108,109]. C-Mpl, the TPO receptor, mostly expressing on MKs, MKPs and HSCs is activated via binding to TPO giving rise to activating downstream

signaling pathways subsequently such as JAK2/STAT, MAPK and PI3K [110-113]. After activation, MK progenitors expand and differentiate to MKs [114]. Some studies proved that TPO treatment gave rise to more maturation of MKs and more platelets production in *vivo* or in *vitro* [113,115,116]. It was reported that the survival of HSCs was relevant to TPO, and TPO also induced the differentiation of HSCs together with IL-3 or SCF [117]. The main sources of TPO are the liver and kidney, and some bone marrow stromal cells provide a small amount of TPO [118,119]. The degradation of TPO occurs when it is binding to c-Mpl on platelets. Therefore, less degradation of TPO takes place in the circulation contributing to replenishing the platelet source under thrombocytopenia [120]. In a previous study we have shown that the highest level of TPO in the circulation occurs after 12h of platelets depletion (Figure 7) [121]. And after 3 days TPO treatment, the quantity of MKs as well as MKPs all increased significantly (Figure 8) [121].

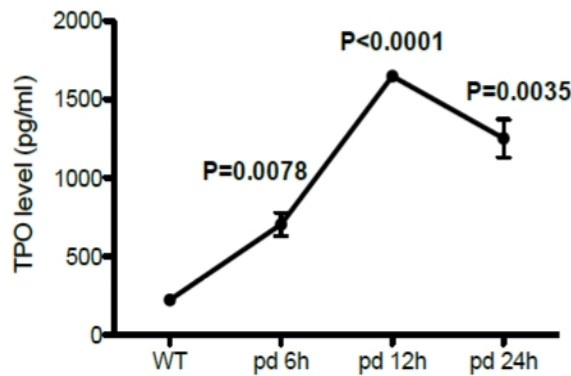


**Figure 7 TPO measurements after platelet depletion.** TPO levels were measured in the serum after 6, 12 and 24 h of platelet depletion. The higher peak is seeing after 12 h of platelet depletion. Wide type mice (WT) n= 6. Platelet depleted mice (pd) n= 4. (from Fu, Wenwen, dissertation, LMU. [121])

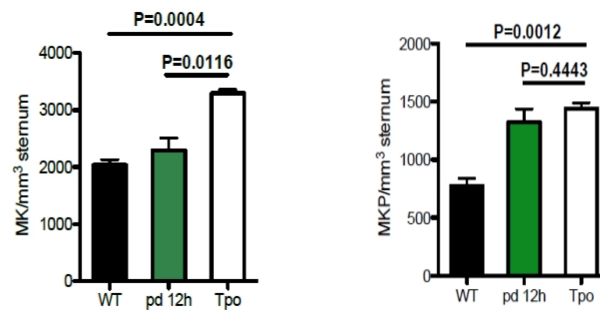


**Figure 8 Quantification of MKs and MKPs in the bone marrow after TPO treatment.** Mice were treated with TPO or injected with antibodies to deplete platelets for 12 h. Histograms display the numbers of MK and MKP quantified in the bone marrow after the respective treatments. Wide type (WT) mice n= 3. Platelet depleted (pd) mice n= 4, and TPO treated mice n= 3 were included (from Fu, Wenwen, dissertation, LMU. [121])

Taking together, TPO is recognized as an indispensable cytokine for megakaryopoiesis, especially promoting the formation of MK progenitors and their differentiation into MKs.

#### 1.1.3.2.3 The potential role of pDCs in megakaryopoiesis

It is clear that the vascular niche microenvironment provides some regulators like SDF-1 and SCF to promote the megakaryopoiesis, and TPO as a potent cytokine globally accelerating the megakaryopoiesis as well. However, it is still not clear how the megakaryopoiesis is triggered, after the mature MKs finished releasing platelets. As before described in our previous study, MKPs were located very close to the mature MKs, therefore we hypothesized that vanishing MKs that accomplished platelet release may themselves act as local stimuli fueling their progenitors. However, how the vanishing MKs regulate megakaryopoiesis is not yet well understood. It is reported that MKs finishing thrombopoiesis turn into “degenerate senescent” MKs with “naked” nuclei [51]. Since remnant MKs are hardly found within BM sections, it has been

suggested that they undergo rapid apoptosis and are cleared by bone marrow phagocytes that sense apoptotic bodies and DNA [35]. As before mentioned, pDCs are migratory cells that are specialized in detecting apoptotic cells and nucleic acids [72,80]. Hence, we hypothesize that pDCs may detect the apoptotic MKs, and then secreting some cytokines to induce MKPs developing into MKs. Actually, pDCs can secrete many cytokines, if these cytokines play a role in megakaryopoiesis is unknown. The main function of pDCs is secreting IFN- $\alpha$  [67], and some studies have proved that both MKs and MKPs express the IFN- $\alpha$  receptor [68]. Furthermore, a study by Haas et al, indicated that IFN- $\alpha$  mediated inflammation can promote MKPs to develop into MKs [94]. Based on these previous reports and our own preliminary results, we hypothesize that pDCs may regulate megakaryopoiesis by sensing apoptotic MKs and then releasing IFN- $\alpha$  to trigger the maturation of MKPs.

## 1.2 Objective

Despite many factors impact megakaryopoiesis in the bone marrow, it is not clear how megakaryopoiesis is triggered after MKs accomplish thrombopoiesis under the steady state or acute thrombocytopenia. In this thesis, It will be investigated if and how pDCs regulate megakaryopoiesis *in vivo* and *in vitro* under the steady state as well as acute thrombocytopenia.

### **Aim 1: To investigate the role of pDCs in megakaryopoiesis under the steady state**

At the first, we will use two-photon intravital microscopy and whole-mount immunostaining to investigate the pDC-MK interaction *in vivo* under the steady state. To study if this interaction is further enhanced in response to apoptotic MKs, we will conditionally induce apoptosis in the megakaryocytic lineage in *PF4-Cre<sup>+</sup>; iDTR<sup>flox</sup>; vWF-eGFP* mice (MK-iDTR-mice) treated with diphtheria-toxin (DT). At the last, to

investigate if pDCs impact megakaryopoiesis, we will use a murine model for pDC depletion (BDCA-2DTR) mouse. Under these conditions, the MKs, MKPs, pDCs and platelets numbers will be quantified via whole-mount immunostaining images in wide type (WT) and pDCs depleted mice.

**Aim 2: To characterize the role of pDCs in megakaryopoiesis under thrombocytopenia**

In order to study if pDCs have an influence on megakaryopoiesis under acute platelets depletion, first, the emergency thrombocytopenia will be performed by injecting the antibodies into the mice to induce acute deplete platelets. By using two-photo intravital microscopy, the pDC-MK interaction *in vivo* under thrombocytopenia conditions will be investigated. The numbers of platelets, MKs and MKPs will be determined after 24 hours of platelets depletion in WT and pDC-depleted mice.

**Aim 3: To investigate if IFN- $\alpha$  regulate megakaryopoiesis**

To investigate if the IFN- $\alpha$  release in the bone marrow impact megakaryopoiesis, we will use murine models for IFN- $\alpha$  treatment, IFN $\alpha$ R depletion and pDC-IFN $\alpha$ R-depletion mice. First, we will count the number of platelets, MKs and MKPs in mice under IFN- $\alpha$  treatment as well as in IFN- $\alpha$  receptor knock out mice to check if the IFN- $\alpha$  affects megakaryopoiesis *in vivo*. Then, we will do megakaryocyte colony forming unit (CFU-MK) assay under different concentrations of IFN- $\alpha$ , to discover the effects of IFN- $\alpha$  for MK proliferation *in vitro*. Last, the number of platelets, MKs and MKPs will be quantified in the absence of pDCs by using the mice lines pDC-DTR-IFN $\alpha$ R and pDC-DTR to analyze the impact of pDCs in megakaryopoiesis.

## 2 Materials & Methods

### 2.1 Mouse strains

Wild type C57BL/6J, Rosa26-iDTR, PF4-Cre, BDCA2-DTR, IFN $\alpha$ R<sup>-/-</sup> and IFN $\alpha$ R1<sup>fllox</sup> were bought from the Jackson Laboratory. vWF-Cre mice were obtained from W. Aird and vWF-eGFP mice were generated by C. Nerlov. The crossbreed of PF4-Cre and Rosa26-iDTR mice was used to induce MK cell death *in vivo* (PF4-Cre; RS26-iDTR). The crossbreed of PF4-Cre; RS26-iDTR and vWF-eGFP mice was used to visualize the megakaryocytic lineage following induction of MK cell death (referred to as MK-iDTR). vWF-Cre mice were crossed with IFN $\alpha$ R1<sup>fllox</sup> to conditionally delete IFN $\alpha$ R in the megakaryocytic lineage. pDC-DTR and IFN $\alpha$ R<sup>-/-</sup> were cross bred to achieve pDC depletion in IFN $\alpha$ R<sup>-/-</sup> animals (pDC-DTR; IFN $\alpha$ R<sup>-/-</sup>). 6-12 weeks old, male and female mice were used in this study. There were no differences of the sexes and ages for the mice in control and experimental groups. Mice were bred and kept in the animal facilities of the Walter-Brendel Zentrum, the Zentrum für Neuropathologie und Prionforschung (ZNP) or the Biomedical center of the LMU in Munich, Germany. The whole murine experiments were followed by the law of animal-production in Munich, Germany.

### 2.2 Reagents and antibodies

Diphtheria Toxin (DT) (Sigma-Aldrich-Saint Louis, MO, USA) was injected intraperitoneally into pDC-DTR and pDC-DTR-IFN $\alpha$ R<sup>-/-</sup> mice in 8 ng/g per day for 3 days [122,123]. A single dose was injected into MK-iDTR mice 24h before the experiment. Platelet depleting antibody (R300, anti-GPIb $\alpha$ , used as 2 $\mu$ g/g bodyweight) and isotype control (C301) from Emfret (Eibelstadt, Germany), were injected intraperitoneally into the mice for 24h to induce platelet depletion. pDC depleting antibody (ultra-LEAF<sup>TM</sup> purified anti-PDCA-1, clone 927, BioLegend) was injected i.p.

for 9 consecutive days with a concentration of 150 µg per mouse at day 1 and 100 µg per mouse the following days. The isotype control (ultra-LEAF™ purified rat IgG2bk Isotype Ctrl, clone RTK4530, BioLegend) was injected accordingly. Type I interferon alpha was applied by injecting universal interferon alpha (PBL, assay science) with 5000U / mouse i.p in 200 µl PBS. Both CD41-fluorescein isothiocyanate (FITC) and CD41-Streptavidin-phycoerythrin (PE) were purchased from Biolegend (San Diego, USA) and were used for labeling MKs. Siglec-H-PE and purified anti-mouse BST2 (CD317) were used to label pDCs (Biolegend, San Diego, USA). Ultra-LEAF™ purified anti-mouse IFNAR-1 purchased from Biolegend (San Diego, USA) was used for labeling IFN-α receptor. Both Cleaved Caspase-3 and BAK, purchased from Cell Signaling (Massachusetts, USA), were used for marking apoptotic MKs. Secondary antibodies goat anti-rat Alexa Fluor 647, goat anti-rabbit Alexa Fluor 488 and 647, and Hoechst 33342 were all bought from Thermo Fisher Scientific (Massachusetts, USA).

## **2.3 Measurement of Platelets**

### **2.3.1 Platelets measurement**

Mice were anesthetized first with 5.0 Vol. % Isoflurane (cp-pharma, Burgdorf, Germany) and 0.25 l/l oxygen. After, one dose of the anesthesia mix (MMF) composed by 90 µl Midazolam (5 mg/kg body weight, B.Braun, Melsungen, Hessen, Germany), 15 µl Medetomidine (0.5 mg/kg body weight, Zoetis, Germany) and 90 µl Fentanyl (0.05 mg/kg body weight, Albrecht GmbH, Aulendorf, Germany), was injected peritoneal. Once the mouse was under deep anesthesia, the blood was drawn from the heart percutaneously between the first rib and the second rib by a syringe containing 100 µl of anticoagulant solution (Sartedt Monovette, Wuppertal, Germany) with a 26 G needle. Then, the mouse was sacrificed by cervical dislocation and the bones were harvested for further analysis. Platelets were counted by the blood reader XN-1000 Pure instrument (Sysmex Europe GmbH, Nordestedt, Germany).

### 2.3.2 Consecutive platelets measurement

Mouse was placed in one restrainer where the tail was exposed outside to get access to the vessels. The tail venous blood was collected through a catheter filled with 10ul of anticoagulant solution (Sartedt Monovette, Wuppertal, Germany) connected by a 1 ml syringe. Platelets were counted by using the XN-1000 Pure system (Sysmex Europe GmbH, Nordestedt, Germany).

### 2.4 Whole-mount immunofluorescence staining and imaging

As previous described, mouse was anesthetized with Isoflurane and one dose intraperitoneal injection of MMF. After collecting the blood, mice were sacrificed by cervical dislocation. Then, humeri, femora, sternums and tibias were isolated and fixed in 4% paraformaldehyde (PFA) for 30 min at room temperature (RT). After fixation the bones were incubated with 30% Sucrose solution 24 h at 4°C. At the following day, the bones were put in Tissue-Tek® Cryomold filled with O.C.T. (Staufen, Germany) and frozen at -80 °C. The frozen bones with O.C.T were sliced on Histo Serve NX70 cryostat (Celle, Germany) to expose the maximal bone marrow area. Later, the bones were gently removed from the O.C.T. and carefully washed with 1×PBS. Next, they were incubated in 4 % PFA for 15min RT. Then after washed with 1×PBS, they were incubated in 0.5 % Triton X-100 (Sigma-Alrich, Saint Louis, MO, USA) solution diluted with 1×PBS for 45 min RT for permeabilization. After permeabilization, the cut bones were washed again within 1×PBS and then incubated in 10% Normal Goat Serum (NGS, Thermo Fisher Scientific, Massachusetts, USA) for 2 h RT for blocking. Next, the primary antibodies were added into the blocking solution with the bones for 24 h in 4 °C. After the incubation with the primary antibodies, the bones were washed with 1x PBS, and the secondary antibodies were added for 2 h RT. For the labeling of MKs and MKPs, CD41-FITC or CD41-PE were used with the dilution of 1:100. MKPs were

recognized as small (diameter < 15  $\mu\text{m}$ ), round and mononuclear CD41<sup>+</sup> cells, and MKs were identified as CD41<sup>+</sup> multinucleated cells with a diameter more than 15  $\mu\text{m}$ . Primary antibody anti-BST2 diluted in 1:100 and second antibody goat anti-rat Alexa Fluor (AF) 647 diluted in 1:100 was used for labeling the pDCs. Primary antibody Cleaved Caspase-3 or BAK diluted in 1:200 and second antibody goat anti-rabbit AF 488 diluted in 1:100 was used to mark the apoptotic MKs. Primary antibody IFNAR-1 diluted in 1:100 and second antibody goat anti-mouse AF 647 diluted in 1:100 was used to label the IFN- $\alpha$  receptor. Hoechst 33342 (1:1000 dilution) was used for labeling the nucleus. After staining, the bone was embedded in the custom-built ring filled with plasticine and then a glass slide was glued to fix the bones and make the exposed surface of the bone marrow attach to the glass slide tightly (Figure 9).



**Figure 9 Model of the whole-mount staining of the tibial bone marrow in mice.** The tibia was fixed in the ring that was full of plasticine under the glass slide.

Next, the bone marrow was imaging with a LSM 880 confocal microscopy using the Airyscan module, objective Plan-Apo 20x Objective NA, 0.8 or with 63x/1.46 oil Plan-Apo. Images were taken with step size of 2  $\mu\text{m}$ , range in z-stack of 40  $\mu\text{m}$ , and analyzed with Zen Blue software. 3D projections and rendering were done with Imaris 8.4.2 (Bitplane) software.

## 2.5 Calvarium bone marrow intravital imaging by Two-Photon microscopy

Multiphoton intravital imaging of the calvarium bone was performed using anesthetized mouse under MMF mix as described above. In short, the anesthetized mouse was placed on a warming pad and the hair over the skull was shaved by the hairclippers and further cleaned by depilatory cream. Then, the middle part of skull was exposed by cutting and clearing the skin and membranes. Later, the exposed skull was fixed tightly by a ring which was glued directly to the skull bone to maintaining immobility. The ring was filled with ultrasonic gel for the imaging. Half dose of the MMF was injected i.p. each 35 min to keep the mouse be under narcosis during the imaging process. The mouse calvarium was imaged by using a multiphoton TrimScope II LaVision Biotech (Bielefeld, Germany) system connected to an upright Olympus microscope. The microscope is equipped with a tunable laser with the range of 700-1080 nm (Ti:Sa Chameleon Ultra II laser). An objective 16x water immersion (numerical aperture 0.8, Nikon) was used. 3D- time series images were recorded within 30-40  $\mu\text{m}$  depth, with step size of 2  $\mu\text{m}$  and a frame rate of 1 min. The excitation wavelength 840 nm was used. The emitted signal was detected by Photomultipliers (G6780-20, Hamamatsu Photonics, Hamamatsu, Japan). ImSpector Pro (LaVision) software was used for imaging acquisition. Imaging was performed at 37 °C using a customized incubator. Blood vessels were visualized by i.v. injection of Dextran Cascade Blue 10.000 MW (D1976, ThermoFisher Scientific) before imaging. *vWF-eGFP* mouse was used to visualize the megakaryocytic lineage and pDCs were labeled with anti-SiglecH-PE antibody (Biolegend) injected intravenously 20 min before imaging (20  $\mu\text{l}$  diluted with 100  $\mu\text{l}$  NaCl). After imaging, the mouse was put to death by cervical dislocation.

## **2.6 Image processing**

The 3D-time series videos, 3D rendering images and cell speeds were analyzed with Imaris software version 8.4.2 (Bitplane). Other measurements as the numbers of MKs, MKPs and pDCs were counted using ZEN software (Carl Zeiss).

## **2.7 Isolation of bone marrow cells**

All bones including the humeri, femora, sternums, tibiae, and spines were collected from the sacrificed mice and were transferred into sterile ice-cold PBS. The bones were first washed shortly with 70 % ethanol, rinsed with sterile ice-cold 1xPBS on a clean bench. Later, for the long bones containing femoras, tibiae and humeri, the two ends' bones were cut by using a blade (Feather, Osaka, Japan). Then, a 26-Gauge needle connected to a syringe with 1x PBS + 2 % fetal calf serum (FCS) was used to flush the bone marrow until the bones were empty. For the other bones containing sternums, ilia and spines were grinded by a syringe to squeeze all the bone marrow out. The liquid containing bone marrow was put into a sterile dish and then resuspended by passing through inside a 20-Gauge needle several times. Afterwards, the resuspension was passed through the 70  $\mu\text{m}$  cell filter (Miltenyl Bioec GmbH, Bergisch Gladbach, Germany) to reach a cleaner cell solution. The solution was centrifuged 4°C at 350xg for 5 min. After centrifugation, the supernatant was discarded and the pellet was resuspended with 1 ml Dulbecco's Modified Eagle's Medium (DMEM, Thermo Fisher Scientific, Massachusetts, USA).

## **2.8 Megakaryocyte colony forming unit (CFU-MK) assay**

The isolated BM cells were counted manually by using Neubauer counting chamber. After counting, the total number of  $2.2 \times 10^6$  cells were needed. Next, 0.3 ml IMDM, 1.2 ml Collagen Solution (STEMCELL Technologies, Cologne, Germany) and  $1 \times 10^5$  cells

were added into each tube of MegaCult™-C medium (STEMCELL Technologies, Cologne, Germany). 6 tubes with the prepared medium were divided into 6 groups, and different cytokines were added into the groups. 50 ng/ml recombinant murine (rm) TPO was added into group 1, 50 ng/ml rm TPO + 5 U/ml IFN- $\alpha$ , (PBL Assay Science, Piscataway, USA) were added into group 2, 50 ng/ml rm TPO + 10 U/ml IFN- $\alpha$  were added into group 3, 50 ng/ml rm TPO + 100 U/ml IFN- $\alpha$  were added into group 4, 50 ng/ml rm TPO + 500 U/ml IFN- $\alpha$  were added into group 5 and 50 ng/ml rm TPO + 1000 U/ml IFN- $\alpha$  were added into group 6. Then all the medium with cytokines were mixed into the tubes with the medium and placed into 6-well plate (Corning Costar, Sigma-Aldrich, Saint Louis, MO, USA) gently avoiding the bubbles. Each group was equally divided into two wells of the 6-well plate. The plates were put into the incubator at a constant air humidity (95 %) and temperature (37 °C) as well as a stable concentration of CO<sub>2</sub> (5 %) for culturing 7 days.

## **2.9 Megakaryocyte colony staining and imaging**

According to the protocol of MK colony staining, staining reagents containing 0.1 M sodium phosphate buffer, 0.1 M sodium citrate solution, 30 mM copper sulfate solution and 5 mM potassium ferricyanide solution were prepared. 10 mg of acetylthiocholine iodide (Sigma-Aldrich, Saint Louis, MO, USA) was added into 0.1 M sodium phosphate buffer to prepare the acetylthiocholonioidide solution. Then 0.1 M sodium citrate solution 1 ml, 30 mM copper sulfate solution 2 ml and 5 mM potassium ferricyanide solution 2 ml were successively added into the acetylthiocholonioidide solution with continuous stirring to prepare the staining solution. MK-colony samples were placed on the sterile bench, and the mediums were discarded to expose the gel. Ice-cold acetone was gently added on the top of the gel for 15 min to fix the samples and simultaneously, the samples were placed on ice. Later, the acetone was gently removed and let evaporated for 10 min. Then, 1 ml of the staining solution was put into each well of the 6-well plate of MK-colony samples and the samples were placed in

dark at least for 8 h. Axiozoom v16 microscope (ZEISS, Oberkochen, Germany) connected to ZEN microscope software (ZEISS, Oberkochen, Germany) was used to perform the MK-colony samples imaging at a magnification of 16.8x with TL bright field channel.

## **2.10 Statistics**

The statistical analysis was performed by using the GraphPad Prism software (San Diego, USA). Before performing statistical analysis, F test was used for ensuring the data with equal variances, and Student's unpaired t-test was used to compare the two groups; if not, when the variances were obviously different, unpaired t-test with Welch's correction was used. One-way ANOVA was used to compare multiple groups for univariate analysis, and Dunnett's multiple comparisons test was used; While two-way ANOVA was used to compare multiple groups for double factor analysis, and Sidak's multiple comparisons test was used. Error bar indicates standard error of the mean (SEM). P value less than 0.05 was considered significant.

### 3 Results

#### 3.1 The regulation of pDCs on megakaryopoiesis in the steady state

##### 3.1.1 Interaction between pDCs and MKs in the steady state

###### 3.1.1.1 Observation of the interaction between pDCs and MKs by bone marrow whole-mount immunostaining

First, we investigated if pDCs can detect MKs, especially apoptotic MKs. We used bone marrow whole-mount immunostaining of *PF4-Cre<sup>+</sup> × Rosa26-iDTR* mice compared with *PF4-Cre<sup>-</sup> × Rosa26-iDTR* mice to characterize pDC-MK interactions. Since after injection of diphtheria toxin (DT) for 24 hours, MKs are going to be depleted, we could use this mouse model as MK apoptosis model. For the control group, we use the same amount of DT treatment on the *PF4-Cre<sup>-</sup> × Rosa26-iDTR* mice where the MKs are not depleted. After DT treatment, we isolated the femurs from the respective mice, and performed the whole-mount immunostaining. We used anti-CD41 antibodies to label MKs, anti-cleaved caspase 3 antibodies to label apoptotic MKs, anti-BST2 antibodies to label pDCs, and Hoechst to label the nucleus. After staining, we performed the imaging of the bone marrow by using confocal microscope. We found that pDCs were interacting with mature MKs (big and multinucleate MKs) and with apoptotic MKs (Figure 10). After quantification, we found that slight decrease of pDCs and significant decrease of MKs in the MK apoptotic group compared with control group (Figure 11), but the percent of apoptotic MKs (apoptotic MKs/total MKs) increased in MK apoptotic group compared with control group demonstrating the efficiency of the *PF4-Cre<sup>+</sup> × Rosa26-iDTR* mice as MK apoptotic model (Figure 12). Besides, we also found that there were more interactions between pDCs and MKs in MK apoptotic group (Figure 13), further indicating that pDCs are capable of detecting apoptotic MKs.

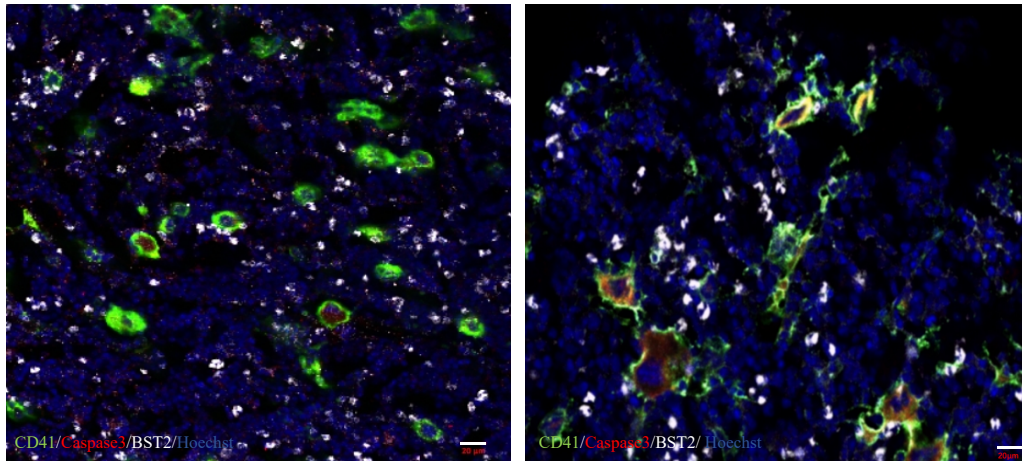


**Figure 10** Representative whole-mount staining images of pDC-MK interactions in control (left) and MK apoptotic (right) groups. 24 hours after DT treatment of *PF4-Cre* × *Rosa26-iDTR* and *PF4-Cre*<sup>+</sup> × *Rosa26-iDTR* mice were included in control group and MK apoptotic group respectively. CD41 labeled MKs, CD41 and cleaved caspase 3 double labeled apoptotic MKs, BST2 labeled pDCs, Hoechst labeled nucleus. Scale bar= 20 µm.

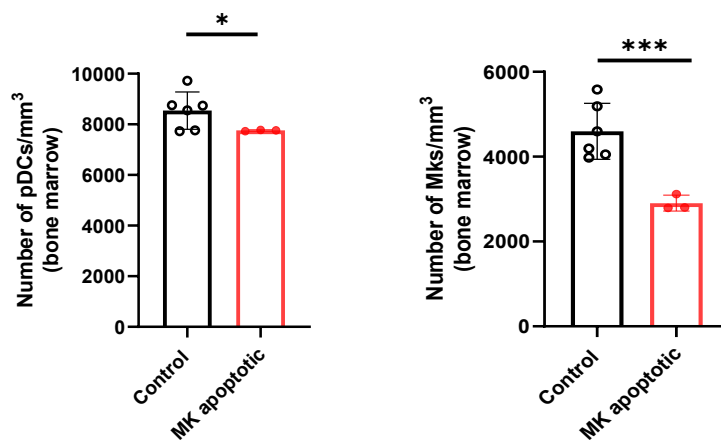


**Figure 11** Quantification of pDC and MK numbers under MK apoptotic conditions. Number of pDCs (left) and MKs (right) in control group and MK apoptotic group. n= 6 in control group; n= 3 in MK apoptotic group. Unpaired t-test with Welch's correction; Error bar= SEM. P= 0.0487 for pDC comparison; P= 0.0009 for MK comparison.

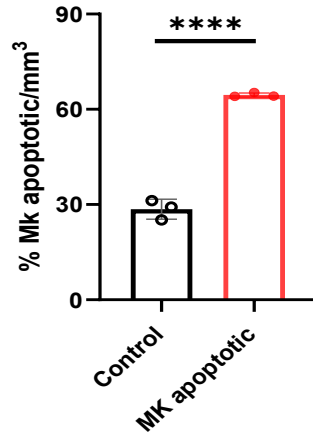


**Figure 12 MK apoptotic quantification.** Percent of apoptotic MKs in control group and MK apoptotic group. n= 3 mice. Unpaired t-test; Error bar= SEM. P< 0.001.

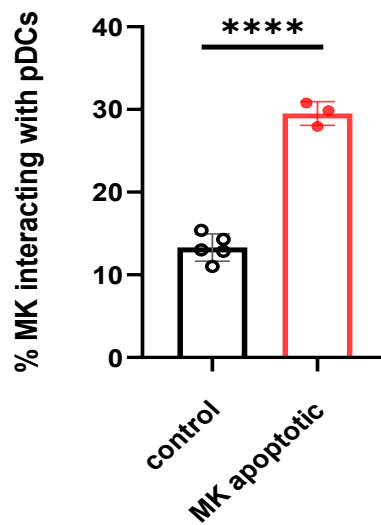


**Figure 13 Quantification of pDC interacting with MK in the bone marrow.** Percent of MK interacting with pDCs in control group and MK apoptotic group. n= 5 in control group; n= 3 in MK apoptotic group. Unpaired t-test with Welch's correction; Error bar= SEM. P< 0.001.

### 3.1.1.2 Observation of the dynamic interaction between pDCs and MKs *in vivo*

To analyze the dynamic interaction between pDCs and MKs *in vivo*, we performed intravital calvarial bone marrow imaging by two-photon microscopy. We used *PF4-Cre<sup>-</sup> × Rosa26-iDTR × vWF-eGFP* mice as control group and *PF4-Cre<sup>+</sup> × Rosa26-iDTR × vWF-eGFP* mice as MK apoptotic group. After injection DT 24 hours for each group, we injected anti-Siglec-H-PE antibodies to label the pDCs, and MKs were marked by vWF-eGFP. We clearly observed the dynamic interaction between pDCs and MKs in the calvarial bone marrow shown by two-photon microscopy (Figure 14). By tracing the single pDC which is interacting with MKs in the MK apoptotic group, we found that some pDCs were interacting on the surface of MKs (Figure 15), and some pDCs were diving into the bodies of MKs (Figure 16). We also observed that pDCs moved faster in MK apoptotic group compared with control group. To verifying this phenomenon, we used the Imaris software to create a 3D rendered image of the calvarial bone marrow imaging, for tracking the pDCs interacting with MKs (Figure 17) and for the pDC speed calculation (Figure 18). The results show that pDCs move faster in the MK apoptotic group further suggesting that pDCs are adept in detecting apoptotic MKs in the bone marrow.

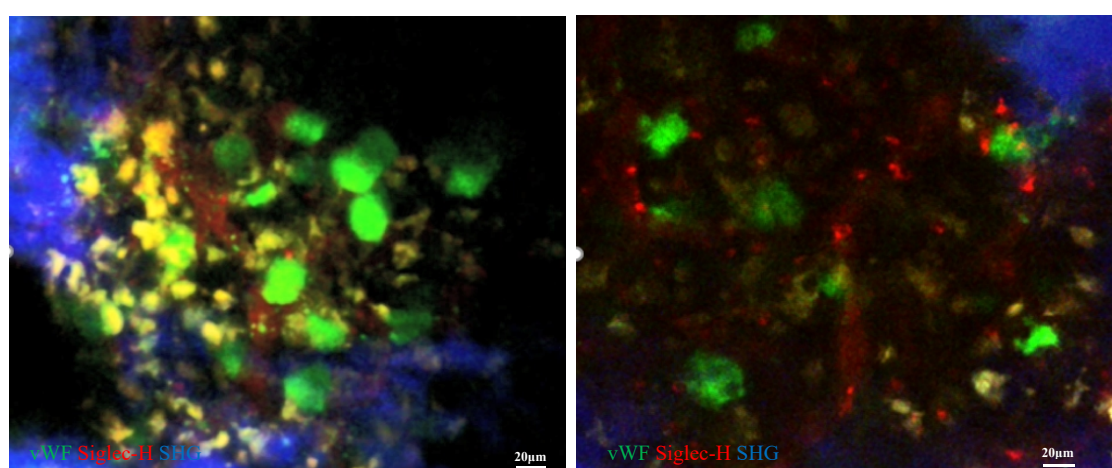


**Figure 14** Representative intravital calvarial bone marrow imaging in control group (left) and MK apoptotic group (right) by two-photon microscopy. vWF-eGFP labeled MKs, Siglec-H-PE labeled pDCs, SHG labeled bone structure shown by the blue signal. Scale bar

=20  $\mu\text{m}$

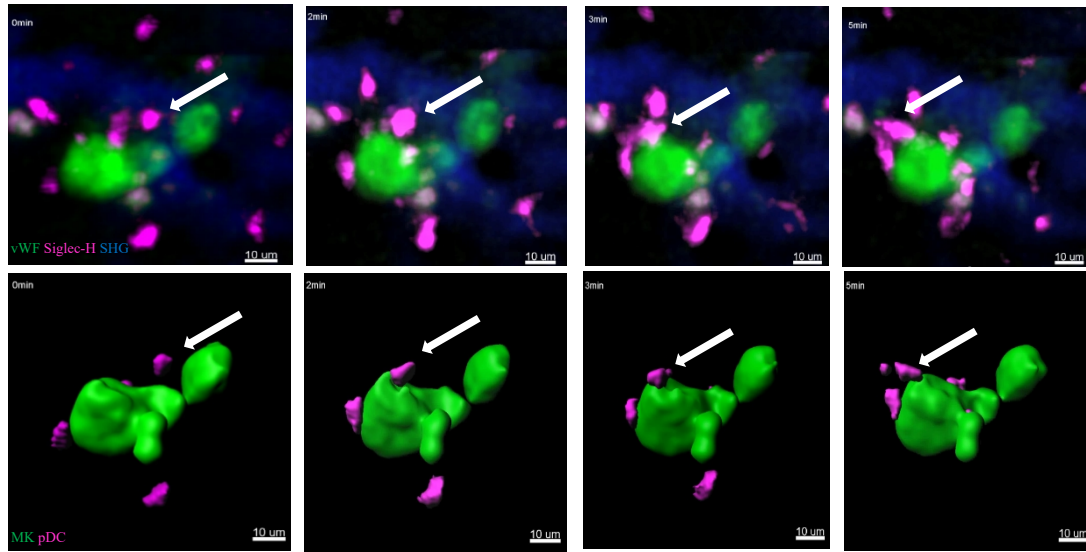


**Figure 15 Single pDC dynamical interaction with MK surface.** Arrow indicated the single pDC (pink). Upper, intravital calvarial bone marrow images, vWF-eGFP labeled MKs (green), Siglec-H-PE antibody labeled pDCs, SHG labeled bone structure in blue signal. Lower, 3D reconstructed images of the same pDC dynamical interaction with MK surface. The pDC was interacting with MK surface at 3 min and left at 5 min. Scale bar= 10  $\mu\text{m}$ .

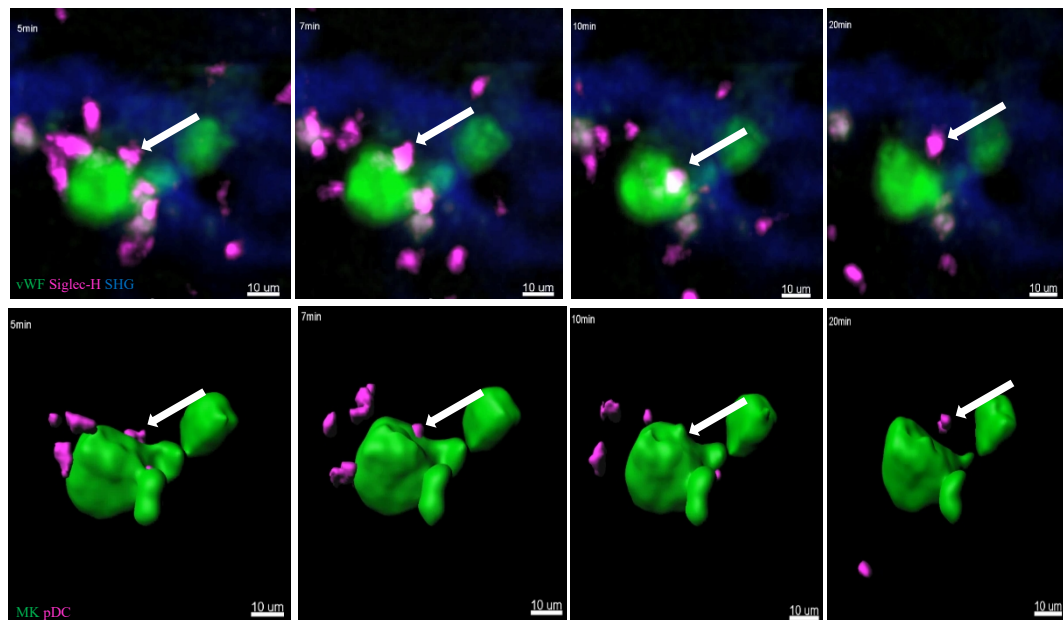


**Figure 16 Single pDC dynamical diving into MK body.** Arrow indicated the single pDC (pink). Upper, intravital calvarial bone marrow images, vWF-eGFP labeled MKs (green), Siglec-H-PE antibody labeled pDCs, SHG labeled bone structure (blue). Lower, 3D reconstructed

images of the same pDC diving into MK body. The pDC was interacting with MK surface at 5min, then was diving into the body of MK at 7 min and left at 20 min. Scale bar= 10  $\mu$ m.

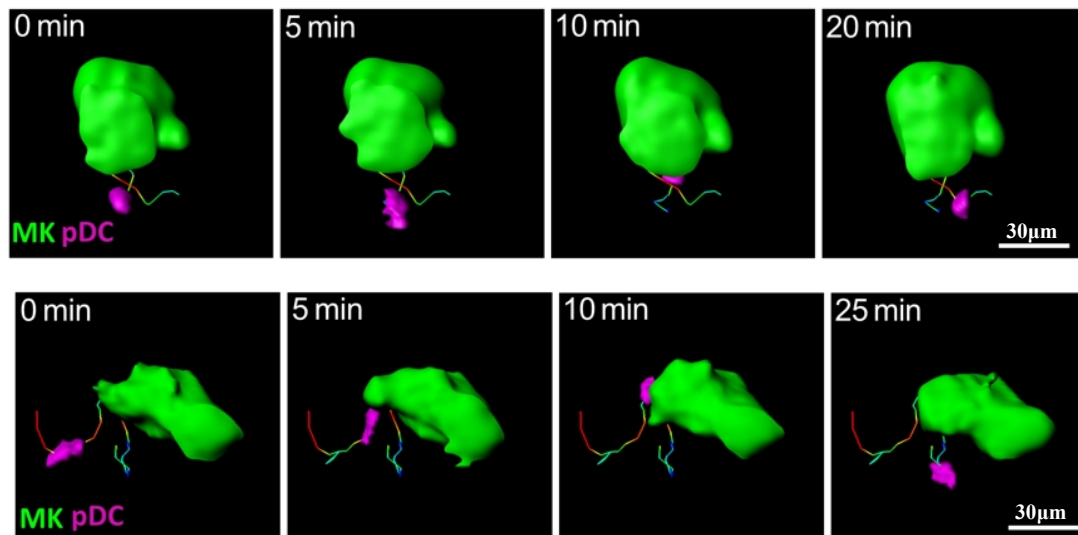


**Figure 17** 3D reconstructed images of single pDC dynamic interaction with MK in control group (upper) and MK apoptotic group (lower). Scale bar= 30  $\mu$ m.

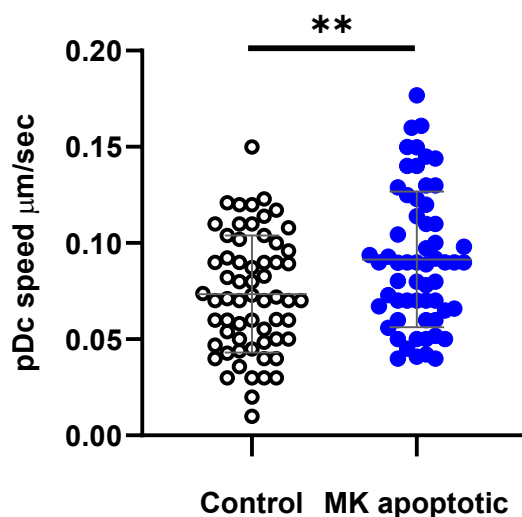


**Figure 18** Speed of each pDC processing the interaction with MKs in control group compared with MK apoptotic group. n= 62 in control group; n= 60 in MK apoptotic group.

Unpaired t-test; Error bar= SEM. P= 0.0029.

### 3.1.2 The impact of pDCs depletion on megakaryopoiesis in the steady state

In order to investigate if pDCs impact megakaryopoiesis *in vivo*, we used pDC depletion models. *BDCA2-iDTR* mice which specifically express DT receptor on pDCs treated with DT were recognized as pDC depletion group, and WT mice treated with DT were recognized as control group. After DT consecutive injections of 3 days for *BDCA2-iDTR* mice and WT mice, about 80 percent of pDCs were depleted in pDC group compared with control group (Figure 19).

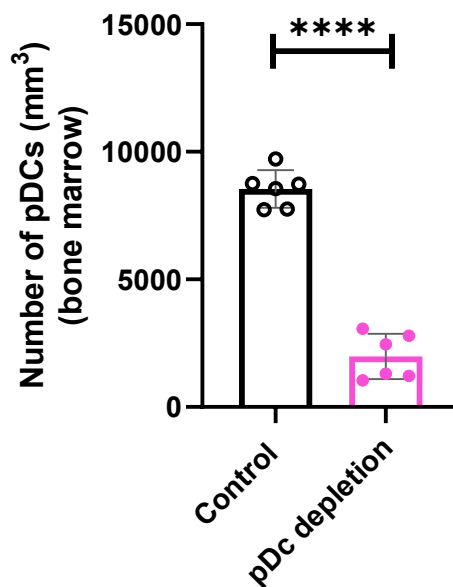


**Figure 19 pDC depletion in the bone marrow.** Number of pDCs in control group (n= 6 mice) and pDC depletion group (n= 6 mice). pDC number was quantified on whole-mount immunostaining. Unpaired t-test; Error bar= SEM. P< 0.001.

Then we collected the blood to measure the number of platelets and isolated the femurs to perform the whole-mount immunostaining in both control group and pDC depletion

group. The number of platelets decreased prominently in pDC depletion group compared with control group ((Figure 20). For the whole-mount immunostaining, we used anti-CD41 antibodies to label MKs, anti-BST2 antibodies to label pDCs and Hoechst to label the nucleus (Figure 21). Besides, we defined MKPs as small (diameter<15  $\mu\text{m}$ ), round and mononuclear CD41<sup>+</sup> cells, and MKs as CD41<sup>+</sup> multinucleated cells with a diameter more than 15  $\mu\text{m}$ . After quantifying the number of MKs and MKPs in each group, we observed that both cell types decreased in pDC depletion group compared with control group (Figure 22). All the data suggested that pDCs directly impact megakaryopoiesis, and consequently affect thrombopoiesis.

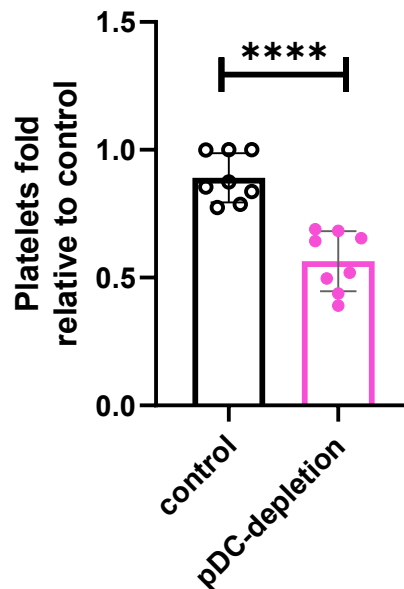


**Figure 20 Platelet quantification under pDC depletion conditions.** Platelets fold relative to control mice. Control mice (n= 6) and pDC depletion mice (n= 6). Unpaired t-test; Error bar= SEM. p< 0.001.

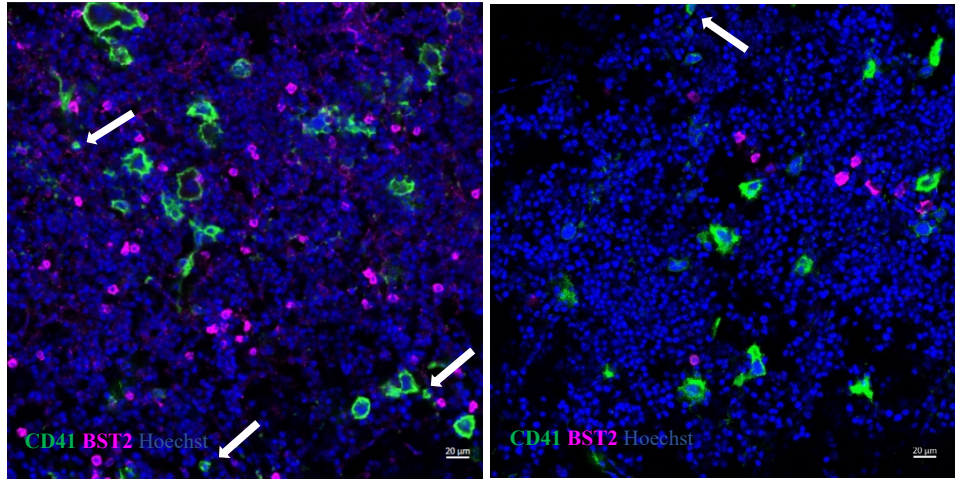


**Figure 21** Representative whole-mount immunostaining in control group (left) and pDC depletion group (right). CD41 labeled MKs, BST2 labeled pDCs, Hoechst labeled nucleus. MKPs were identified as small (diameter < 15 $\mu$ m), round and mononuclear CD41<sup>+</sup> cells. MKs were identified as CD41<sup>+</sup> multinucleated cells with a diameter more than 15  $\mu$ m. Arrows indicated MKPs. Scale bar= 20  $\mu$ m.

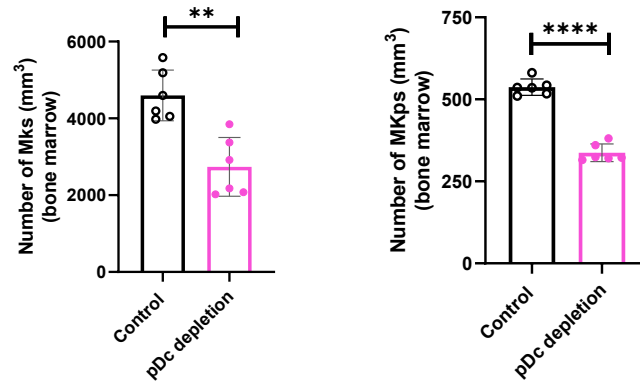


**Figure 22** MK and MKP quantifications under pDC depletion conditions. Number of MK and MKP in control group (n= 6 mice) and pDC depletion group (n= 6 mice). Unpaired t-test; Error bar=SEM. MK contrast (P= 0.0011); MKP contrast (P< 0.001).

## 3.2 The regulation of pDCs in megakaryopoiesis under thrombocytopenia

### 3.2.1 The interaction of pDCs with MKs under thrombocytopenia

We have demonstrated the role of pDCs in enhancing megakaryopoiesis at steady state. Next, we would like to investigate the role of pDCs in megakaryopoiesis under emergency thrombocytopenia. R300 injection into WT mice for 24 h was used to induce emergency thrombocytopenia. To investigate the interaction of pDCs with MKs under thrombocytopenia, we performed whole-mount immunostaining of bone marrow for WT mice (control group) and thrombocytopenia mice (platelet depletion group) (Figure 23). We used anti-CD41 antibodies to label MKs and anti-BST2 antibodies to label pDCs. After counting, we found there were more interactions in platelet depletion group compared with control group (Figure 24).

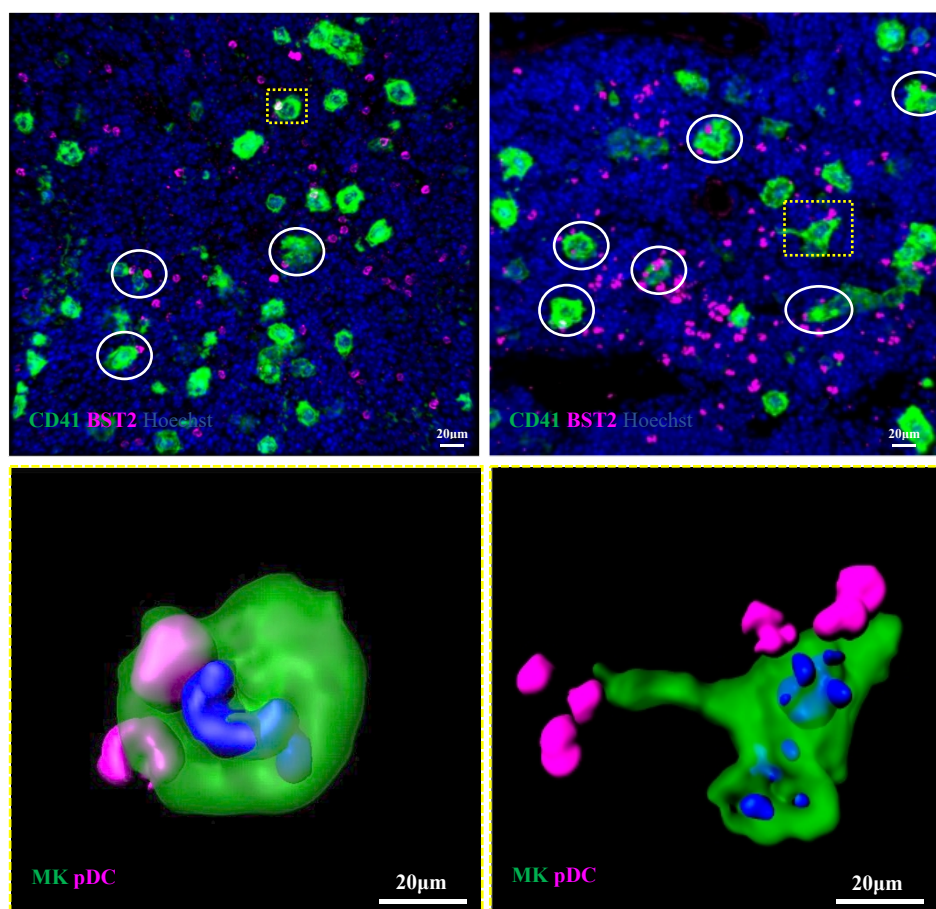
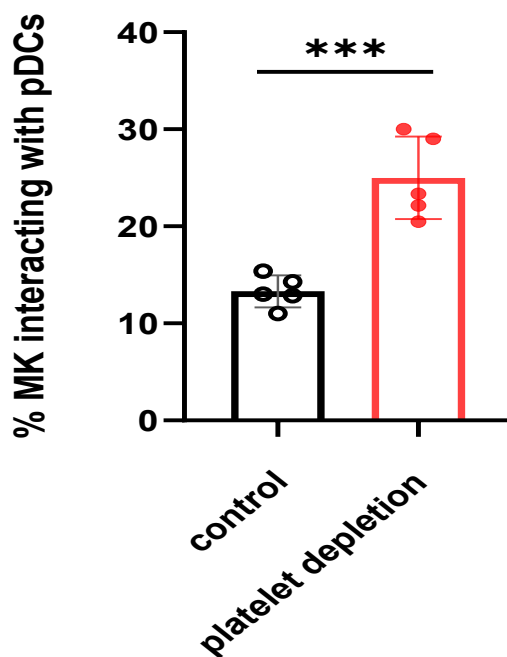


Figure 23 Representative bone marrow whole-mount immunostaining (upper) and 3D

reconstructed images (lower) in control group (left) and platelet depletion group (right). CD41 labeled MKs and MKPs (green), BST2 labeled pDCs (pink), Hoechst labeled nuclei (blue). Circles indicated interactions between MKs and pDCs. Scale bar= 20  $\mu$ m.



**Figure 24 MK-pDC interaction under thrombocytopenia.** Percent of MK interacting with pDCs in control group (n= 5) and platelet depletion group (n= 5). Unpaired t-test; Error bar= SEM. P= 0.004.

In addition, we performed intravital calvarial bone marrow imaging by two-photon microscopy using the *vWF-eGFP* mice after R300 injection 24 hours. MK was labeled with vWF-eGFP and pDC was labeled with anti-siglecH-PE antibodies (Figure 25). The speed of single pDC interacting with MKs was calculated by tracing the tract of the single pDC through 3D reconstructed images (Figure 26). We found that pDCs migrate faster in the platelet depletion mice compared with WT mice (Figure 27) demonstrating that pDCs had more activity under thrombocytopenia.

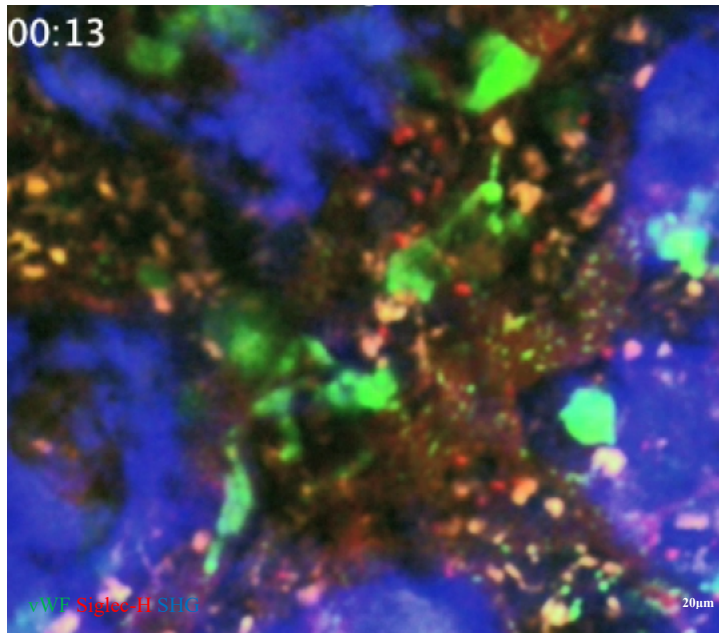


**Figure 25** Representative intravital calvarial bone marrow imaging in platelet depleted mice by two-photon microscopy. vWF-eGFP labeled MKs, Siglec-H-PE labeled pDCs, SHG labeled bone structure in blue signal. Scale bar= 20  $\mu$ m.

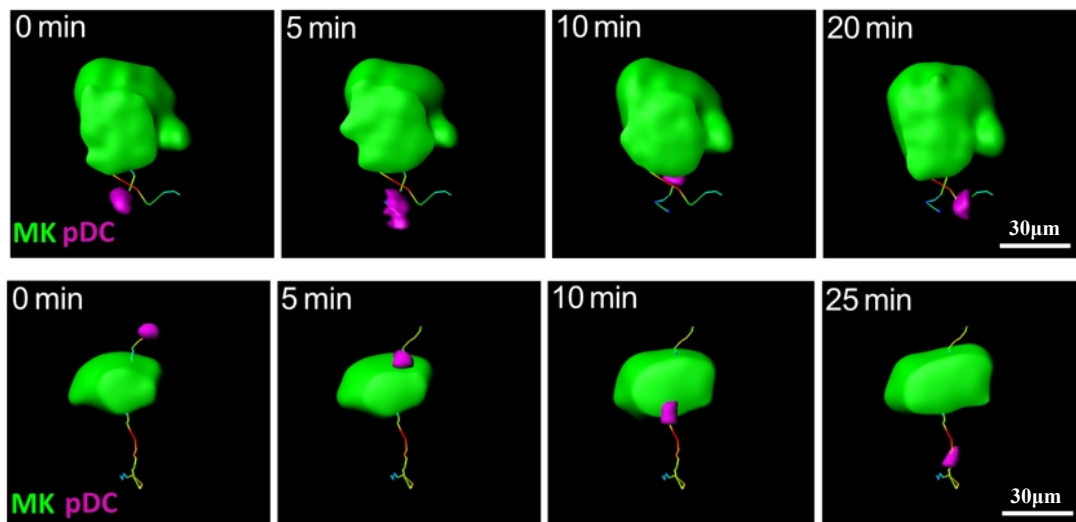


**Figure 26** 3D reconstructed images of single pDC dynamic interaction with MK in control group (upper) and platelet depletion group (lower). Scale bar= 30  $\mu$ m.

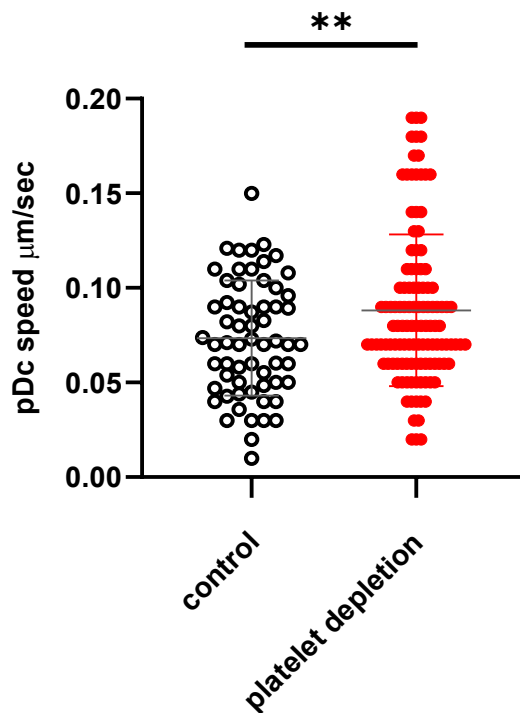


**Figure 27 Speed of each pDC interacting with MKs in control group compared with platelet depletion group.** n= 62 in control group; n= 98 in platelet depletion group. Unpaired t-test with Welch’s correction; Error bar= SEM. P= 0.0064.

### 3.2.2 Apoptotic MK numbers under thrombocytopenia

Platelet production involves the exhaustion of MKs by producing cytoplasmic extension denominate proplatelets. This MK consumption leads to MK death as shown in Figure 28 and Figure 29, where under thrombocytopenia conditions the number of apoptotic MKs increased. We used anti-CD41 antibodies to label MKs and anti-BST2 antibodies to label pDCs, apoptotic MKs were double marked by anti-BAK antibodies which are used for labeling apoptotic cells [127,128] and anti-CD41 antibodies. After quantifying the number of apoptotic MKs, results showed that there were more apoptotic MKs and more interactions between pDCs and apoptotic MKs in platelet depletion mice (Figure 30).

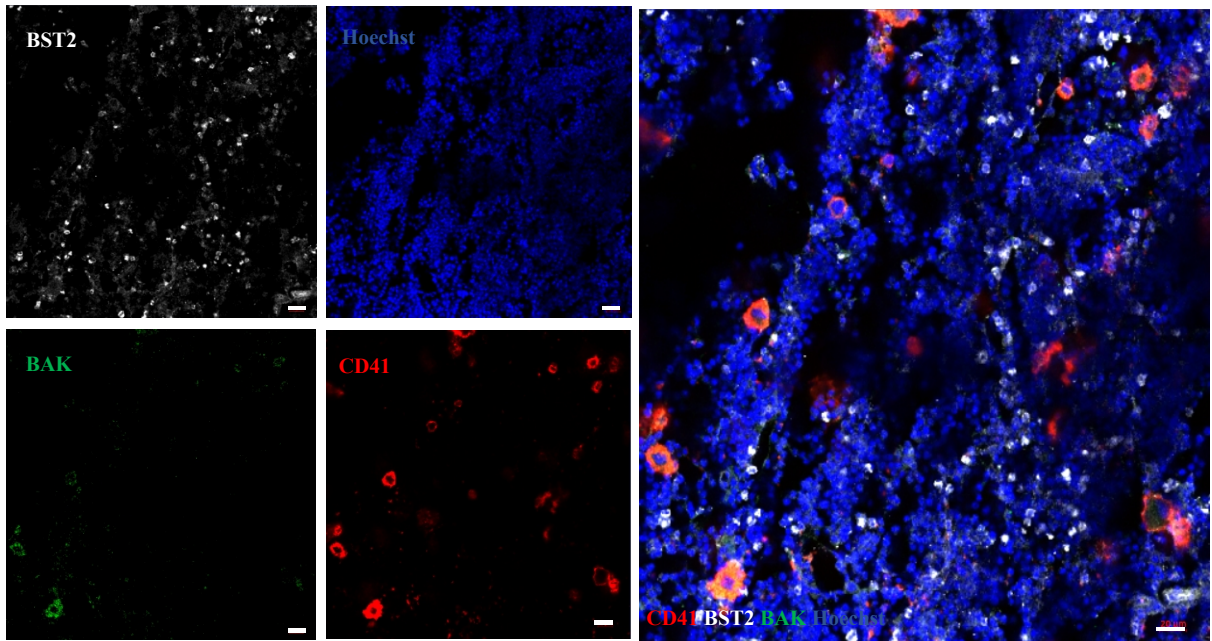


**Figure 28 Representative whole-mount staining images in control group.** CD41 labeled MKs, CD41 and BAK double labeled apoptotic MKs, BST2 labeled pDCs, Hoechst labeled nucleus. Scale bar= 20  $\mu$ m.

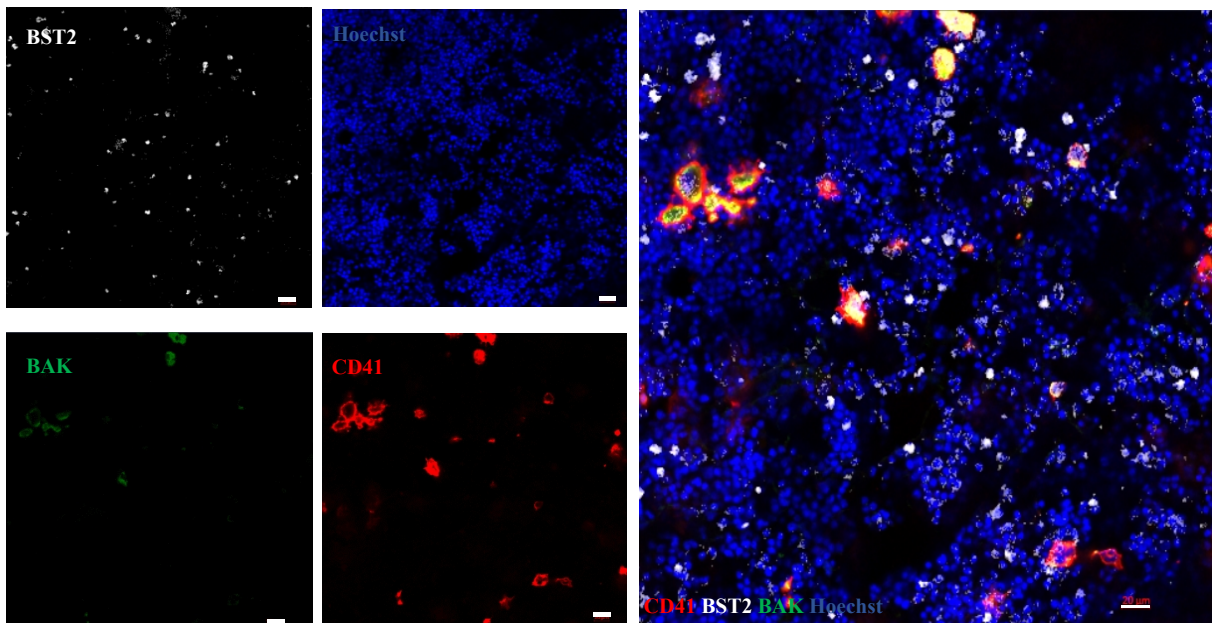


**Figure 29 Representative whole-mount staining images in thrombocytopenia group.** CD41 labeled MKs, CD41 and BAK double labeled apoptotic MKs, BST2 labeled pDCs, Hoechst labeled nucleus. Scale bar= 20  $\mu$ m.

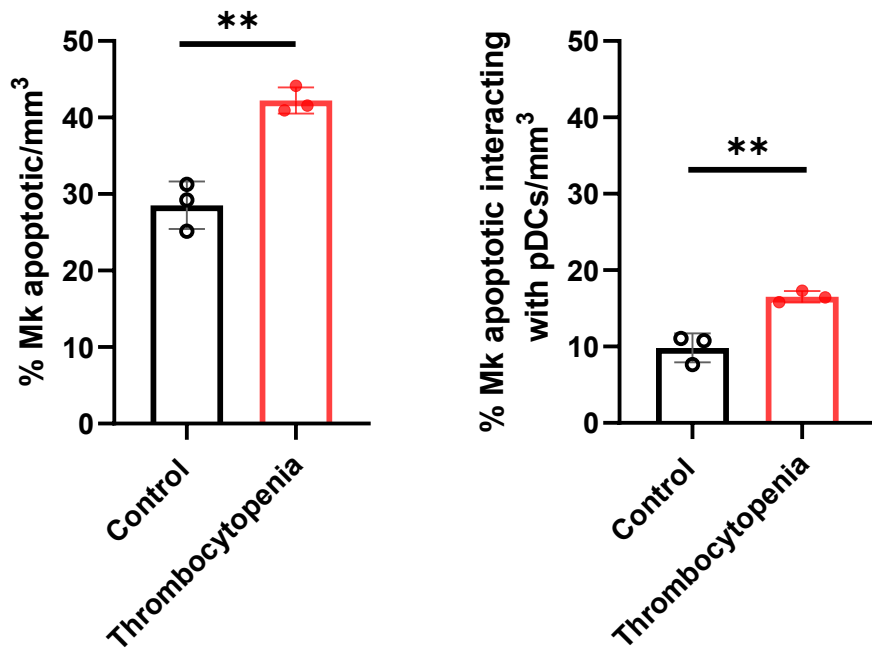


**Figure 30 MK apoptotic quantification under thrombocytopenia.** Percent of apoptotic MKs in control and thrombocytopenia group (left, n= 3). Percent of apoptotic MKs interacting with pDCs in control group and thrombocytopenia group (right, n= 3). Unpaired t-test; Error bar= SEM. P= 0.0026 for percent of apoptotic MKs; P= 0.0047 for percent of apoptotic MKs interacting with pDCs.

### 3.2.3 The impact of pDCs absence on megakaryopoiesis under thrombocytopenia

In order to investigate if pDCs impact megakaryopoiesis under thrombocytopenia, we performed pDC depletion mice under emergency thrombocytopenia. We treated WT (control) and WT (treated for pDC depletion with PDCA-1 antibodies) mice with the R300 antibodies for platelet depletion for 24 h. The peripheral blood was analyzed for platelets numbers before injection, and after injection 1 day, 2 days, 4 days, 6 days, 8 days, 9 days, 10 days and 13 days. WT mice recovered the platelets count after R300 injection at Day 8, while pDC depletion mice recovered the platelets count at Day 10 (Figure 31) illuminating that absence of pDCs delayed the recovery of platelets.

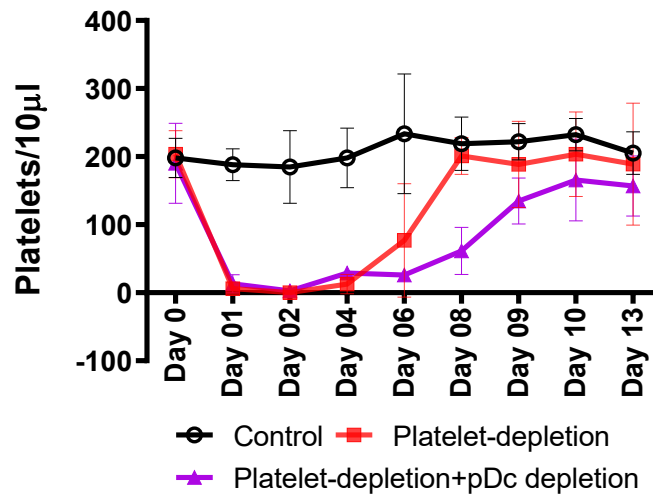


**Figure 31 Platelets recovery under emergency thrombocytopenia.** Numbers of peripheral blood platelet in control mice (n= 3), platelet depleted mice (n= 3) and pDC-platelet depleted mice (n= 3). R300 was injected for WT mice and WT mice treated with PDCA-1 antibodies to reach the thrombocytopenia condition. Two-way ANOVA, Sidak's multiple comparisons test; Error bar=SEM. Contrast to control: Day 0 (P= 0.9884 in platelet-depletion; P= 0.9741 in platelet-depletion + pDC depletion); Day 1 (P< 0.001 in platelet-depletion; P< 0.001 in platelet-depletion + pDC depletion); Day 2 (P< 0.001 in platelet-depletion; P< 0.001 in platelet-depletion + pDC depletion); Day 4 (P< 0.001 in platelet-depletion; P< 0.001 in platelet-depletion + pDC depletion); Day 6 (P= 0.002 in platelet-depletion; P< 0.001 in platelet-depletion + pDC depletion); Day 8 (P= 0.8759 in platelet-depletion; P= 0.002 in platelet-depletion + pDC depletion); Day 9 (P= 0.6313 in platelet-depletion; P= 0.0534 in platelet-depletion + pDC depletion); Day 10 (P= 0.7102 in platelet-depletion; P= 0.1734 in platelet-depletion + pDC depletion); Day 13 (P= 0.8966 in platelet-depletion; P= 0.3914 in platelet-depletion + pDC depletion).

Next, we did bone marrow whole-mount immunostaining in platelet depleted and pDC-platelet depleted mice and quantified the numbers of pDCs, MKs and MKPs (Figure 32). We used anti-CD41 antibodies to label MKs and MKPs, anti-BST2 antibodies to label pDCs and Hoechst to label the nucleus. MKP were identified as small (diameter< 15 µm), round and mononuclear CD41<sup>+</sup> cells. MKs were identified as CD41<sup>+</sup> multinucleated cells with a diameter more than 15 µm. We found a slight increase (not statistically significant) of MK counts and significant increase of MKP counts in platelet depletion mice compared with WT mice (control). However, there were less MKs and MKPs in pDC-platelet depleted mice compared with platelet depleted mice

(Figure 33) suggesting that pDCs are crucial for maintenance of MK and MKP numbers under thrombocytopenia conditions.

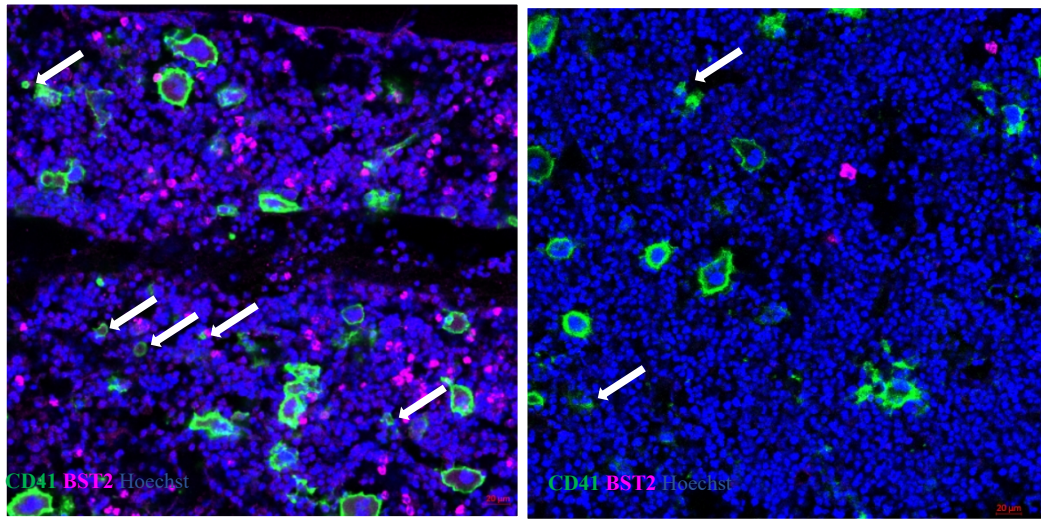


**Figure 32 Representative whole-mount staining images in platelet depletion mice (left) and platelet depletion + pDC depletion mice (right).** CD41 labeled MKs and MKPs, BST2 labeled pDCs, Hoechst labeled nucleus. MKP was identified as small (diameter < 15 μm), round and mononuclear CD41<sup>+</sup> cells. MKs were identified as CD41<sup>+</sup> multinucleated cells with a diameter more than 15 μm. Arrows indicated MKPs. Scale bar= 20 μm.

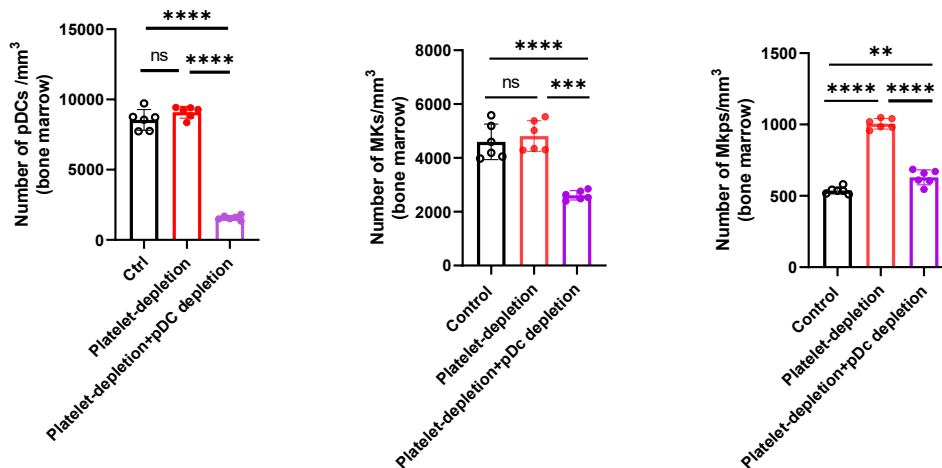


**Figure 33 pDC, MK and MKP quantifications under thrombocytopenia.** The numbers of pDC, MK and MKP in control group (n= 6), platelet depletion group (n= 6) and platelet depletion + pDC depletion group (n= 6). Unpaired t-test; Error bar= SEM. For pDC comparison (P= 0.1458 for comparing control with platelet depletion group; P< 0.001 for comparing control

with platelet depletion + pDC depletion group;  $P < 0.001$  for comparing platelet depletion with platelet depletion + pDC depletion group). For MK comparison ( $P = 0.5612$  for comparing control with platelet depletion group;  $P < 0.001$  for comparing control with platelet depletion + pDC depletion group;  $P = 0.0005$  for comparing platelet depletion with platelet depletion + pDC depletion group); For MKP comparison ( $P < 0.001$  for comparing control with platelet depletion group;  $P = 0.0030$  for comparing control with platelet depletion + pDC depletion group;  $P < 0.001$  for comparing platelet depletion with platelet depletion + pDC depletion group).

### 3.3 The impact of IFN- $\alpha$ on megakaryopoiesis

#### 3.3.1 The impact of IFN- $\alpha$ on megakaryopoiesis *in vivo*

The previous results revealed that pDCs can promote megakaryopoiesis both in the steady state and under thrombocytopenia, next we would like to explore the mechanism involved in this process. As described before, the main function of pDCs is producing IFN- $\alpha$ , and the question arise here is if IFN could promote MK development in the bone marrow. To answer this question, primarily, we performed experiments in which wild-type mice were treated with universal type I interferon for 2 h, 4 h, and 24 h. After the treatments, we analyzed the changes of platelets, MKs and MKPs numbers. The blood profile showed that the platelet number of mice treated with IFN- $\alpha$  increased compared with untreated mice (Figure 34).

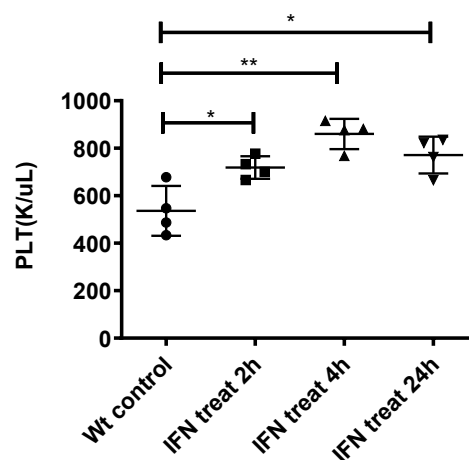


**Figure 34 Platelet numbers under interferon treatment.** The numbers of platelets in control and IFN- $\alpha$  treatment mice. 4 mice were included in control group and IFN- $\alpha$  treatment 2 h, 4 h

as well as 24 h group respectively. Unpaired t-test; Error bar= SEM. P= 0.0320 for IFN- $\alpha$  treatment 2 h compared with control; P= 0.0034 for IFN- $\alpha$  treatment 4 h compared with control; P= 0.0132 for IFN treatment 24 h compared with control.

The bone marrow whole-mount staining show more MKs and MKPs in mice with IFN- $\alpha$  treatment (especially IFN- $\alpha$  treatment 2h and 4h) than in IFN- $\alpha$  untreated mice (Figure 35, Figure 36) indicating that IFN- $\alpha$  can trigger fast and immediate megakaryopoiesis *in vivo*.

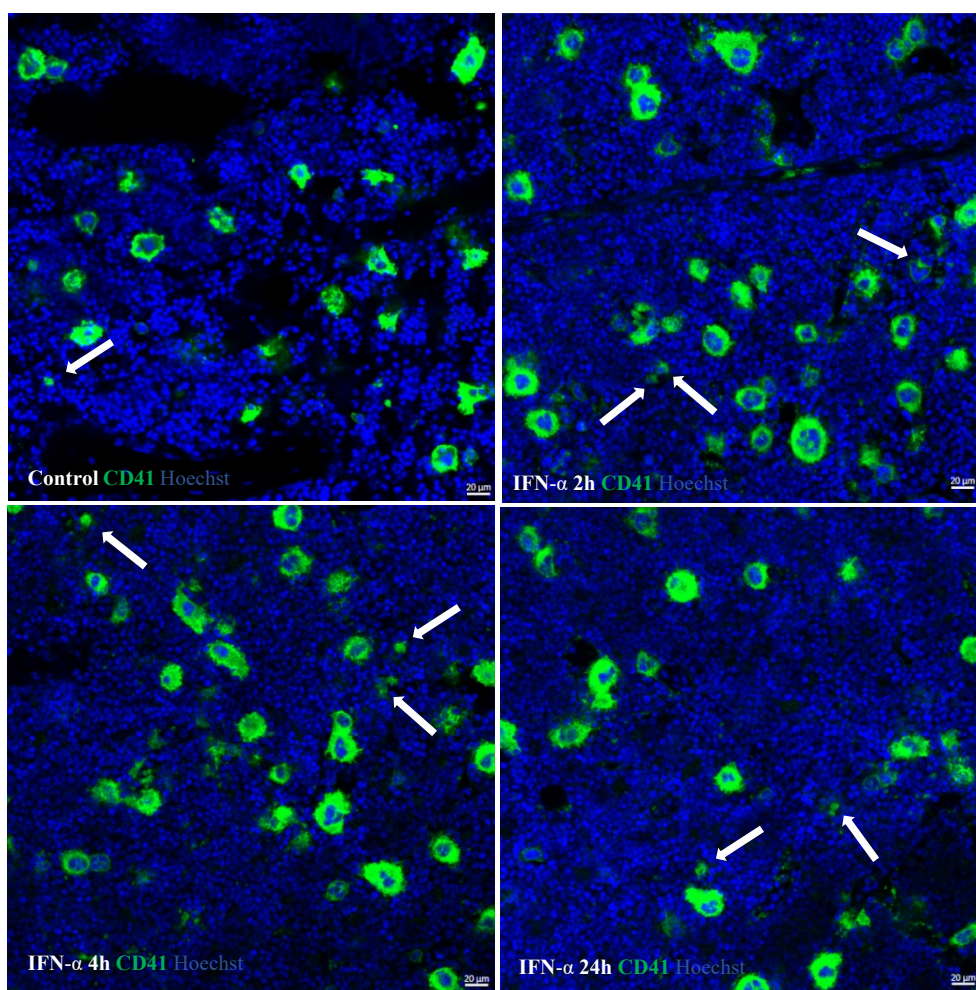


**Figure 35** Representative whole-mount immunostaining in control (upper-left), IFN- $\alpha$  treated 2 h (upper-right), IFN- $\alpha$  treated 4 h (lower-left) and IFN- $\alpha$  treated 24 h (lower-right) mice. CD41 labeled MKs and MKPs, Hoechst labeled nucleus. MKPs were identified as small (diameter < 15  $\mu$ m), round and mononuclear CD41<sup>+</sup> cells. MKs were identified as CD41<sup>+</sup> multinucleated cells with a diameter more than 15  $\mu$ m. Arrows indicated MKPs. Scale bar= 20  $\mu$ m.

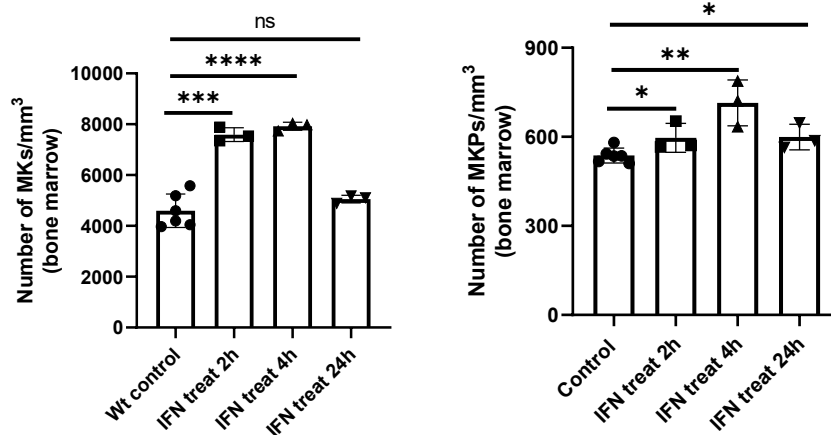


**Figure 36 MK and MKP quantifications under interferon treatment.** Number of MKs and MKPs in control group (n= 6 mice) and IFN- $\alpha$  treatment group (3 mice were included in IFN- $\alpha$  treatment 2 h, 4 h as well as 24 h group respectively). Unpaired t-test; Error bar= SEM. For MKs comparison: contrasted to control, P= 0.002 in IFN- $\alpha$  treatment 2 h; P< 0.01 in IFN- $\alpha$  treatment 4 h; P= 0.2854 in IFN- $\alpha$  treatment 24 h. For MKPs comparison: contrasted to control, P= 0.0401 in IFN- $\alpha$  treatment 2 h; P= 0.0010 in IFN- $\alpha$  treatment 4 h; P=0.0253 in IFN- $\alpha$  treatment 24 h.

### 3.3.2 Impact of IFN- $\alpha$ on megakaryopoiesis *in vitro*

To further analyze if IFN- $\alpha$  could enhance megakaryopoiesis, we performed MK colony forming unit (MK-CFU) assay. BM cells from vWF  $\times$  IFN $\alpha$ Rflox cre<sup>+</sup> mice (IFN $\alpha$ R was specifically knocked out in vWF<sup>+</sup> cells as experimental group) and vWF  $\times$  IFN $\alpha$ Rflox cre<sup>-</sup> mice (control group) were isolated. Then each 1  $\times$  10<sup>5</sup> cells were cultivated with TPO 50 ng/ml, TPO 50 ng/ml + IFN- $\alpha$  5 U/ml, TPO 50 ng/ml + IFN- $\alpha$  10 U/ml, TPO 50 ng/ml + IFN- $\alpha$  100 U/ml, TPO 50 ng/ml + IFN- $\alpha$  500 U/ml and TPO 50 ng/ml + IFN- $\alpha$  1000 U/ml respectively for 7 days in two groups. Next, we did the MK colony staining and imaging by microscope (16.8x) in experimental group (Figure 37) and control group (Figure 38). It is defined that one MK colony must include at least 3 MKs that are clustered together. After counting the number of MK colonies, we found that there were more colonies with IFN- $\alpha$  5, 10 or 100 U/ml plus TPO than TPO only in control group, and there were less colonies with IFN- $\alpha$  500 or 1000 U/ml plus TPO than TPO only (Figure 39). While there were no obvious differences in

experimental group (Figure 40). Additionally, according to comparing two groups, we found that there were more colonies with IFN- $\alpha$  5, 10 or 100 U/ml plus TPO in control group contrasted to those in experimental group, while there were less colonies with IFN- $\alpha$  500 or 1000 U/ml plus TPO in control group contrasted to those in experimental group, and there were no obvious differences of TPO only in two groups (Figure 41). These data illustrated that IFN- $\alpha$  in a proper concentration such as 5 to 100 U/ml can promote the development of MKs *in vitro*.

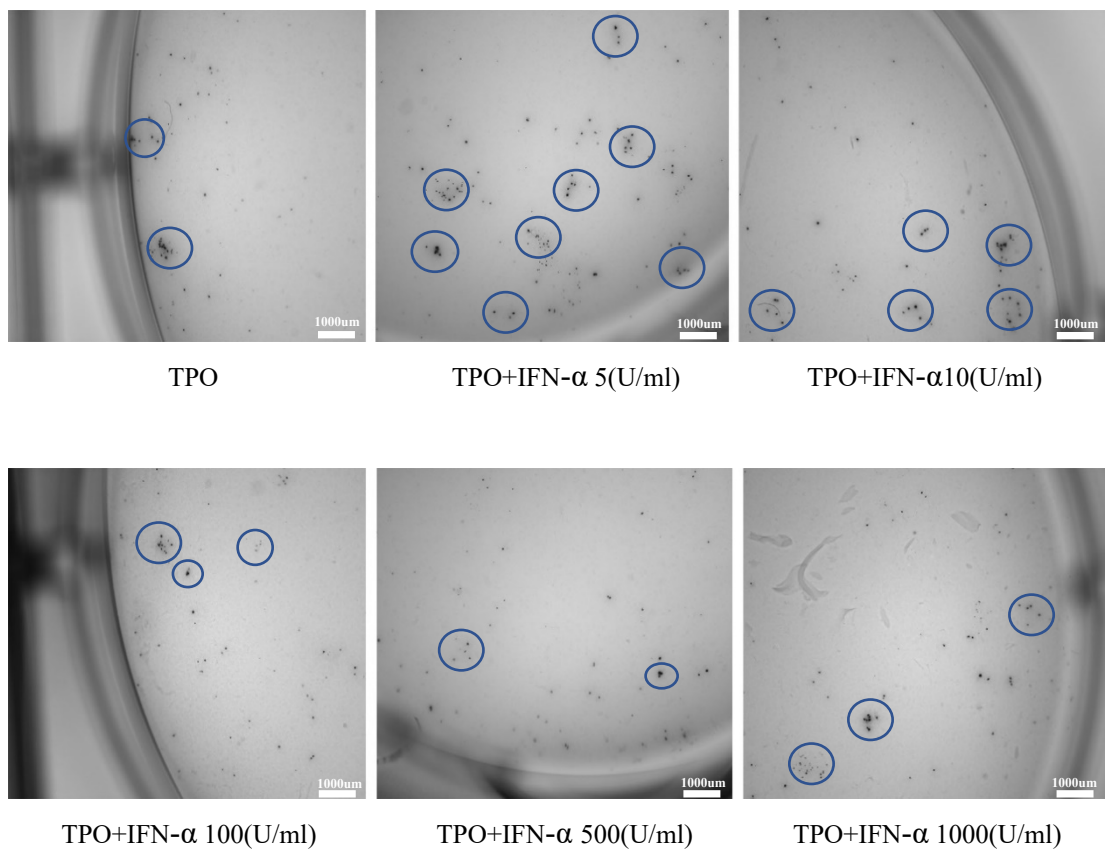


**Figure 37 Representative MK-CFU staining images in control group.** Circles indicated MK colonies. Scale bar= 1000  $\mu$ m.

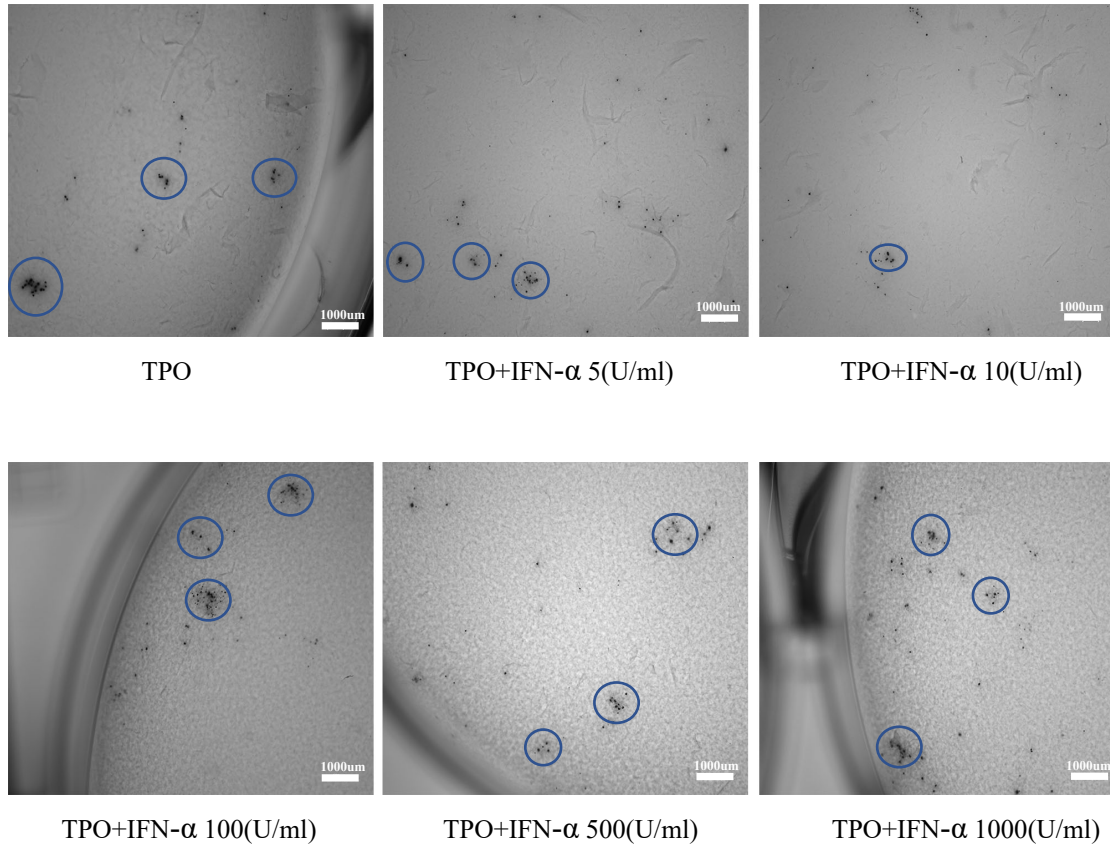


**Figure 38 Representative MK-CFU staining images in experimental group.** Circles indicated MK colonies. Scale bar= 1000  $\mu$ m.

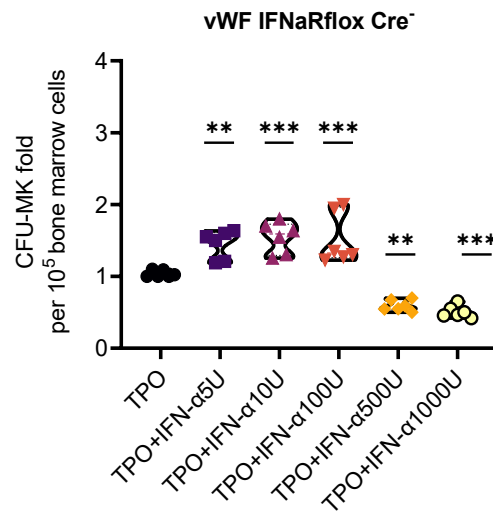


**Figure 39 CFU-MK fold in vWF  $\times$  IFN $\alpha$ Rflox cre<sup>-</sup> mice (control group) (n=6 mice).** TPO only was compared by others. One-way ANOVA, Dunnett's multiple comparisons test; Error bar=SEM. Contrasted to TPO: TPO+IFN- $\alpha$  5(U/ml) (P=0.0045); TPO+IFN- $\alpha$  10 (U/ml)

(P=0.0005); TPO+IFN- $\alpha$  100 (U/ml) (P=0.0009); TPO+IFN- $\alpha$  500 (U/ml) (P=0.0022); TPO+IFN- $\alpha$  1000(U/ml) (P=0.0003).

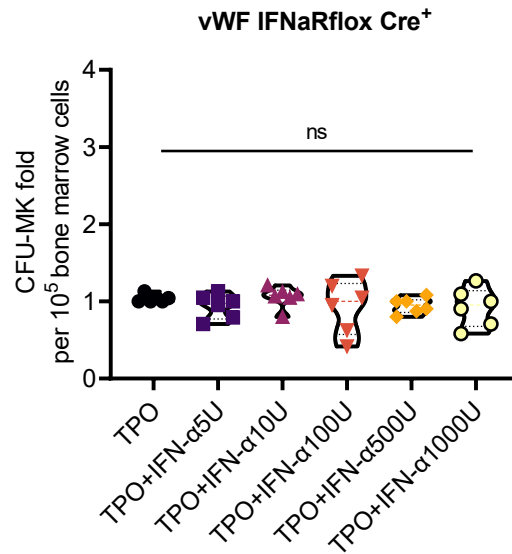


**Figure 40 CFU-MK fold in vWF  $\times$  IFN $\alpha$ Rflox cre<sup>+</sup> mice (experimental group) (n= 6 mice).** TPO only was compared to the other treatments. One-way ANOVA, Dunnett's multiple comparisons test; Error bar=SEM. Contrasted to TPO: TPO+IFN- $\alpha$  5(U/ml) (P= 0.8644); TPO+IFN- $\alpha$  10(U/ml) (P= 0.9997); TPO+IFN- $\alpha$  100(U/ml) (P= 0.8200); TPO+IFN- $\alpha$  500(U/ml) (P= 0.8884); TPO+IFN- $\alpha$  1000(U/ml) (P= 0.8055).

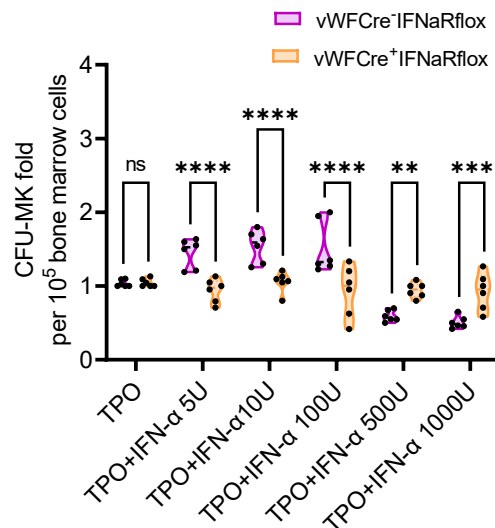


**Figure 41 CFU-MK fold in vWF  $\times$  IFN $\alpha$ Rflox cre<sup>-</sup> mice (control group) and vWF  $\times$  IFN $\alpha$ Rflox cre<sup>+</sup> mice (experimental group).** n= 6 mice for each group. Two-way ANOVA, Sidak's multiple comparisons test; Error bar=SEM. P> 0.9999 for TPO only; P< 0.0001 for

TPO+IFN- $\alpha$  5(U/ml); P< 0.0001 for TPO+IFN- $\alpha$  10(U/ml); P< 0.0001 for TPO+IFN- $\alpha$  100(U/ml); P= 0.0022 for TPO+IFN- $\alpha$  500(U/ml); P= 0.0002 for TPO+IFN- $\alpha$  1000(U/ml).

### 3.3.3 Effects of IFNaR deficiency on megakaryopoiesis *in vivo*

To further analyze the effects of IFN- $\alpha$  on megakaryopoiesis, we used a mouse where the IFN receptor is absent in all cell type. In the absence of the IFNaR, the platelet numbers in the blood decreased in steady state (Figure 42). To quantify the MK and MKPs numbers, we isolated the femurs and performed the bone marrow whole-mount immunostaining in WT mice and IFNaR-KO mice. We used anti-CD41 antibodies to label MKs and MKPs, anti-BST2 antibodies to label pDCs and Hoechst to label the nuclei (Figure 43). MKP were identified as small (diameter< 15  $\mu$ m), round and mononuclear CD41<sup>+</sup> cells, and MK as CD41<sup>+</sup> cells (diameter more than 15  $\mu$ m). After quantifying the number of pDCs, MKs and MKPs in each group, we found that there was slight decrease of pDCs and conspicuous decrease of MKs as well as MKPs in IFNaR-KO group compared with control group (Figure 44). Taking all the data together, it suggested that IFN- $\alpha$  may play a role on effective megakaryopoiesis and thrombocytopoiesis.

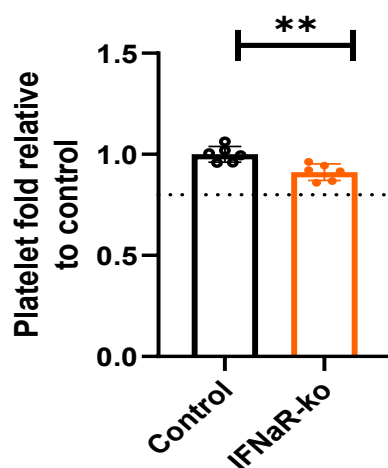


**Figure 42 Platelets fold relative to control group.** n= 6 mice in each group. Unpaired t-test; Error bar= SEM. P= 0.0035.

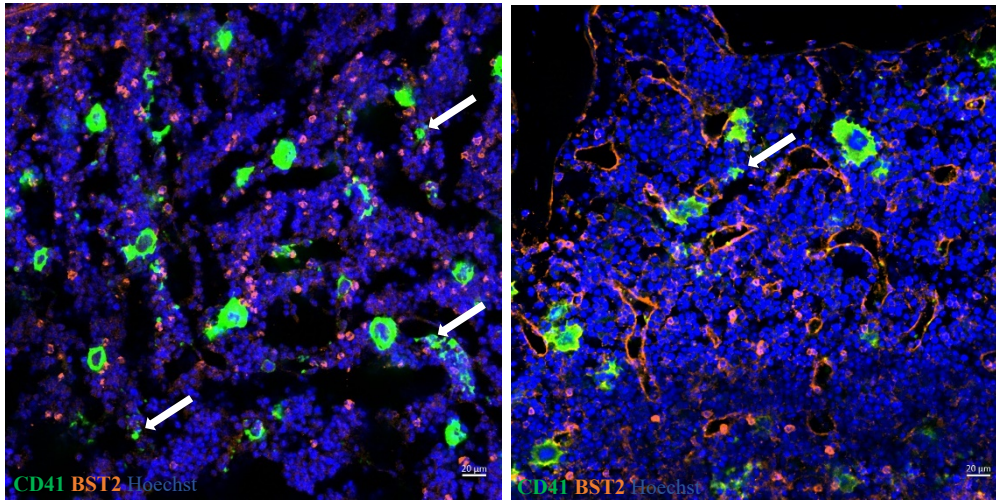


**Figure 43 Representative whole-mount immunostaining in control group (left) and IFNaR-KO group (right).** CD41 labeled MKs and MKPs, BST2 labeled pDCs, Hoechst labeled nucleus. MKP was identified as small (diameter < 15  $\mu\text{m}$ ), round and mononuclear CD41<sup>+</sup> cells. MKs were identified as CD41<sup>+</sup> multinucleated cells with a diameter more than 15  $\mu\text{m}$ . Arrows indicated MKPs. Scale bar = 20  $\mu\text{m}$ .

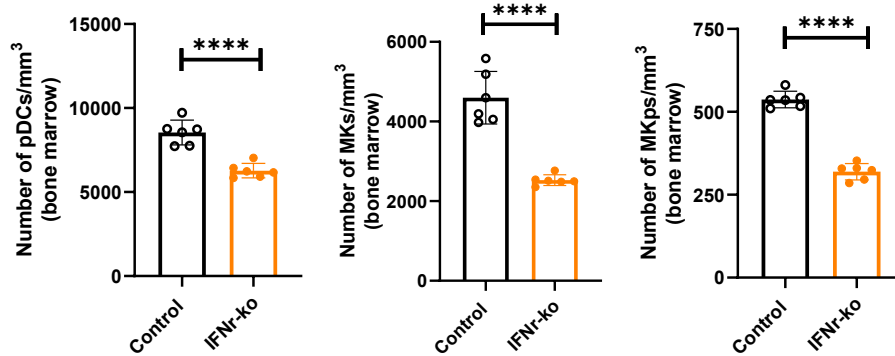


**Figure 44 pDC, MK and MKP quantifications under IFNaR deficiency condition.** The numbers of pDC, MK and MKP in control group (n = 6 mice) and IFNaR-KO group (n = 6 mice). Unpaired t-test; Error bar = SEM. pDC contrast (P < 0.01); MK contrast (P < 0.01); MKP contrast (P < 0.01).

### 3.3.4 IFN- $\alpha$ impacting megakaryopoiesis mainly released by pDCs

In order to verify if the IFN- $\alpha$  acting on megakaryopoiesis is mainly sourced from pDCs, we did the whole-mount staining in bone marrow of pDC depletion and *pDC-iDTR x IFNaR<sup>-/-</sup>* mice both in the steady state (Figure 45) and under emergency thrombocytopenia (Figure 46). The results showed that IFNaR deficiency in the absence of the pDCs had no impact on MK and MKP numbers both in the steady state (Figure 47) and under emergency thrombocytopenia (Figure 48) suggesting that IFN- $\alpha$  which triggers megakaryopoiesis is mainly released from pDCs.

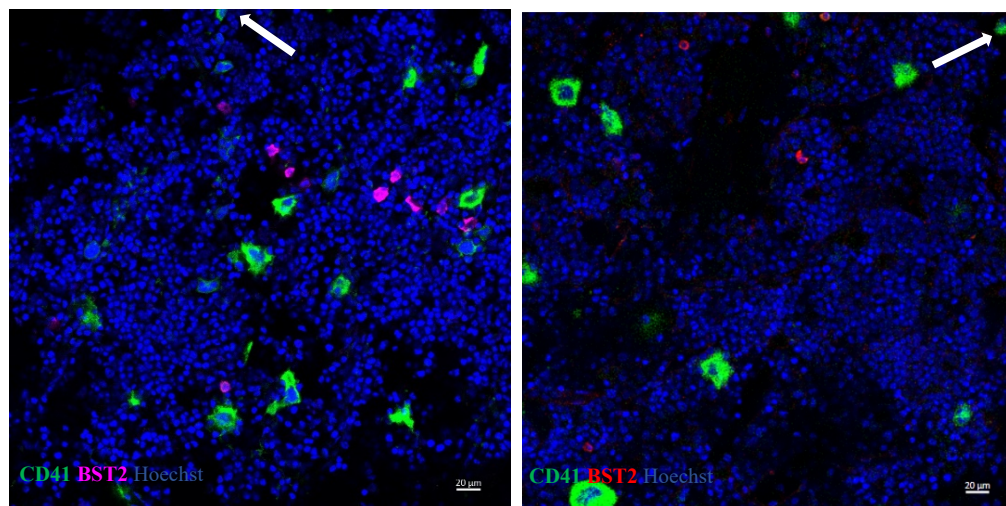


**Figure 45** Representative whole-mount immunostaining in pDC depletion group (left) and pDC-DTR x IFNaR-KO group (right). CD41 labeled MKs and MKPs, BST2 labeled pDCs, Hoechst labeled nucleus. MKP was identified as small (diameter < 15  $\mu\text{m}$ ), round and mononuclear CD41<sup>+</sup> cells. MKs were identified as CD41<sup>+</sup> multinucleated cells with a diameter more than 15  $\mu\text{m}$ . Arrows indicated MKPs. Scale bar = 20  $\mu\text{m}$ .

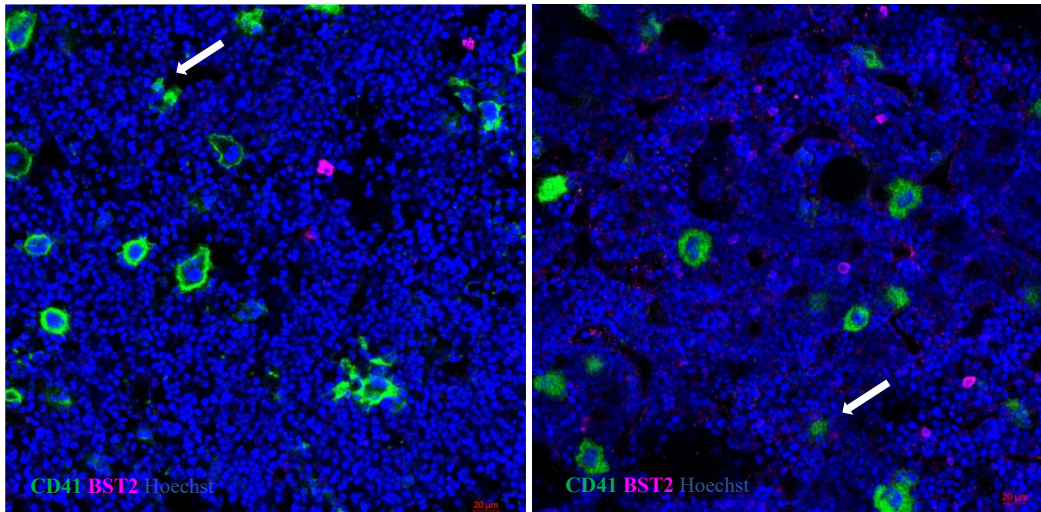


**Figure 46** Representative whole-mount immunostaining in platelet depletion + pDC depletion mice (left) and platelet depletion + pDC-DTR x IFN $\alpha$ R-KO mice (right). CD41 labeled MKs and MKPs, BST2 labeled pDCs, Dapi labeled nucleus. MKP was identified as small (diameter < 15  $\mu$ m), round and mononuclear CD41<sup>+</sup> cells. MKs were identified as CD41<sup>+</sup> multinucleated cells with a diameter more than 15  $\mu$ m. Arrows indicated MKPs. Scale bar= 20  $\mu$ m

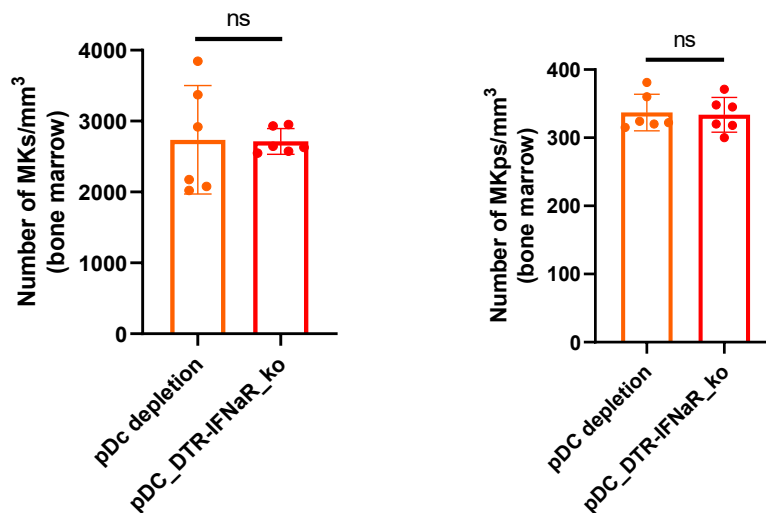


**Figure 47** MK and MKP quantifications under absence of pDC and IFN $\alpha$ R knock out condition. The numbers of MK and MKP in pDC depletion group (n= 6 mice) and pDC-DTR x IFN $\alpha$ R-KO group (n= 6 mice). Unpaired t-test; Error bar= SEM. MK contrast (P= 0.9465); MKP contrast (P= 0.8308).

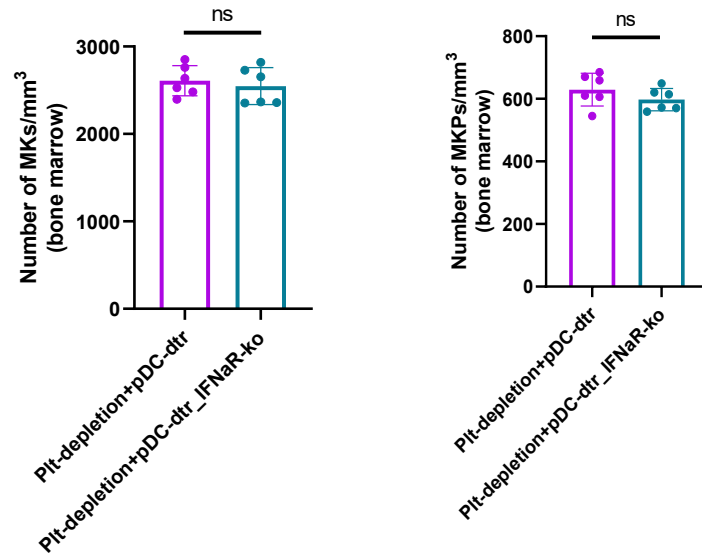


**Figure 48 MK and MKP quantifications in the absence of pDC and IFNaR knock out under thrombocytopenia.** The numbers of MK and MKP in platelet depletion + pDC depletion (n= 6) and platelet depletion + pDC-DTR x IFNaR-KO group (n= 6). Unpaired t-test; Error bar=SEM. P= 0.5868 for MK comparison; P= 0.2456 for MKP comparison.

## 4. Discussion

### 4.1 Methodology discussion

#### 4.1.1 Identification of MKs, MKPs and pDCs

CD 41 is the mostly common surface marker to identify MKs and it is extensively accepted for characterize all stages of the megakaryocytes [11]. It has been described that there is expression of CD41 on embryonic HSCs [129], but CD41 is still widely recognized as a lacking antigen of adult stem cells. One study by Gekas showed that there was expression of CD41 increasing with age in some adult HSCs, but the number of CD41<sup>+</sup> HSCs in mice older than 8 weeks is extremely low [130]. In this study, all mice we used were older than 8 weeks, therefore, CD41<sup>+</sup> cells were considered as MKPs and MKs in our whole-mount staining analysis. CD42 is a recognized cell marker for mature MK [12,13,131], but some studies reported some MK progenitors were double labeled by CD41 and CD42 [132]. Considering this condition, we just used only CD41 to label MKs and MKPs, and defined MKPs as small (diameter<15  $\mu$ m), round and mononuclear CD41<sup>+</sup> cells, since MKPs were reported to be 10-15  $\mu$ m in diameter, round and small cells with single nucleus [6,133]. MK were defined as CD41<sup>+</sup> multinucleated cells with a diameter more than 15  $\mu$ m.

For MK intravital staining in mice, in the traditional concept, fluorescently labeled antibodies were injecting into the blood of the mice to mark MKs populations as some studies reported [134,135]. It is simple and effective to label the cells that are exposed in the blood by using this method. Nowadays, it is widely known to use transgenic mouse models to label the MKs populations, which is more convenient than injection of antibodies. In our previous study, vWF-eGFP mouse model was used to label MKs and MKPs and showed an efficient mark for MKs and MKPs. There are other MK labeled mouse models such as CD41-YFP and PF4 Cre  $\times$  Rosa26-mT/mG mice [136, 137]. But for CD41-YFP mouse, it was showed low efficiency marking the MK populations according to our previous studies from our lab. As to PF4 Cre  $\times$  Rosa26-

mT/mG, it was reported that some part of other cells containing monocytes, macrophages and dendritic cells were also labeled by PF4 [138] implying it could be not specific to MKs. Therefore, the vWF-eGFP mouse model was used for MKs labeling *in vivo* in this thesis.

BST2, Siglec-H, CD11c, B220 and Ly6C are the most common markers to identify pDCs in mice. And BST2 and Siglec-H are more specific to label pDCs compared other markers in the bone marrow [63-65]. However, Siglec-H is also expressed on some subtypes of macrophages [66]. Therefore, BST2 was used to label the pDCs in bone marrow whole-mount staining. But for intravital calvarial bone marrow imaging by two-photo microscope, anti-siglec-H-PE antibodies were much efficient to label pDCs than anti-BST2 antibodies applied in our experiments. pDCs could be differentiated from macrophages by their specific morphology. Therefore, we choose to use anti-siglec-H-PE antibodies to label the pDCs in the intravital calvarial bone marrow imaging *in vivo*.

## **4.2 Results discussion**

How pDCs regulate megakaryopoiesis in the bone marrow is the main goal of this study.

The main findings in this study are: (1) pDCs can interact with vital and apoptotic MKs. (2) Absence of pDCs decreases the numbers of MK as well as MKP both in steady state and under thrombocytopenia. (3) IFN- $\alpha$  stimulates MK proliferation both *in vivo* and *in vitro*. (4) Deficiency of IFN- $\alpha$  receptor decreases the numbers of MK and MKP both in steady state and under thrombocytopenia. (5) Deficiency of IFN- $\alpha$  receptor in the pDC depletion mice does not further decrease the numbers of MK and MKP.

#### 4.2.1 pDCs serve as the BM scanners sensing apoptotic MKs

It was reported that platelets production is followed by MKs apoptosis [38-45], and remnant MKs are naked nuclei after MK apoptosis [51]. In addition, it was reported that pDCs can sense apoptotic cells and nuclei acids [69,80,139]. In this study, through the bone marrow whole-mount staining, we found that pDCs were surrounding with the mature MKs and interacting with vital MKs and apoptotic MKs especially under the MK-depletion (MK apoptotic) and thrombocytopenia conditions where the number of apoptotic MKs significantly increase. Furthermore, according to the analysis of dynamic MK-pDC interactions by two-photon bone marrow imaging *in vivo*, we found that pDCs were interacting with the surface of MKs, even some ones were diving into the bodies of MKs, a process similar to emperipolesis [140]. And by tracing the single pDC interacting with the MKs, pDCs moved faster in the presence of more apoptotic MKs. These findings suggest that pDCs can be a bone marrow scanner to sense and interact with apoptotic MKs.

#### 4.2.2 Absence of pDCs impair megakaryopoiesis both in the steady state and under emergency thrombocytopenia

To further investigate the effect of pDCs in megakaryopoiesis *in vivo*, pDC-depleted models were used. It was reported that about 90% of pDCs in the circulation, spleen and lymph nodes were depleted after DT injection in *BDCA2-iDTR* mice, therefore, these mice were usually used for investigating the functions of pDCs in the immune responses to viral infections [123,141,142]. In this study, we found that approximately 80% of pDCs were depleted on the BM after 3 days of DT treatment in the *BDCA2-iDTR* mice, thus they were used for investigating the impact of pDCs in bone marrow for megakaryopoiesis. After analyzing the megakaryocytic lineage by whole-mount immunostainings, we found that there were substantial decreases in MKPs (50%) and MKs (25%) in the steady state as well as significant decreases in MKPs (40%) and MKs

(50%) under the emergency thrombocytopenia indicating that absence of pDCs severely impaired megakaryopoiesis in the bone marrow. Furthermore, under the condition of immune-mediated thrombocytopenia, the platelets were recovered in around one week for WT mice, but it was delayed by more than 2 days and never reached a standard level in pDC depletion mice indicating that the absence of pDCs impairs self-restoring capacity encountering the emergency thrombocytopenia. In addition, we found that there were slight increase of MKs and significant increase of MKPs in WT mice, but significant decrease of MKs and MKPs in pDC depletion mice under thrombocytopenia further suggesting that absence of pDCs impairs the megakaryopoiesis resulting in impairing the restoring capacity. Therefore, pDCs could be triggered as therapeutic target for controlling platelet production via modulation of its progenitors.

#### 4.2.3 IFN- $\alpha$ promotes megakaryopoiesis of the bone marrow

##### 4.2.3.1 IFN- $\alpha$ plays a role in promoting the development of MKs

IFN- $\alpha$  has a crucial protective role in viral infections [143]. Recently, more and more studies have found that IFN- $\alpha$  also impacts several physiological processes including immunomodulation, cell cycle regulating, as well as cell surviving and differentiating [144,145]. It was reported that IFN- $\alpha$  is required for maintenance of the HSC niche in bone marrow, but long-term systemic elevation of IFN- $\alpha$  levels causes exhaustion of HSCs [146,147]. Additionally, some studies have declared that both MKs and MKPs express IFN $\alpha$ R [68], and one study by Haas and his colleagues revealed that IFN- $\alpha$  mediated some inflammations can promote MKPs to develop into MKs [94]. These findings illustrate that IFN- $\alpha$  could be a trigger to promote the megakaryopoiesis in the bone marrow. In our study, we find that a proper concentration of IFN- $\alpha$  (5-100U/ml) with TPO synergistically induced MKPs to develop into MKs in an IFN $\alpha$ R-dependent way, as analyzed by CFU assays *in vitro*. However, some studies indicated that IFN- $\alpha$  inhibits MK-colony forming *in vitro* [148,149]. In these studies, the concentration of IFN- $\alpha$  was more than 100U/ml, and it was similar in our study with the concentrations

(500U/ml and 1000U/ml) illustrating that constitutive IFN- $\alpha$  could promote the megakaryopoiesis, while excess IFN- $\alpha$  could inhibit the megakaryopoiesis. Additionally, there was a significant increase of MKPs, MKs and circulating platelets numbers after 2-4h of IFN- $\alpha$  treatment indicating that systemic treatment of mice with IFN- $\alpha$  triggered fast and immediate megakaryopoiesis *in vivo*. Furthermore, it is similar to pDC-iDTR mice, IFNaR-deficient mice showed remarkable reduced MKP numbers insufficient to maintain MK and platelet homeostasis, both in the steady state and emergency thrombocytopenia. Take all the findings together, constitutive IFN- $\alpha$  can promote the megakaryopoiesis both *in vivo* and *in vitro*.

#### 4.2.3.2 The source of IFN- $\alpha$ for promoting megakaryopoiesis in the bone marrow

IFN- $\alpha$  is produced by many cells in the bone marrow such as macrophages, endothelial cells and osteoblasts. However, pDCs are releasing 1000-fold higher levels than other cells and they are recognized as the major IFN- $\alpha$  producers [150-152]. It was reported that pDCs encountering apoptotic cells release large amounts of IFN- $\alpha$  and then triggering local inflammation [80, 137]. In our study, we found that deficiency of IFNaR in pDC depletion mice (*BDCA2-DTR x IFNaR*<sup>-/-</sup> mice) had no additive effect on MK and MKP numbers in the steady state and under thrombocytopenia, indicating that IFN- $\alpha$ -mediated regulation of megakaryopoiesis is mainly from pDCs. Together, these data show that pDCs detecting and interacting with apoptotic MKs trigger local inflammation by probably releasing IFN- $\alpha$  to promote the differentiation of MKPs maintaining MK homeostasis.

### 4.3 Clinical implications

Thrombocytopenia is a very common complication in some severe viral diseases, as in HIV, influenza and SARS-CoV-2 infected patients [153-155]. The mechanism leading to thrombocytopenia in viral infections is complicated and still not clear. It is known

that pDCs play an important role in antiviral infections by sensing viral RNA/DNA through the TLR7/9 to activate the genes responsible for production of type I interferon [67,68]. During some viral infections such as HIV and SARS-CoV-2, the number of circulating pDCs is reduced and their function in IFN- $\alpha$  production is decreased [156-159]. One of the reasons for it, maybe come from the pDCs precursors mismanagement promoted by these viral infections and resulting in less and dysfunctional pDCs development [160,161]. Indeed, the increase of apoptotic pDCs were found in HIV and SARS-CoV-2 infections in humans as well as HSV infection in mice [162-164]. In this context, pDCs apoptosis was partly induced by a burst release of type I IFN in murine HSV infection [163]. Furthermore, the increase of some cytokines as IL-10 and TNF- $\alpha$  which can restrain the function of pDCs, were found in SARS-CoV-2 infection patients [165,166]. In this study, we found that pDCs can promote megakaryopoiesis by probably releasing IFN- $\alpha$  resulting in platelet production. And the depletion of pDCs results in thrombocytopenia, given strong evidence of their role on controlling the platelet turnover in the blood. Thus, given the evidence of pDCs involvement in antiviral immune responses and platelet production, it brings to the clinical field an excellent target for therapeutics approaches to treat cases of thrombocytopenia.

## 5. References

1. Odell T, Jackson CJ, Reiter R. Generation cycle of rat megakaryocytes. *Exp Cell Res*, 1968. 53, 321. 1. Odell T, Jackson CJ, Reiter R. Generation cycle of rat megakaryocytes. *Exp Cell Res*, 1968. 53, 321.
2. Ebbe S, Stohlman F Jr. Megakaryocytopoiesis in the rat. *Blood*, 1965. 26, 20-34.
3. Ebbe, S. Biology of megakaryocytes. *Prog Hemost Thromb*, 1976. 3, 211-229.
4. Therman, E., Sarto, G., & Stubblefields, P. Endomito- sis: A reappraisal. *Hum Genet*, 1983. 63,3-18.
5. Machlus KR, Italiano JE Jr. The incredible journey: From megakaryocyte development to platelet formation. *J Cell Biol*, 2013. 201(6): 785-96.
6. Y.X.Ru, S.X.Zhao, S.X.Dong, Y.Q.Yang, and B.Eyden, "On the Maturation of Megakaryocytes: A Review with Original Observations on Human In Vivo Cells Emphasizing Morphology and Ultrastructur,"*Ultrastructural Pathology*, vol. 39, no. 2. pp. 79-87, 2015.
7. K.Miyawaki, H. Iwasaki, T. Jiromaru, H. Kusumoto, A. Yurino, T. Sugio, Y. Uehara, J. Odawara, S. Daitoku, Y. Kunisaki, Y. Mori, Y. Arinobu, H. Tsuzuki, Y. Kikushige, T. Iino, K. Kato, K. Takenaka, T. Miyamoto, T. Maeda, and K. Akashi,"Identification of unipotent megakaryocyte progenitors in human hematopoiesis," *Blood*, vol. 129, no. 25, pp. 3332-3343, 2017.
8. R. F. Levine, K. C. Hazzard, and J. D. Lamberg, "The significance of megakaryocyte size.," *Blood*, vol. 60, no. 5, pp. 1122-31, 1982.
9. J. N. Thon, A. Montalvo, S. PatelaHett, M. T. Devine, J. L. Richardson, A. Ehrlicher, M. K. Larson, K. Hoffmeister, J. H. Hartwig, and J. E. Italiano, "Cytoskeletal mechanics of proplatelet maturation and platelet release," *J. Cell Biol.*, vol. 191, no. 4, pp. 861-874, 2010.
10. E. S. Choi, J. L. Nichol, M. M. Hokom, A. C. Hornkohl, and P. Hunt, "Platelets generated in vitro from proplateletdisplaying human megakaryocytes are functional." *Blood*, vol. 85, no. 2, pp. 402-413, 1995.

11. Debili N, Robin C, Schiavon V, Letestu R, Pflumio F, Mitjavila-Garcia MT, Coulombel L, Vainchenker W. Different expression of CD41 on human lymphoid and myeloid progenitors from adults and neonates. *Blood*, 2001. 97(7): 2023-30.
12. Klimchenko O, Mori M, Distefano A, Langlois T, Larbret F, Lecluse Y, Feraud O, Vainchenker W, Norol F, Debili N. A common bipotent progenitor generates the erythroid and megakaryocyte lineages in embryonic stem cell-derived primitive hematopoiesis. *Blood*, 2009. 114(8): 1506-17.
13. Lagrue-Lak-Hal AH, Debili N, Kingbury G, Lecut C, Le Couedic JP, Villeval JL, Jandrot-Perrus M, Vainchenker W. Expression and function of the collagen receptor GPVI during megakaryocyte maturation. *J Biol Chem*, 2001. 276(18): 15316-25.
14. Chang Y, Bluteau D, Debili N, Vainchenker W. From hematopoietic stem cells to platelets. *J Thromb Haemost*. 2007 Jul;5 Suppl 1:318-27.
15. Seita J, Weissman IL. Hematopoietic stem cell: self-renewal versus differentiation. *Wiley Interdiscip Rev Syst Biol Med*. 2010 Nov-Dec;2(6):640-53.
16. Clay D, Rubinstein E, Mishal Z, Anjo A, Prenant M, Jasmin C, Boucheix C, Le Bousse-Kerdilès MC. CD9 and megakaryocyte differentiation. *Blood*, 2001. 97(7): 1982-9.
17. Nakorn TN, Miyamoto T, Weissman IL. Characterization of mouse clonogenic megakaryocyte progenitors. *Proc Natl Acad Sci U S A*, 2003. 100(1): 205-10.
18. Bush LM, Healy CP, Marvin JE, Deans TL. High-throughput enrichment and isolation of megakaryocyte progenitor cells from the mouse bone marrow. *Sci Rep*. 2021 Apr 15;11(1):8268.
19. Trowbridge EA, Martin JF, Slater DN, Kishk YT, Warren CW, Harley PJ, Woodcock B. The origin of platelet count and volume. *Clin Phys Physiol Meas*. 1984 Aug;5(3):145-70.
20. Harker LA, Finch CA. Thrombokinetics in man. *J Clin Invest*. 1969 Jun;48(6):963-74.

21. Kaufman RM, Airo R, Pollack S, Crosby WH. Circulating megakaryocytes and platelet release in the lung. *Blood*. 1965 Dec;26(6):720-31.
22. Long MW, Williams N, Ebbe S. Immature megakaryocytes in the mouse: physical characteristics, cell cycle status, and in vitro responsiveness to thrombopoietic stimulatory factor. *Blood*. 1982 Mar;59(3):569-75.
23. Ravid K, Lu J, Zimmet JM, Jones MR. Roads to polyploidy: the megakaryocyte example. *J Cell Physiol*. 2002 Jan;190(1):7-20.
24. Patel SR, Hartwig JH, Italiano JE Jr. The biogenesis of platelets from megakaryocyte proplatelets. *J Clin Invest*. 2005 Dec;115(12):3348-54.
25. Behnke O. An electron microscope study of the megakaryocyte of the rat bone marrow. I. The development of the demarcation membrane system and the platelet surface coat. *J Ultrastruct Res*. 1968 Sep;24(5):412-33.
26. Nakao K, Angrist AA. Membrane surface specialization of blood platelet and megakaryocyte. *Nature*. 1968 Mar 9;217(5132):960-1.
27. Italiano JE Jr, Lecine P, Shivdasani RA, Hartwig JH. Blood platelets are assembled principally at the ends of proplatelet processes produced by differentiated megakaryocytes. *J Cell Biol*. 1999 Dec 13;147(6):1299-312.
28. Andrews NC, Erdjument-Bromage H, Davidson MB, Tempst P, Orkin SH. Erythroid transcription factor NF-E2 is a haematopoietic-specific basic-leucine zipper protein. *Nature*. 1993 Apr 22;362(6422):722-8.
29. Kerr JF, Wyllie AH, Currie AR. Apoptosis: a basic biological phenomenon with wideranging implications in tissue kinetics. *Br J Cancer*. 1972;26(4):239-257.
30. Youle RJ, Strasser A. The BCL-2 protein family: opposing activities that mediate cell death. *Nat Rev Mol Cell Biol*. 2008 Jan;9(1):47-59.
31. Fearnhead HO, Vandenabeele P, Vanden Berghe T. How do we fit ferroptosis in the family of regulated cell death? *Cell Death Differ*. 2017 Dec;24(12):1991-1998.
32. Scaffidi C, Fulda S, Srinivasan A, Friesen C, Li F, Tomaselli KJ, Debatin KM, Krammer PH, Peter ME. Two CD95 (APO-1/Fas) signaling pathways. *EMBO J*. 1998 Mar 16;17(6):1675-87.

33. Yin XM, Wang K, Gross A, Zhao Y, Zinkel S, Klocke B, Roth KA, Korsmeyer SJ. Bid-deficient mice are resistant to Fas-induced hepatocellular apoptosis. *Nature*. 1999 Aug 26;400(6747):886-91.
34. Jost PJ, Grabow S, Gray D, McKenzie MD, Nachbur U, Huang DC, Bouillet P, Thomas HE, Borner C, Silke J, Strasser A, Kaufmann T. XIAP discriminates between type I and type II FAS-induced apoptosis. *Nature*. 2009 Aug 20;460(7258):1035-9.
35. McArthur K, Chappaz S, Kile BT. Apoptosis in megakaryocytes and platelets: the life and death of a lineage. *Blood*. 2018 Feb 8;131(6):605-610.
36. Kodama T, Hikita H, Kawaguchi T, Shigekawa M, Shimizu S, Hayashi Y, Li W, Miyagi T, Hosui A, Tatsumi T, Kanto T, Hiramatsu N, Kiyomizu K, Tadokoro S, Tomiyama Y, Hayashi N, Takehara T. Mcl-1 and Bcl-xL regulate Bak/Bax-dependent apoptosis of the megakaryocytic lineage at multistages. *Cell Death Differ*. 2012 Nov;19(11):1856-69.
37. Debrincat MA, Josefsson EC, James C, Henley KJ, Ellis S, Lebois M, Betterman KL, Lane RM, Rogers KL, White MJ, Roberts AW, Harvey NL, Metcalf D, Kile BT. Mcl-1 and Bcl-x(L) coordinately regulate megakaryocyte survival. *Blood*. 2012 Jun 14;119(24):5850-8.
38. Morison IM, Cramer Bordé EM, Cheesman EJ, Cheong PL, Holyoake AJ, Fichelson S, Weeks RJ, Lo A, Davies SM, Wilbanks SM, Fagerlund RD, Ludgate MW, da Silva Tatley FM, Coker MS, Bockett NA, Hughes G, Pippig DA, Smith MP, Capron C, Ledgerwood EC. A mutation of human cytochrome c enhances the intrinsic apoptotic pathway but causes only thrombocytopenia. *Nat Genet*. 2008 Apr;40(4):387-9.
39. Houwerzijl EJ, Blom NR, van der Want JJ, Esselink MT, Koornstra JJ, Smit JW, Louwes H, Vellenga E, de Wolf JT. Ultrastructural study shows morphologic features of apoptosis and para-apoptosis in megakaryocytes from patients with idiopathic thrombocytopenic purpura. *Blood*. 2004 Jan 15;103(2):500-6.
40. Clarke MC, Savill J, Jones DB, Noble BS, Brown SB. Compartmentalized

- megakaryocyte death generates functional platelets committed to caspase-independent death. *J Cell Biol.* 2003 Feb 17;160(4):577-87.
41. Kaluzhny Y, Yu G, Sun S, Toselli PA, Nieswandt B, Jackson CW, Ravid K. BclxL overexpression in megakaryocytes leads to impaired platelet fragmentation. *Blood.* 2002 Sep 1;100(5):1670-8.
  42. De Botton S, Sabri S, Daugas E, Zermati Y, Guidotti JE, Hermine O, Kroemer G, Vainchenker W, Debili N. Platelet formation is the consequence of caspase activation within megakaryocytes. *Blood.* 2002 Aug 15;100(4):1310-7.
  43. Brown SB, Clarke MC, Magowan L, Sanderson H, Savill J. Constitutive death of platelets leading to scavenger receptor-mediated phagocytosis. A caspase-independent cell clearance program. *J Biol Chem.* 2000 Feb 25;275(8):5987-96.
  44. Ogilvy S, Metcalf D, Print CG, Bath ML, Harris AW, Adams JM. Constitutive Bcl-2 expression throughout the hematopoietic compartment affects multiple lineages and enhances progenitor cell survival. *Proc Natl Acad Sci U S A.* 1999 Dec 21;96(26):14943-8.
  45. Bouillet P, Metcalf D, Huang DC, Tarlinton DM, Kay TW, Köntgen F, Adams JM, Strasser A. Proapoptotic Bcl-2 relative Bim required for certain apoptotic responses, leukocyte homeostasis, and to preclude autoimmunity. *Science.* 1999 Nov 26;286(5445):1735-8.
  46. Josefsson EC, Burnett DL, Lebois M, Debrincat MA, White MJ, Henley KJ, Lane RM, Moujalled D, Preston SP, O'Reilly LA, Pellegrini M, Metcalf D, Strasser A, Kile BT. Platelet production proceeds independently of the intrinsic and extrinsic apoptosis pathways. *Nat Commun.* 2014 Mar 17;5:3455.
  47. Josefsson EC, James C, Henley KJ, Debrincat MA, Rogers KL, Dowling MR, White MJ, Kruse EA, Lane RM, Ellis S, Nurden P, Mason KD, O'Reilly LA, Roberts AW, Metcalf D, Huang DC, Kile BT. Megakaryocytes possess a functional intrinsic apoptosis pathway that must be restrained to survive and produce platelets. *J Exp Med.* 2011 Sep 26;208(10):2017-31.
  48. Kodama T, Takehara T, Hikita H, Shimizu S, Shigekawa M, Li W, Miyagi T,

- Hosui A, Tatsumi T, Ishida H, Kanto T, Hiramatsu N, Yin XM, Hayashi N. BH3-only activator proteins Bid and Bim are dispensable for Bak/Bax-dependent thrombocyte apoptosis induced by Bcl-xL deficiency: molecular requisites for the mitochondrial pathway to apoptosis in platelets. *J Biol Chem*. 2011 Apr 22;286(16):13905-13.
49. Kodama T, Takehara T, Hikita H, Shimizu S, Li W, Miyagi T, Hosui A, Tatsumi T, Ishida H, Tadokoro S, Ido A, Tsubouchi H, Hayashi N. Thrombocytopenia exacerbates cholestasis-induced liver fibrosis in mice. *Gastroenterology*. 2010 Jun;138(7):2487-98, 2498.e1-7.
50. White MJ, Schoenwaelder SM, Josefsson EC, Jarman KE, Henley KJ, James C, Debrincat MA, Jackson SP, Huang DC, Kile BT. Caspase-9 mediates the apoptotic death of megakaryocytes and platelets, but is dispensable for their generation and function. *Blood*. 2012 May 3;119(18):4283-90. doi: 10.1182/blood-2011-11-394858. Epub 2012 Jan 31.
51. Radley JM, Haller CJ. Fate of senescent megakaryocytes in the bone marrow. *Br J Haematol*. 1983;53(2):277-287.
52. Lennert K, Remmele W. Karyometric research on lymph node cells in man. I. Germinoblasts, lymphoblasts & lymphocytes. *Acta Haematol*. 1958; 19:99-113.
53. Shalin H Naik, Priyanka Sathe, Hae-Young Park, Donald Metcalf, Anna I Proietto, Aleksander Dakic, Sebastian Carotta, Meredith O'Keeffe, Melanie Bahlo, Anthony Papenfuss, Jong-Young Kwak, Li Wu1 & Ken Shortman. Development of plasmacytoid and conventional dendritic cell subtypes from single precursor cells derived in vitro and in vivo. *Nat Immunol*. 2007; 8:1217-1226.
54. Nobuyuki Onai, Aya Obata-Onai, Michael A Schmid1, Toshiaki Ohteki, David Jarrossay1 & Markus G Manz. Identification of clonogenic common Flt3+M-CSFR+ plasmacytoid and conventional dendritic cell progenitors in mouse bone marrow. *Nat Immunol*. 2007; 8:1207-1216.
55. Reizis B. Regulation of plasmacytoid dendritic cell development. *Curr Opin Immunol*. 2010; 22:206-211.

56. Satpathy AT, Wu X, Albring JC, Murphy KM. Re(de)fining the dendritic cell lineage. *Nat Immunol.* 2012; 13:1145-1154.
57. Belz GT, Nutt SL. Transcriptional programming of the dendritic cell network. *Nat Rev Immunol.* 2012; 12:101-113.
58. Onai N, Kurabayashi K, Hosoi-Amaike M, Toyama-Sorimachi N, Matsushima K, Inaba K, et al. A clonogenic progenitor with prominent plasmacytoid dendritic cell developmental potential. *Immunity.* (2013) 38:943-57.
59. Onai N, Asano J, Kurosaki R, Kuroda S, Ohteki T. Flexible fate commitment of E2–2high common DC progenitors implies tuning in tissue microenvironments. *Int Immunol.* (2017) 29:443-56.
60. Andreas Schlitzer, Jakob Loschko, Katrin Mair, Roger Vogelmann, Lynette Henkel, Henrik Einwa"chter, Matthias Schiemann, Jan-Hendrik Niess, Wolfgang Reindl, and Anne Krug. Identification of CCR9– murine plasmacytoid DC precursors with plasticity to differentiate into conventional DCs. *Blood.* 2011; 117:6562-6570.
61. Andreas Schlitzer, Alexander F. Heiseke, Henrik Einwa"chter, Wolfgang Reindl, Matthias Schiemann, Calin-Petru Manta, Peter See, Jan-Hendrik Niess, Tobias Suter, Florent Ginhoux, and Anne B. Krug. Tissue-specific differentiation of a circulating CCR9– pDC-like common dendritic cell precursor. *Blood.* 2012; 119:6063-6071.
62. Andrea Musumeci, Konstantin Lutz, Elena Winheim and Anne Barbara Krug. What Makes a pDC: Recent Advances in Understanding Plasmacytoid Development and Heterogeneity.
63. Amanda L. Blasius, Emanuele Giurisato, Marina Cella, Robert D. Schreiber, Andrey S. Shaw, and Marco Colonna. Bone marrow stromal cell antigen 2 is a specific marker of type I IFN-producing cells in the naive mouse, but a promiscuous cell surface antigen following IFN stimulation. *J Immunol.* 2006; 177:3260–3265.
64. Blasius AL, Cella M, Maldonado J, Takai T, Colonna M. Siglec-H is an IPC-specific receptor that modulates type I IFN secretion through DAP12. *Blood.*

- 2006; 107:2474–2476. [PubMed: 16293595]
65. Jiquan Zhang, Anna Raper, Noriko Sugita, Ravi Hingorani, Mariolina Salio, Michael J. Palmowski, Vincenzo Cerundolo, and Paul R. Crocker. Characterization of Siglec-H as a novel endocytic receptor expressed on murine plasmacytoid dendritic cell precursors. *Blood*. 2006; 107:3600–3608.
  66. Jens Kopatz, Clara Beutner, Kristian Welle, Liviu G. Bodea, Julia Reinhardt, Janine Claude, Bettina Linnartz-Gerlach, and Harald Neumann. Siglec-h on activated microglia for recognition and engulfment of glioma cells. *Glia*. 2013; 61:1122–1133.
  67. Honda K, Ohba Y, Yanai H, Negishi H, Mizutani T, Takaoka A, Taya C, Taniguchi T. Spatiotemporal regulation of MyD88-IRF-7 signalling for robust type-I interferon induction. *Nature*. 2005 Apr 21;434(7036):1035-40.
  68. Negrotto S, J De Giusti C, Laponi MJ, Etulain J, Rivadeneyra L, Pozner RG, Gomez RM, Schattner M. Expression and functionality of type I interferon receptor in the megakaryocytic lineage. *J Thromb Haemost*. 2011 Dec;9(12):2477-85. doi: 10.1111/j.1538-7836.2011.04530.x. PMID: 22136495.
  69. Gilliet M, Cao W, Liu YJ. Plasmacytoid dendritic cells: sensing nucleic acids in viral infection and autoimmune diseases. *Nat Rev Immunol*. 2008; 8:594–606.
  70. Blasius AL, Beutler B. Intracellular toll-like receptors. *Immunity*. 2010; 32:305-315.
  71. Kawai T, Akira S. Toll-like receptors and their crosstalk with other innate receptors in infection and immunity. *Immunity*. 2011; 34:637–650.
  72. Cella, M., Facchetti, F., Lanzavecchia, A., Colonna, M., 2000. Plasmacytoid dendritic cells activated by influenza virus and CD40L drive a potent TH1 polarization. *Nat. Immunol*. 1, 305–310.
  73. Tough, D.F., Borrow, P., Sprent, J., 1996. Induction of bystander T cell proliferation by viruses and type I interferon in vivo. *Science* 272, 1947–1950.
  74. Jego, G., Palucka, A.K., Blanck, J.P., Chalouni, C., Pascual, V., Banchereau, J., 2003. Plasmacytoid dendritic cells induce plasma cell differentiation through

- type I interferon and interleukin 6. *Immunity* 19, 225–234.
75. Villadangos JA, Young L. Antigen-presentation properties of plasmacytoid dendritic cells. *Immunity*. 2008; 29:352–361.
  76. Reizis B, Bunin A, Ghosh HS, Lewis KL, Sisirak V. Plasmacytoid Dendritic Cells: Recent Progress and Open Questions. *Annu Rev Immunol*. 2011; 29:163–183.
  77. Adriano Boasso, Jean-Philippe Herbeuval, Andrew W. Hardy, Stephanie A. Anderson, Matthew J. Dolan, Dietmar Fuchs, and Gene M. Shearer. HIV inhibits CD4<sup>+</sup> T-cell proliferation by inducing indoleamine 2,3-dioxygenase in plasmacytoid dendritic cells. *Blood*. 2007; 109:3351–3359.
  78. Tomoki Ito, Maria Yang, Yui-Hsi Wang, Roberto Lande, Josh Gregorio, Olivia A Perng, Xiao-Feng Qin, Yong-Jun Liu, and Michel Gilliet. Plasmacytoid dendritic cells prime IL-10-producing T regulatory cells by inducible costimulator ligand. *J Exp Med*. 2007; 204:105–115.
  79. Julien Diana, Thibault Griseri, Sylvie Lagaye, Lucie Beaudoin, Elodie Autrusseau, Anne-Sophie Gautron, Céline Tomkiewicz, André Herbelin, Robert Barouki, Matthias von Herrath, Marc Dalod, and Agnès Lehuen. NKT cell-plasmacytoid dendritic cell cooperation via OX40 controls viral infection in a tissue-specific manner. *Immunity*. 2009; 30:289–299.
  80. Simpson, J., Miles, K., Trub, M., Macmahon, R., Gray, M., 2016. Plasmacytoid dendritic cells respond directly to apoptotic cells by secreting immune regulatory IL-10 or IFN $\alpha$ . *Front. Immunol*. 7, 590.
  81. Dana Mitchell, Sreenivasulu Chintala, Mahua Dey. Plasmacytoid dendritic cell in immunity and cancer. *Journal of Neuroimmunology*, 322(2018)63-73.
  82. Golde D. The stem cell. *Sci Am*, 1991. 265, 86–93. 2.
  83. Ogawa, M. Differentiation and proliferation of hematopoietic stem cells. *Blood*, 1993. 81, 2844–2853.
  84. Morrison SJ, Wandycz AM, Hemmati HD, Wright DE, Weissman IL. Identification of a lineage of multipotent hematopoietic progenitors. *Development*, 1997. 124(10): 1929-39.

85. Akashi K, Traver D, Miyamoto T, Weissman IL. A clonogenic common myeloid progenitor that gives rise to all myeloid lineages. *Nature*, 2000. 404(6774): 193-7.
86. Debili N, Coulombel L, & Croisille L. Characterization of a bipotent erythro-megakaryocytic progenitor in human bone marrow. *Blood*, 1996. 88, 1284-1296.
87. McDonald TP, Sullivan PS. Megakaryocytic and erythrocytic cell lines share a common precursor cell. *Exp Hematol*, 1993. 21, 1316–1320.
88. Nakeff A, Daniels–McQueen S. In vitro colony assay for a new class of megakaryocyte precursor: Colony- forming unit megakaryocyte (CFU-M). *Proc Soc Exp Biol Med*, 1976. 151, 587–590.
89. Yamamoto R, Morita Y, Ooehara J, Hamanaka S, Onodera M, Rudolph KL, Ema H, Nakauchi H. Clonal analysis unveils self-renewing lineage-restricted progenitors generated directly from hematopoietic stem cells. *Cell*. 2013 Aug 29;154(5):1112-1126.
90. Paul F, Arkin Y, Giladi A, Jaitin DA, Kenigsberg E, Keren-Shaul H, Winter D, Lara-Astiaso D, Gury M, Weiner A, David E, Cohen N, Lauridsen FK, Haas S, Schlitzer A, Mildner A, Ginhoux F, Jung S, Trumpp A, Porse BT, Tanay A, Amit I. Transcriptional Heterogeneity and Lineage Commitment in Myeloid Progenitors. *Cell*. 2015 Dec 17;163(7):1663-77.
91. Woolthuis CM, Park CY. Hematopoietic stem/progenitor cell commitment to the megakaryocyte lineage. *Blood*. 2016 Mar 10;127(10):1242-8. doi: 10.1182/blood-2015-07-607945.
92. Noetzli LJ, French SL, Machlus KR. New Insights into the Differentiation of Megakaryocytes From Hematopoietic Progenitors. *Arterioscler Thromb Vasc Biol*. 2019 Jul;39(7):1288-1300.
93. Sanjuan-Pla A, Macaulay IC, Jensen CT, Woll PS, Luis TC, Mead A, Moore S, Carella C, Matsuoka S, Bouriez Jones T, Chowdhury O, Stenson L, Lutteropp M, Green JC, Facchini R, Boukarabila H, Grover A, Gambardella A, Thongjuea S, Carrelha J, Tarrant P, Atkinson D, Clark SA, Nerlov C, Jacobsen SE. Platelet-biased stem cells reside at the apex of the haematopoietic stem-cell hierarchy.

- Nature, 2013. 502(7470): 232-6.
94. Haas S, Hansson J, Klimmeck D, Loeffler D, Velten L, Uckelmann H, Wurzer S, Prendergast ÁM, Schnell A, Hexel K, Santarella-Mellwig R, Blaszkiewicz S, Kuck A, Geiger H, Milsom MD, Steinmetz LM, Schroeder T, Trumpp A, Krijgsveld J, Essers MA. Inflammation-Induced Emergency Megakaryopoiesis Driven by Hematopoietic Stem Cell-like Megakaryocyte Progenitors. *Cell Stem Cell*, 2015. 17(4): 422-34.
  95. Tavassoli M, Aoki M. Localization of megakaryocytes in the bone marrow. *Blood Cells*, 1989.15(1): 3-14.
  96. Avecilla ST, Hattori K, Heissig B, Tejada R, Liao F, Shido K, Jin DK, Dias S, Zhang F, Hartman TE, Hackett NR, Crystal RG, Witte L, Hicklin DJ, Bohlen P, Eaton D, Lyden D, de Sauvage F, Rafii S. Chemokine-mediated interaction of hematopoietic progenitors with the bone marrow vascular niche is required for thrombopoiesis. *Nat Med*, 2004. 10(1): 64-71.
  97. Greenbaum A, Hsu YM, Day RB, Schuettpelz LG, Christopher MJ, Borgerding JN, Nagasawa T, Link DC. CXCL12 in early mesenchymal progenitors is required for haematopoietic stem-cell maintenance. *Nature*, 2013. 495(7440): 227-30.
  98. Ding L, Morrison SJ. Haematopoietic stem cells and early lymphoid progenitors occupy distinct bone marrow niches. *Nature*, 2013. 495(7440):231-5.
  99. Ding L, Saunders TL, Enikolopov G, Morrison SJ. Endothelial and perivascular cells maintain haematopoietic stem cells. *Nature*, 2012. 481(7382): 457–462.
  100. Williams DE, Eisenman J, Baird S, Rauch C, Ness KV, March CJ, Park LS, Martin U, Mochizuki DY, Boswell HS, Burgess GS, Cosman D, Lyman SD: Identification of a ligand for the c-kit proto-oncogene. *Cell*, 1990. 63:163.
  101. Zsebo KM, Williams DA, Geissler EN, Broudy VC, Martin FH, Atkins HL, Hsu R-Y, Birkett NC, Okino KH, Murdock DC, Jacobsen FW, Langley KE, Smith KA, Takeishi T, Cattanch BM, Galli SJ, Suggs SV: Stem cell factor is encoded at the S1 locus of the mouse and is the ligand for c-kit tyrosine kinase receptor. *Cell*, 1990. 63: 213.

102. Huang E, Nocka K, Beier DR, Chu T-Y, Buck J, Lahm H-W, Wellner D, Leder P, Besmer P: The hematopoietic growth factor KL is encoded by the SI locus and is the ligand of the c-kit receptor, the gene product of the W locus. *Cell*, 1990. 63: 225.
103. Ogawa M, Nishikawa S, Yoshinaga K, Hayashi S, Kunisada T, Nakao J, Kina T, Sudo T, Kodama H, Nishikawa S. Expression and function of c-Kit in fetal hemopoietic progenitor cells: transition from the early c-Kit-independent to the late c-Kit-dependent wave of hemopoiesis in the murine embryo. *Development*, 1993. 117(3): 1089-98.
104. Tsuji K, Zsebo KM, Ogawa M. Enhancement of murine blast cell colony formation in culture by recombinant rat stem cell factor, ligand for c-kit. *Blood*, 1991. 78(5): 1223-9.
105. Ogawa M, Matsuzaki Y, Nishikawa S, Hayashi S, Kunisada T, Sudo T, Kina T, Nakauchi H, Nishikawa S. Expression and function of c-kit in hemopoietic progenitor cells. *J Exp Med*, 1991. 174(1): 63-71.
106. Avraham H, Vannier E, Cowley S, Jiang SX, Chi S, Dinarello CA, Zsebo KM, Groopman JE. Effects of the stem cell factor, c-kit ligand, on human megakaryocytic cells. *Blood*, 1992. 79(2): 365-71.
107. Avraham H, Scadden DT, Chi S, Broudy VC, Zsebo KM, Groopman JE. Interaction of human bone marrow fibroblasts with megakaryocytes: role of the c-kit ligand. *Blood*, 1992. 80(7): 1679-84.
108. Kaushansky K, Lok S, Holly RD, Broudy VC, Lin N, Bailey MC, Forstrom Buddle MM, Oort PJ, Hagen FS, Roth GJ, Papayannopoulou T, Foster DC. Promotion of megakaryocyte progenitor expansion and differentiation by the c-Mpl ligand thrombopoietin. *Nature*, 1994. 369(6481): 568-71.
109. Gurney AL, Carver-Moore K, de Sauvage FJ, Moore MW. Thrombocytopenia in c-mpl-deficient mice. *Science*, 1994. 265(5177):1445-7.
110. de Graaf CA, Metcalf D. Thrombopoietin and hematopoietic stem cells. *Cell Cycle*, 2011. 10(10): 1582-9.
111. Debili N, Wendling F, Cosman D, Titeux M, Florindo C, Dusanter-Fourt I,

- Schooley K, Methia N, Charon M, Nador R. The Mpl receptor is expressed in the megakaryocytic lineage from late progenitors to platelets. *Blood*, 1995. 85(2): 391-401.
112. Fishley B, Alexander WS. Thrombopoietin signalling in physiology and disease. *Growth Factors*, 2004. 22(3): 151-5.
113. Geddis AE, Linden HM, Kaushansky K. Thrombopoietin: a pan-hematopoietic cytokine. *Cytokine Growth Factor Rev*, 2002. 13(1): 61-73.
114. Debili N, Wendling F, Katz A, Guichard J, Breton-Gorius J, Hunt P, Vainchenker W. The Mpl-ligand or thrombopoietin or megakaryocyte growth and differentiative factor has both direct proliferative and differentiative activities on human megakaryocyte progenitors. *Blood*, 1995. 86(7): 2516-25.
115. Lok S, Kaushansky K, Holly RD, Kuijper JL, Lofton-Day CE, Oort PJ, Grant FJ, Heipel MD, Burkhead SK, Kramer JM, et al. Cloning and expression of murine thrombopoietin cDNA and stimulation of platelet production in vivo. *Nature*, 1994. 369(6481): 565-8.
116. Zucker-Franklin D, Kaushansky K. Effect of thrombopoietin on the development of megakaryocytes and platelets: an ultrastructural analysis. *Blood*, 1996. 88(5): 1632-8.
117. Broudy VC, Lin NL, Kaushansky K. Thrombopoietin (c-mpl ligand) acts synergistically with erythropoietin, stem cell factor, and interleukin-11 to enhance murine megakaryocyte colony growth and increases megakaryocyte ploidy in vitro. *Blood*, 1995. 85(7): 1719-26.
118. Qian S, Fu F, Li W, Chen Q, de Sauvage FJ. Primary role of the liver in thrombopoietin production shown by tissue-specific knockout. *Blood*, 1998.92(6): 2189-91.
119. Grozovsky R, Begonja AJ, Liu K, Visner G, Hartwig JH, Falet H, Hoffmeister KM. The Ashwell-Morell receptor regulates hepatic thrombopoietin production via JAK2-STAT3 signaling. *Nat Med*, 2015. 21(1): 47-54.
120. Emmons RV, Reid DM, Cohen RL, Meng G, Young NS, Dunbar CE, Shulman

- NR. Human thrombopoietin levels are high when thrombocytopenia is due to megakaryocyte deficiency and low when due to increased platelet destruction. *Blood*, 1996. 87(10): 4068-71.
121. Fu, Wenwen (2017): Megakaryopoietic islands in the bone marrow balance platelet production and maintain megakaryocyte homeostasis. Dissertation, LMU München: Faculty of Medicine
  122. Buch T, Heppner FL, Tertilt C, Heinen TJ, Kremer M, Wunderlich FT, Jung S, Waisman A. A Cre-inducible diphtheria toxin receptor mediates cell lineage ablation after toxin administration. *Nat Methods*, 2005. 2(6): 419-26.
  123. Swiecki M, Gilfillan S, Vermi W, Wang Y, Colonna M. Plasmacytoid dendritic cell ablation impacts early interferon responses and antiviral NK and CD8(+) T cell accrual. *Immunity*. 2010;33(6):955–66.
  124. Lassailly F, Foster K, Lopez-Onieva L, Currie E, Bonnet D. Multimodal imaging reveals structural and functional heterogeneity in different bone marrow compartments: functional implications on hematopoietic stem cells. *Blood*, 2013. 122(10): 1730-40.
  125. Mazo IB, Gutierrez-Ramos JC, Frenette PS, Hynes RO, Wagner DD, von Andrian UH. Hematopoietic progenitor cell rolling in bone marrow microvessels: parallel contributions by endothelial selectins and vascular cell adhesion molecule 1. *J Exp Med*, 1998. 188(3): 465-74.
  126. Schulze H. Culture of murine megakaryocytes and platelets from fetal liver and bone marrow. *Methods Mol Biol*, 2012. 788: 193-203.
  127. Kim EJY, Anko ML, Flensberg C, Majewski IJ, Geng FS, Firas J, Huang DCS, van Delft MF, Heath JK. BAK/BAX-Mediated Apoptosis Is a Myc-Induced Roadblock to Reprogramming. *Stem Cell Reports*. 2018 Feb 13;10(2):331-338.
  128. Iyer S, Uren RT, Dengler MA, Shi MX, Uno E, Adams JM, Dewson G, Kluck RM. Robust autoactivation for apoptosis by BAK but not BAX highlights BAK as an important therapeutic target. *Cell Death Dis*. 2020 Apr 23;11(4):268.
  129. Robin C, Ottersbach K, Boisset JC, Oziemlak A, Dzierzak E. CD41 is developmentally regulated and differentially expressed on mouse hematopoietic

- stem cells. *Blood*, 2011. 117(19): 5088-91.
130. Gekas C, Graf T. CD41 expression marks myeloid-biased adult hematopoietic stem cells and increases with age. *Blood*, 2013. 121(22): 4463-72.
  131. Bluteau D, Lordier L, Di Stefano A, Chang Y, Raslova H, Debili N, Vainchenker W. Regulation of megakaryocyte maturation and platelet formation. *J Thromb Haemost*. 2009. 7 Suppl 1:227-34.
  132. Nishikii H, Kanazawa Y, Umemoto T, Goltsev Y, Matsuzaki Y, Matsushita K, Yamato M, Nolan GP, Negrin R, Chiba S. Unipotent Megakaryopoietic Pathway Bridging Hematopoietic Stem Cells and Mature Megakaryocytes. *Stem Cells*, 2015. 33(7): 2196-207.
  133. Lefrançais E, Ortiz-Muñoz G, Caudrillier A, Mallavia B, Liu F, Sayah DM, Thornton EE, Headley MB, David T, Coughlin SR, Krummel MF, Leavitt AD, Passegué E, Looney MR. The lung is a site of platelet biogenesis and a reservoir for haematopoietic progenitors. *Nature*, 2017. 544(7648): 105-109.
  134. Dütting S, Gaits-Iacovoni F, Stegner D, Popp M, Antkowiak A, van Eeuwijk JMM, Nurden P, Stritt S, Heib T, Aurbach K, Angay O, Cherpokova D, Heinz N, Baig AA, Gorelashvili MG, Gerner F, Heinze KG, Ware J, Krohne G, Ruggeri ZM, Nurden AT, Schulze H, Modlich U, Pleines I, Brakebusch C, Nieswandt B. A Cdc42/RhoA regulatory circuit downstream of glycoprotein Ib guides transendothelial platelet biogenesis. *Nat Commun*, 2017. 8: 15838.
  135. McArdle S, Mikulski Z, Ley K. Live cell imaging to understand monocyte, macrophage, and dendritic cell function in atherosclerosis. *J Exp Med*, 2016. 213(7): 1117-31.
  136. Zhang J, Varas F, Stadtfeld M, Heck S, Faust N, Graf T. CD41-YFP mice allow in vivo labeling of megakaryocytic cells and reveal a subset of platelets hyperreactive to thrombin stimulation. *Exp Hematol*, 2007. 35(3): 490-499.
  137. Muzumdar MD, Tasic B, Miyamichi K, Li L, Luo L. A global double-fluorescent Cre reporter mouse. *Genesis*, 2007. 45(9): 593-605.
  138. Pertuy F, Aguilar A, Strassel C, Eckly A, Freund JN, Duluc I, Gachet C, Lanza F, Léon C. Broader expression of the mouse platelet factor 4-cre transgene

- beyond the megakaryocyte lineage. *J Thromb Haemost*, 2015. 13(1): 115-25.
139. Swiecki, M. & Colonna, M. The multifaceted biology of plasmacytoid dendritic cells. *Nat. Rev. Immunol.* 15, 471–485 (2015).
140. Pierre Cunin, Rim Bouslama, Kellie R Machlus, Marta Martínez-Bonet, Pui Y Lee, Alexandra Wactor, Nathan Nelson-Maney, Allyn Morris, Li Guo, Andrew Weyrich, Martha Sola-Visner, Eric Boilard, Joseph E Italiano, Peter A Nigrovic. Megakaryocyte emperipolesis mediates membrane transfer from intracytoplasmic neutrophils to platelets. *Elife* 8, doi:10.7554/eLife.44031 (2019).
141. Anne Lippitsch, Nelli Baal, Yuri Chukovetskyi, Sarah Cunningham, Gabriela Michel, Kristina Dietert, Corinne Gurtner, Achim D Gruber, Gregor Bein, Holger Hackstein. Plasmacytoid dendritic cell depletion modifies FoxP3+ T cell homeostasis and the clinical course of bacterial pneumonia in mice. *J Leukoc Biol*, 2019.106(4):977-985.
142. Mandl M, Drechsler M, Jansen Y, Neideck C, Noels H, Faussner A, Soehnlein O, Weber C, Döring Y. Evaluation of the BDCA2-DTR Transgenic Mouse Model in Chronic and Acute Inflammation. *PLoS One*. 2015 Aug 7;10(8):e0134176.
143. Mesev, E. V., LeDesma, R. A. & Ploss, A. Decoding type I and III interferon signalling during viral infection. *Nat Microbiol* 4, 914-924 (2019).
144. Gough, D. J., Messina, N. L., Clarke, C. J., Johnstone, R. W. & Levy, D. E. Constitutive type I interferon modulates homeostatic balance through tonic signaling. *Immunity* 36, 166-174 (2012).
145. Lazear HM, Schoggins JW, Diamond MS. Shared and Distinct Functions of Type I and Type III Interferons. *Immunity*. 2019 Apr 16;50(4):907-923.
146. Essers MA, Offner S, Blanco-Bose WE, Waibler Z, Kalinke U, Duchosal MA, Trumpp A. IFN $\alpha$  activates dormant haematopoietic stem cells in vivo. *Nature*. 2009 Apr 16;458(7240):904-8.
147. Sato T, Onai N, Yoshihara H, Arai F, Suda T, Ohteki T. Interferon regulatory factor-2 protects quiescent hematopoietic stem cells from type I interferon-

- dependent exhaustion. *Nat Med*. 2009 Jun;15(6):696-700.
148. Wang Q, Miyakawa Y, Fox N, Kaushansky K. Interferon-alpha directly represses megakaryopoiesis by inhibiting thrombopoietin-induced signaling through induction of SOCS-1. *Blood*. 2000 Sep 15;96(6):2093-9.
  149. Shida N, Oritani K, Shiraga M, Yoshida H, Kawamoto S, Ujiie H, Masaie H, Ichii M, Tomiyama Y, Kanakura Y. Differential effects of a novel IFN-zeta/limitin and IFN-alpha on signals for Daxx induction and Crk phosphorylation that couple with growth control of megakaryocytes. *Exp Hematol*. 2005 Apr;33(4):495-503.
  150. Siegal FP, Kadowaki N, Shodell M, Fitzgerald-Bocarsly PA, Shah K, Ho S, Antonenko S, Liu YJ. The nature of the principal type 1 interferon-producing cells in human blood. *Science*. 1999 Jun 11;284(5421):1835-7.
  151. Cella M, Jarrossay D, Facchetti F, Alebardi O, Nakajima H, Lanzavecchia A, Colonna M. Plasmacytoid monocytes migrate to inflamed lymph nodes and produce large amounts of type I interferon. *Nat Med*. 1999 Aug;5(8):919-23.
  152. Diebold SS, Montoya M, Unger H, Alexopoulou L, Roy P, Haswell LE, Al-Shamkhani A, Flavell R, Borrow P, Reis e Sousa C. Viral infection switches non-plasmacytoid dendritic cells into high interferon producers. *Nature*. 2003 Jul 17;424(6946):324-8. *w. Methods Mol Biol*, 2012. 788: 193-203.
  153. Durandt C, Potgieter JC, Mellet J, Herd C, Khoosal R, Nel JG, Rossouw T, Pepper MS. HIV and haematopoiesis. *S Afr Med J*. 2019 Sep 10;109(8b):40-45.
  154. Jansen AJG, Spaan T, Low HZ, Di Iorio D, van den Brand J, Tieke M, Barendrecht A, Rohn K, van Amerongen G, Stittelaar K, Baumgärtner W, Osterhaus A, Kuiken T, Boons GJ, Huskens J, Boes M, Maas C, van der Vries E. Influenza-induced thrombocytopenia is dependent on the subtype and sialoglycan receptor and increases with virus pathogenicity. *Blood Adv*. 2020 Jul 14;4(13):2967-2978.
  155. Wool GD, Miller JL. The Impact of COVID-19 Disease on Platelets and Coagulation. *Pathobiology*. 2021;88(1):15-27.

156. Tilton JC, Manion MM, Luskin MR, Johnson AJ, Patamawenu AA, Hallahan CW, Cogliano-Shutta NA, Mican JM, Davey RT Jr, Kottlilil S, Lifson JD, Metcalf JA, Lempicki RA, Connors M. Human immunodeficiency virus viremia induces plasmacytoid dendritic cell activation in vivo and diminished alpha interferon production in vitro. *J Virol.* 2008 Apr;82(8):3997-4006.
157. Schwartz JA, Clayton KL, Mujib S, Zhang H, Rahman AK, Liu J, Yue FY, Benko E, Kovacs C, Ostrowski MA. Tim-3 is a Marker of Plasmacytoid Dendritic Cell Dysfunction during HIV Infection and Is Associated with the Recruitment of IRF7 and p85 into Lysosomes and with the Submembrane Displacement of TLR9. *J Immunol.* 2017 Apr 15;198(8):3181-3194.
158. Peruzzi B, Bencini S, Capone M, Mazzoni A, Maggi L, Salvati L, Vanni A, Orazzini C, Nozzoli C, Morettini A, Poggesi L, Pieralli F, Peris A, Bartoloni A, Vannucchi AM, Liotta F, Caporale R, Cosmi L, Annunziato F. Quantitative and qualitative alterations of circulating myeloid cells and plasmacytoid DC in SARS-CoV-2 infection. *Immunology.* 2020 Dec;161(4):345-353.
159. Arunachalam PS, Wimmers F, Mok CKP, Perera RAPM, Scott M, Hagan T, Sigal N, Feng Y, Bristow L, Tak-Yin Tsang O, Wagh D, Collier J, Pellegrini KL, Kazmin D, Alaaeddine G, Leung WS, Chan JMC, Chik TSH, Choi CYC, Huerta C, Paine McCullough M, Lv H, Anderson E, Edupuganti S, Upadhyay AA, Bosinger SE, Maecker HT, Khatri P, Roupheal N, Peiris M, Pulendran B. Systems biological assessment of immunity to mild versus severe COVID-19 infection in humans. *Science.* 2020 Sep 4;369(6508):1210-1220.
160. Macal M, Jo Y, Dallari S, Chang AY, Dai J, Swaminathan S, Wehrens EJ, Fitzgerald-Bocarsly P, Zúñiga EI. Self-Renewal and Toll-like Receptor Signaling Sustain Exhausted Plasmacytoid Dendritic Cells during Chronic Viral Infection. *Immunity.* 2018 Apr 17;48(4):730-744.e5.
161. Greene TT, Zuniga EI. Type I Interferon Induction and Exhaustion during Viral Infection: Plasmacytoid Dendritic Cells and Emerging COVID-19 Findings. *Viruses.* 2021 Sep 15;13(9):1839.
162. Lehmann C, Lafferty M, Garzino-Demo A, Jung N, Hartmann P, Fätkenheuer

- G, Wolf JS, van Lunzen J, Romerio F. Plasmacytoid dendritic cells accumulate and secrete interferon alpha in lymph nodes of HIV-1 patients. *PLoS One*. 2010 Jun 14;5(6):e11110.
163. Swiecki M, Wang Y, Vermi W, Gilfillan S, Schreiber RD, Colonna M. Type I interferon negatively controls plasmacytoid dendritic cell numbers in vivo. *J Exp Med*. 2011 Nov 21;208(12):2367-74.
164. Liu C, Martins AJ, Lau WW, Rachmaninoff N, Chen J, Imberti L, Mostaghimi D, Fink DL, Burbelo PD, Dobbs K, Delmonte OM, Bansal N, Failla L, Sottini A, Quiros-Roldan E, Han KL, Sellers BA, Cheung F, Sparks R, Chun TW, Moir S, Lionakis MS; NIAID COVID Consortium; COVID Clinicians, Rossi C, Su HC, Kuhns DB, Cohen JI, Notarangelo LD, Tsang JS. Time-resolved systems immunology reveals a late juncture linked to fatal COVID-19. *Cell*. 2021 Apr 1;184(7):1836-1857.e22.
165. Lucas C, Wong P, Klein J, Castro TBR, Silva J, Sundaram M, Ellingson MK, Mao T, Oh JE, Israelow B, Takahashi T, Tokuyama M, Lu P, Venkataraman A, Park A, Mohanty S, Wang H, Wyllie AL, Vogels CBF, Earnest R, Lapidus S, Ott IM, Moore AJ, Muenker MC, Fournier JB, Campbell M, Odio CD, Casanovas-Massana A; Yale IMPACT Team, Herbst R, Shaw AC, Medzhitov R, Schulz WL, Grubaugh ND, Dela Cruz C, Farhadian S, Ko AI, Omer SB, Iwasaki A. Longitudinal analyses reveal immunological misfiring in severe COVID-19. *Nature*. 2020 Aug;584(7821):463-469.
166. Huang C, Wang Y, Li X, Ren L, Zhao J, Hu Y, Zhang L, Fan G, Xu J, Gu X, Cheng Z, Yu T, Xia J, Wei Y, Wu W, Xie X, Yin W, Li H, Liu M, Xiao Y, Gao H, Guo L, Xie J, Wang G, Jiang R, Gao Z, Jin Q, Wang J, Cao B. Clinical features of patients infected with 2019 novel coronavirus in Wuhan, China. *Lancet*. 2020 Feb 15;395(10223):497-506.

## 6 Appendix

### Abbreviations

min minute

ml milliliter

mm millimeter

n number

µg microgram

µl microliter

µm micrometer

3D 3 dimension

APC antigen present cell

BM bone marrow

BSA bovine serum albumin

BCL-2 B-cell lymphoma 2

cDC classical dendritic cell

CDP common dendritic cell progenitor

CFU colony-forming unit

CFU-MK colony-forming unit-megakaryocyte

CLP common lymphoid progenitor

CMP common myeloid progenitor

CMPR common myeloid repopulating progenitor

DC dendritic cell

DMEM Dulbecco's Modified Eagle Medium

DMS Demarcation membrane system

DT Diphtheria toxin

EGFP Enhanced green fluorescent protein

FCS fetal calf serum

FGF-4 Fibroblast growth factor-4

FITC Fluorescein isothiocyanate

FLT3 Fms-like tyrosine kinase 3  
GFP green fluorescent protein  
HIV Human immunodeficiency virus  
HSC Hematopoietic stem cell  
HSV Herpes simplex virus  
ICOS-L inducible co-stimulator ligand  
IDO indoleamine 2,3-dioxygenase  
IFN Interferon  
IL Interleukin  
LIN lacking lineage markers  
LMPP lymphoid primed multipotent progenitor  
LSK Lin<sup>-</sup> Sca-1<sup>+</sup> c-Kit<sup>+</sup>  
MDP macrophage dendritic cell progenitor  
MEP Megakaryocytic-erythrocytic progenitor  
MERP Megakaryocytic-erythrocytic repopulating progenitor  
MK Megakaryocyte  
MKP Megakaryocyte progenitor  
MKPR Megakaryocyte repopulating progenitor  
MPP Multipotent progenitor  
MSC Mesenchymal stem cell  
NGS Normal goat serum  
PBS Phosphate buffer saline  
pDC plasmatic dendritic cell  
PE Phycoerythrin  
PF4 Platelet factor 4  
PFA Paraformaldehyde  
PMT Photo Multiplier Tube  
rm Recombinant mouse  
RT room temperature  
SEM standard error of the mean

SCF Stem cell factor

SDF-1 Stromal cell-derived factor-1

SHG Second Harmonic Generation

TNF Tumor necrosis factor

Tpo Thrombopoietin

vWF von Willebrand Factor

VEGF Vascular endothelial growth factor

WT Wild type

## **Acknowledgement**

Firstly, I am very grateful to Prof. Dr. med Steffen Massberg for offering me this great project where I could learn a lot of professional knowledge and skills through three years of medical doctor study. I would not have finished this project in time without his distinguished supervision and endless support.

Secondly, I would like to thank my thesis advisory committee, Prof. Dr. med Christian Schulz and Prof. Dr. rer. nat. Annette Müller-Taubenberger for the insightful suggestions and comments that helped me understand and finish this project.

Additionally, I am deeply grateful to Dr. Hellen Ishikawa-Ankerhold, my direct supervisor, for teaching me many experimental skills and led me to finish this project. She is very kind and patient and gave me support and constructive discussions on the research. She always encouraged me when I encountered the failure of the experiments. I also thank my colleagues and cooperation partners, especially Dominic van den Heuvel, Jutta Weitz, Tobias Schübel, Larissa Belz, Michael Lorenz, Lulu Liu, Zhe Zhang, Dr. Florian Gärtner and Dr. Susanne Stutte, for helping me finish the research. It is my pleasure to work with them.

Furthermore, I am grateful that IRTG 914 program provided me 1-year financial support, Dr. Verena Kochan provided me the guidance about the structure MD program. Importantly, I am deeply grateful for China Scholarship Council (CSC) offering me 3-years financial support so that I could finish my doctoral study in Germany.

Finally, I thank my family and my girlfriend for supporting and encouraging me during the study.

## Affidavit

	LUDWIG- MAXIMILIANS- UNIVERSITÄT MÜNCHEN	Promotionsbüro Medizinische Fakultät		
<b>Affidavit</b>				

Guo, Chenglong

\_\_\_\_\_  
Surname, first name

\_\_\_\_\_  
Street

\_\_\_\_\_  
Zip code, town, country

I hereby declare that the submitted thesis entitled:

### **Plasmacytoid Dendritic Cells Play a Role in Megakaryopoiesis in the Bone Marrow**

is my own work. I have only used the sources indicated and have not made unauthorised use of services of a third party. Where the work of others has been quoted or reproduced, the source is always given.

I further declare that the submitted thesis or parts thereof have not been presented as part of an examination degree to any other university.

Munich, 16.05.2022

\_\_\_\_\_  
place, date

Chenglong Guo

\_\_\_\_\_  
Signature doctoral candidate